Effects of aggregate quality on reinforcement corrosion

Syed Imran Ali

Civil Engineering

April 2003

Abstract

The reduction in the useful-service life of concrete structures in the Arabian Gulf, due to chloride-induced reinforcement corrosion is of major concern to the construction industry in this region. There are several options available to minimize concrete deterioration due to reinforcement corrosion. Among these alternatives, the use of good quality concrete is the cheapest one. However, it is difficult to produce good quality concrete locally, as the available limestone aggregates are weak and highly absorptive. Therefore, there is a need to improve the quality of concrete by suitable adjustments in the mix design. Further, the performance of high quality concrete when exposed to thermal variations is not very well documented.

This research was conducted to develop high quality concrete utilizing local aggregates. Three types of coarse aggregates, namely limestone aggregates from Abu-Hadriyah and Riyadh, and steel slag aggregates were selected to produce high quality concrete. The tensile strength and reinforcement corrosion of the high quality concrete produced using local aggregates were investigated.

The data developed in this research indicate that the quality of aggregate has a significant effect on the corrosion resistance of concrete. The steel slag aggregate concrete showed better corrosion resistance and tensile strength followed by Riyadh and Abu-Hadriyah aggregate concretes. Exposure to the thermal variations reduced the corrosion resistance of reinforced concrete specimens prepared with the selected aggregates.

The service life of the concrete prepared with the selected aggregates was predicted using two models, namely Bazant's mathematical model and Morinaga empirical formula. The highest service life was recorded in the concrete specimens prepared with steel slag aggregates, silica fume and steel fibers.

EFFECTS OF AGGREGATE QUALITYON REINFORCEMENT CORROSION

By

SYED IMRAN ALI

A Thesis presented to the

DEANSHIP OF GRADUATE STUDIES

In Partial Fulfillment of the Requirements
for the degree

MASTER OF SCIENCE

IN

CIVIL ENGINEERING

KING FAHD UNIVERSITY
OF PETROLEUM AND MINERALS

Dhahran, Saudi Arabia

MARCH 2003

KING FAHD UNIVERSITY OF PETROLEUM AND MINERALS
DHAHRAN 31261, SAUDI ARABIA

DEANSHIP OF GRADUATE STUDIES

This thesis, written by **SYED IMRAN ALI** under the direction of his Thesis Advisor and approved by his Thesis Committee, has been presented to and accepted by the Dean of Graduate Studies, in partial fulfillment of the requirements for the degree of **MASTER OF SCIENCE IN CIVIL ENGINEERING.**

THESIS COMMITTEE

_____
Prof. Abdullah A. Al-Musallam (Advisor)

_____
Dr. Mohammed Maslehuddin (Co-Advisor)

_____
Dr. Ahmad S. Al- Gahtani (Member)

_____
Dr. Omar S. B. Al-Amoudi (Member)

_____
Dr. Salah U. Al-Dulaijan (Member)

_____
Prof. Hamad. I. Al-AbdulWahab
Department Chairman

_____
Prof. Osama A. Jannadi
Dean of Graduate Studies

_____
Date

In the Name of Allah, Most Gracious, Most Merciful.

*Dedicated to my beloved **Parents** and **Family Members***

ACKNOWLEDGEMENTS

All praises and thanks are due to Allah (subhana wa taala) for bestowing me with health, knowledge and patience to complete this work. May the peace and blessing of Allah be upon Prophet Muhammad (PBUH), his family and his companions. Thereafter, acknowledgement is due to KFUPM for the support given to this research through its tremendous facilities and for granting me the opportunity to pursue graduate studies with financial support.

I acknowledge, with deep gratitude and appreciation, the inspiration, encouragement, valuable time and guidance given to me by my Committee Chairman, Dr. Abdullah A. Al-Musallam. Special thanks are due to my Committee Co-Chairman, Dr. Mohammed Maslehuddin, for his continuous moral support, encouragement and guidance during this research work.

I am grateful to my Committee members, Dr. Ahmad S. Al-Gahtani, Dr. Omar S. B. Al-Amoudi and Dr. Salah U. Al-Dulaijan for their constructive guidance and technical support. I also acknowledge the sincere and untiring efforts of Engr. Mr. Mukarram in preparing the experimental program and set-ups utilized in this study. Thanks are also due to the laboratory personnel, Mr. Hassan Zakaria, Mr. Abbasi, Mr. Omar, Mr. Saleem Mr. Nahash, Mr. Abdullah who assisted me in the experimental work and the Department secretaries, Mr. Mumtaz, Mr. Solano and Mr. Efren for their help and assistance.

Special thanks are due to my senior colleagues at the University, Akber, Faiz Iqbal B., Taufiq A. and Shazali who were always there to help me in my work. I would also like to thank my friends Abdullah, Ali, Anwar, Aurif, Baseer, Faheem, Farooq, Hameed, Jalal, Khasim, Majid, Mujtaba, Rizwan, Saif, Salman, Sohail and all others who provided wonderful company and some memories that will last a lifetime.

Finally, thanks are due to my mother, late father, and all my family members for their emotional and moral support throughout my academic career and also for their love, patience, encouragement and prayers.

TABLE OF CONTENTS

LIST OF TABLES

LIST OF FIGURES

THESIS ABSTRACT

SYED IMRAN ALI

EFFECT OF AGGREGATE QUALITY ON REINFORCEMENT CORROSION

CIVIL ENGINEERING

8 APRIL, 2003

The reduction in the useful-service life of concrete structures in the Arabian Gulf, due to chloride induced reinforcement corrosion, is of major concern to the construction industry in this region. There are several options available to minimize concrete deterioration due to reinforcement corrosion. Among these alternatives, the use of good quality concrete is the cheapest one. However, it is difficult to produce good quality concrete locally, as the available limestone aggregates are weak and highly absorptive. Therefore, there is a need to improve the quality of concrete by suitable adjustments in the mix design. Further, the performance of high quality concrete when exposed to thermal variations is not very well documented.

This research was conducted to develop high quality concrete utilizing local aggregates. Three types of coarse aggregates, namely limestone aggregates from Abu-Hadriyah and Riyadh, and steel slag aggregates were selected to produce high quality concrete. The tensile strength and reinforcement corrosion of the high quality concrete produced using local aggregates were investigated.

The data developed in this research indicate that the quality of aggregate has a significant effect on the corrosion resistance of concrete. The steel slag aggregate concrete showed better corrosion resistance and tensile strength followed by Riyadh and Abu-Hadriyah aggregate concretes. Exposure to thermal variations reduced the corrosion-resistance of concrete specimens prepared with the selected aggregates.

The service life of the concrete prepared with the selected aggregates was predicted using two models, namely Bazant's mathematical model and Morinaga empirical formula. The highest service life was recorded in the concrete specimens prepared with steel slag aggregates, silica fume and steel fibers.

MASTER OF SCIENCE DEGREE

KING FAHD UNIVERSITY OF PETROLEUM AND MINERALS

Dhahran, Saudi Arabia

ABSTRACT (ARABIC)

ملخص الرسالة

اسم مقدم الرسالة: **سيد عمران علي**
عنوان الرسالة: **تأثير جودة الركام على صدأ حديد التسليح**
تخصص مقدم البحث: **الهندسة المدنية**
تاريخ الرسالة: **8 أبريل 2003م**

ان نقصان العمر الافتراضي للمنشآت الخرسانيّة في الخليج العربيّ بسبب صدأ حديد التسليح نتيجة لتغلغل الكلورايد, يعتبر ذا اهمية كبيرة لقطاع التشييد في هذه المنطقة . وهنالك عدّة خيارات متاحة للحدّ من التّدهور بسبب صدأ التسليح مثل: استعمال الخرسانة الجيّدة , حيث أن هذا الاختيار هو الأرخص. ومع ذلك, فانه من الصعوبة انتاج خرسانة محليّة ذات جودة عالية نظراً لأن الركام الجيري المتاح ضعيف وذو خاصية امتصاص عالية. لذلك, هناك حاجة ماسة لتحسين جودة الخرسانة بالتّعديلات المناسبة في تصميم الخلطة. كما أن أداء الخرسانة ذات الجودة العالية غير موثقة عند التعرض لتغيرات حرارية.

تم اجراء هذا البحث لتطوير خرسانة ذات جودة عالية باستخدام ثلاثة انواع من الركام المحلي, وهي ركام جيري من منطقة أبوحدرية ومن منطقة الرياض وركام خبث الحديد لانتاج خرسانة ذات جودة عالية. وتم التحقق من مقاومة الشد وصدأ حديد التسليح للخرسانة عالية الجودة المنتجة باستخدام الركام المحلي.

أشارت الدراسات التي أجريت في هذا البحث الى ان جودة الركام ذات تأثير ملحوظ على مقاومة الخرسانة للصدأ. وأظهرت خرسانة ركام خبث الحديد مقاومة للصدأ وقوة الشد بصورة أفضل من النوعين الآخرين يتبعها ركام الرياض وأخيراً ركام أبو حدرية. كما دلت نتائج الدراسة أن التعرض لتغييرات حرارية قد قللت من مقاومة الصدأ في عينات الخرسانة المعدة باستخدام انواع الركام المختلفة وتم تقدير العمر الافتراضي للخرسانة المعدة باستخدام انواع الركام المختلفة باستعمال نموذجين, وهما نموذج بازنت الرياضي وصيغة مورياناقا العملية. ودلت نتائج الدراسة أن العمرالافتراضي الأطول قد سجلت في عينات الخرسانة المعدة باستخدام ركام خبث الحديد ثم غبار السيليكا وألياف الحديد.

درجة الماجستير في العلوم

جامعة الملك فهد للبترول والمعادن

الظهران, المملكة العربية السعودية

CHAPTER 1

INTRODUCTION

1.1 DURABILITY OF REINFORCED CONCRETE IN AGGRESSIVE ENVIRONMENTS

Concrete has been extensively used in the construction all over the world. It is the most versatile building material and there can be virtually no significant structure being built anywhere in the world that does not use cement and concrete in one way or the other. The use of concrete is immediately apparent in reinforced concrete structures, bridges or in dams. There are perhaps three specific characteristics that make concrete so widely used. Firstly, concrete can be molded into different shapes and sizes either on the site or in a precast concrete plant. Its second dominant virtue is the protection it provides to steel to against corrosion and the third is its low-cost. Its ecologically favorable profile, excellent compressive strength, good fire resistance, high water resistance, low maintenance, and long

service-life coupled with its ease of manufacture at the construction site has established it as a major construction material.

Although concrete is the most widely used construction material, it has its own limitations. It has low tensile strength compared to compressive strength. Tensile strength of concrete is typically 8% to 15% of its compressive strength [1]. This weakness has been dealt with over many decades by using a system of reinforcing steel bars (rebars) to create reinforced concrete; so that concrete primarily resists compressive stresses and rebars resist tensile and shear stresses.

Reinforced concrete is expected to show excellent durability, however, sometimes it does not perform adequately as a result of: inferior design, improper construction, inadequate materials selection, harsh environment or a combination of these factors. Deterioration of reinforced concrete is the major problem facing the construction industry these days. Considerable resources have to be diverted towards the repair and rehabilitation of the deteriorated reinforced concrete structures.

There are several processes that affect reinforced concrete structures leading to loss of serviceability or, in extreme cases, to structural collapse. The most common concerns are corrosion of steel reinforcement, sulfate attack, freeze-thaw damage and alkali-aggregate reactions. The last three are forms of attack on the concrete itself. Much research has been devoted to these subjects, and for the most part these problems have been mitigated.

The most common cause of deterioration is corrosion of reinforcing steel. The reduction in the useful service-life of reinforced concrete structures, mainly due to reinforcement corrosion, in North America, Europe and the arid and semi-arid regions of the world, is of concern to the construction industry. Reinforcement corrosion is caused by the use of deicer salts in the temperate climatic conditions, while in the marine environment it is caused by the wetting and drying cycles and diffusion of chloride ions to the steel surface. In the arid and semi-arid regions, deterioration of reinforced concrete structures is mainly attributed to the environmental conditions of the region.

In the costal areas of the Arabian Gulf, deterioration of reinforced concrete components is noted within a short span of 5 to 10 years. The deterioration of structures in this region is mainly attributed to: (i) severe environment and geomorphic conditions, (ii) inappropriate materials specifications, and (iii) inadequate construction practices. The environmental conditions of Arabian Gulf are characterized by a large variation in the daily and seasonal temperature. The ambient temperature in the summer is as high as 45 to 50 °C and the relative humidity between 40 to 100% over a period of 24 hours [2]. At this ambient temperature, the temperature on the concrete surface may be as high as 70 to 80 °C due to solar radiation. The variation in the day to night temperature may be as much as 20 °C. This variation in the day and night temperature leads to the formation of micro-cracks in the concrete which accelerates the diffusion of aggressive species, such as chlorides, carbon dioxide, oxygen and moisture, to the steel surface causing corrosion of reinforcing steel. The corrosion of embedded steel is accompanied

with considerable expansive force, which results in spalling and cracking of concrete. The reinforced concrete construction in the above environments should be designed for durability in addition to strength. In these regions, concrete quality should be specified in terms of diffusion and permeability indices [3].

The two main causes of corrosion of steel in concrete are chloride attack and carbonation. These two mechanisms are unusual in that they do not attack the integrity of the concrete. Instead, these aggressive chemical species pass through the pores in the concrete and attack the steel. Other acids and aggressive ions, such as sulfates, destroy the integrity of the concrete before the steel is affected. Carbon dioxide and chloride ions are very unusual in penetrating the concrete without considerably damaging it.

Concrete normally provides reinforcing steel with excellent corrosion protection. The high alkaline environment in concrete results in the formation of a tightly adhering film which passivates the steel and protects it from corrosion. In addition, concrete can be proportioned to have a low permeability which minimizes the penetration of corrosion-inducing substances. Low permeability also increases the electrical resistivity of concrete which slows down the flow of electrochemical corrosion currents. Because of these inherent protective attributes, corrosion of steel does not proceed in the majority of concrete elements or structures. Corrosion of steel, however, can occur if the concrete is not of adequate quality, the structure was not properly designed for the service environment, or the environment was not as anticipated or has changed during the service life of a structure. The corrosion of metals, especially steel, in concrete has received increasing attention in recent years

because of its widespread occurrence in certain types of structures and the high cost of repairs.

Concrete is a composite material, and its properties depend on the properties of the component phases and the interaction between them. It is known that the interfaces are the weakest link in concrete, playing a very important role in the process of failure. In ordinary concrete, the strength of coarse aggregate is hardly an issue of consideration. This is because with water-cement ratio in the range of 0.5 to 0.7, it is the hardened cement paste and the transition zone that are normally the weaker components when compared to the coarse aggregates. This is no longer the case with high performance concrete. The quality of aggregates significantly influences the strength and durability characteristics of high performance concrete, particularly when lower water-cement ratio, high cement content, and chemical and/or mineral admixtures are used. The failure in high performance concrete often occurs either within the aggregate or at the aggregate-cement paste interface. The failure at the aggregate-cement paste is further accelerated due to the variation in the daily and seasonal temperature as indicated earlier. The micro-cracks formed at the aggregate-cement paste interface act as conduits for the moisture to penetrate to the steel surface. Therefore, there is need to evaluate the durability of high performance concrete, produced using local aggregates when exposed to temperature variations representative of the local environmental conditions.

1.2 NEED FOR THIS RESEARCH

Corrosion of reinforced concrete structures is a wide spread phenomenon all over the world. Vast resources are directed every year on repair and rehabilitation of structures. It is known that concrete is a highly heterogeneous and complex structure, which contains a heterogeneous distribution of different types and amounts of solid phases, pores, and microcracks [4]. In addition, the structure of concrete is also subject to change with time, environmental humidity and temperature. A large amount of water can exist in the hydrated cement paste, depending on the environmental humidity, porosity and pore size distribution of the hydrated concrete. Low quality porous concrete significantly increases the ingress of chlorides, oxygen, moisture and carbon dioxide to the steel-concrete interface. This situation is ideal for the initiation of reinforcement corrosion, especially if the cover over the reinforcing steel is insufficient. One method to reduce this problem may be to stop the supply of oxygen, moisture and other aggressive ions and gases to the steel surface, which are essential for reinforcement corrosion to occur. This can be achieved by using good quality concrete. The need to improve the quality of concrete in the Arabian Gulf States is all the more important to minimize the prevalent corrosion deterioration problem in this region.

High performance concrete is useful from structural point of view, but its durability performance is not very well investigated. Since the local coarse aggregates are weak and absorptive, considerable modifications in the concrete mix design have to be adopted to produce high performance concrete. Supplementary cementing materials, such as silica fume, are normally utilized, along with chemical

admixtures in conjunction with low water–cementitious materials ratio to produce high performance concrete. Further, fibers are incorporated to improve the ductility of high performance concrete. Since high strength concrete is not a ductile material, it is prone to cracking, particularly at the aggregate-cement interface when exposed to thermal variation. In the Arabian Gulf, the seasonal and daily variations in the temperature may be as high as 50 and 20 ^{o}C, respectively. The micro-cracks formed at the aggregate-paste interface assist the moisture and oxygen to diffuse to the steel-concrete interface thereby accelerating reinforcement corrosion. The effect of thermal variations on the durability of concrete, particularly reinforcement corrosion, has not been evaluated. Hence, there is a need for this study.

1.3 OBJECTIVES

The overall objective of this research program was to evaluate the effect of aggregate quality on reinforcement corrosion. The specific objectives were as follows:

1. To study the effect of aggregate quality and mix constituents on concrete durability, particularly reinforcement corrosion and chloride diffusion,

2. To evaluate the effect of aggregate quality and temperature variation on the tensile properties of concrete, and

3. To provide guidelines on the most suitable aggregates for producing high quality concrete for the local environmental conditions.

CHAPTER 2

LITERATURE REVIEW

2.1 MECHANISIMS OF REINFORCEMENT CORROSION

Corrosion of reinforcing steel in concrete and its damaging impact has generated significant research interest in the past few decades. This is due to the fact that the major cause of concrete deterioration worldwide is reinforcement corrosion. In order to understand the various approaches by which corrosion can be controlled, it is necessary to understand its nature.

A few metals, notably gold, silver, and platinum, exist naturally. Engineering metals, including steel, must be derived from their ores by smelting. During smelting, a metal absorbs the energy required to free it from the ore; and, this energy is retained within the metal after it is recovered. However, in a metallic state the metal is unstable, because it tends to get rid of itself from the extra energy by

recombining with the environment to revert to its more stable and natural state as an ore. This reversion process is known as oxidation.

Corrosion in general terms, means deterioration or destruction of a material due to a reaction with its environment [5]. Corrosion of a metal can be defined as a chemical reaction which returns the metal to compounds that are similar to the minerals from which it was extracted in the first place [6]. A refined metal, such as iron or steel has a natural tendency to corrode and thereby return to the stable state that exists in nature, as iron ore (typically iron oxide, Fe_2O_3). The rate of steel corrosion depends on its composition, grain structure, and the presence of entrained stress from fabrication. It also depends on the nature of the surrounding environment, such as the availability of water, oxygen, and ionic species, pH and temperature.

Concrete normally provides a high degree of protection to the reinforcing steel against corrosion, by virtue of the high alkalinity (pH > 13.5) of the pore solution. Under high alkalinity, steel remains passivated. In addition, well-consolidated and properly-cured concrete with a low w/c ratio has a low permeability, which minimizes the penetration of corrosion-inducing agents, such as chloride, carbon dioxide, moisture, etc., to the steel surface. Further, the high electrical resistivity of concrete restricts the rate of corrosion by reducing the flow of electrical current from the anodic to the cathodic sites.

The presence of calcium hydroxide and alkali elements, such as sodium and potassium, increase the alkalinity of the pore solution, pH being more than 13. It is

widely accepted that, at the early age of the concrete, this high alkalinity results in the transformation of a surface layer of the embedded steel to a tightly adhering submicroscopic γ-Fe_2O_3 film. As long as this film is not disturbed, it keeps the steel passive and protected from corrosion.

Reinforcement corrosion is caused either by the chloride ions or carbonation of concrete or both of them combined together. Both of these ions destroy the chemical protection provided by the concrete to the reinforcing steel. Depassivation of steel occurs by the reduction of the pore solution pH, due to carbonation, or by ingress of chloride ions to the steel-concrete interface. A number of mechanisms by which chlorides break down the passive layer have been proposed, e.g., the chemical dissolution of the film [7], the built up of the metal holes at the film-substrate interface [8], and due to the high chloride concentration at the iron oxide-pore solution interface which leads to local acidification and pitting [9]. Leek and Poole [10], based on SEM-EDS studies of passive film breakdown on steel in mortar prisms, have shown that chloride ions initiate reinforcement corrosion by breaking the bond between the film and the steel.

2.1.1 Basic Principles of Corrosion

The most common form of reinforcement corrosion in aqueous medium is of an electrochemical nature in which the corroding metal behaves like a small electrochemical cell. It requires an anode (where oxidation takes place), a cathode (where reduction occurs), an electrical conductor (steel reinforcement) and an

electrolyte (concrete). At the anode, metallic iron goes into solution by oxidation (loss of electron).

$$Fe \rightarrow Fe^{++} + 2e^{-} \qquad \text{(Oxidation)} \qquad (2.1)$$

At the cathode, dissolved oxygen in the pore water is reduced by electrons supplied by the anodic reaction to form hydroxyl ions:

$$\tfrac{1}{2}O_2 + H_2O + 2e^{-} \rightarrow 2OH^{-} \qquad \text{(Oxygen reduction)} \qquad (2.2)$$

$$Fe^{++} + 2OH^{-} \rightarrow Fe(OH)_2 \qquad (2.3)$$

The OH^- flows back to the anode through the concrete to complete the circuit. The rate of this transfer depends on the temperature, moisture content, ionic concentration and electrical resistivity of concrete. The OH^- at the anode can then combine with the Fe^{++} as in Equation 2.3 to form a fairly soluble ferrous hydroxide, $Fe(OH)_2$. Figure 2.1 schematically represents the mechanisms of reinforcement corrosion.

If sufficient oxygen is available, this product can be further oxidized to form insoluble hydrated red rust. Depending on the type of oxide formed, the rust can have a volume 2 to 10 times of the parent iron from which it is formed, as shown in Figure 2.2. The rust product can exert tensile stresses of the order of 4000 psi, which is 10 times the tensile strength of concrete. This excessive pressure causes

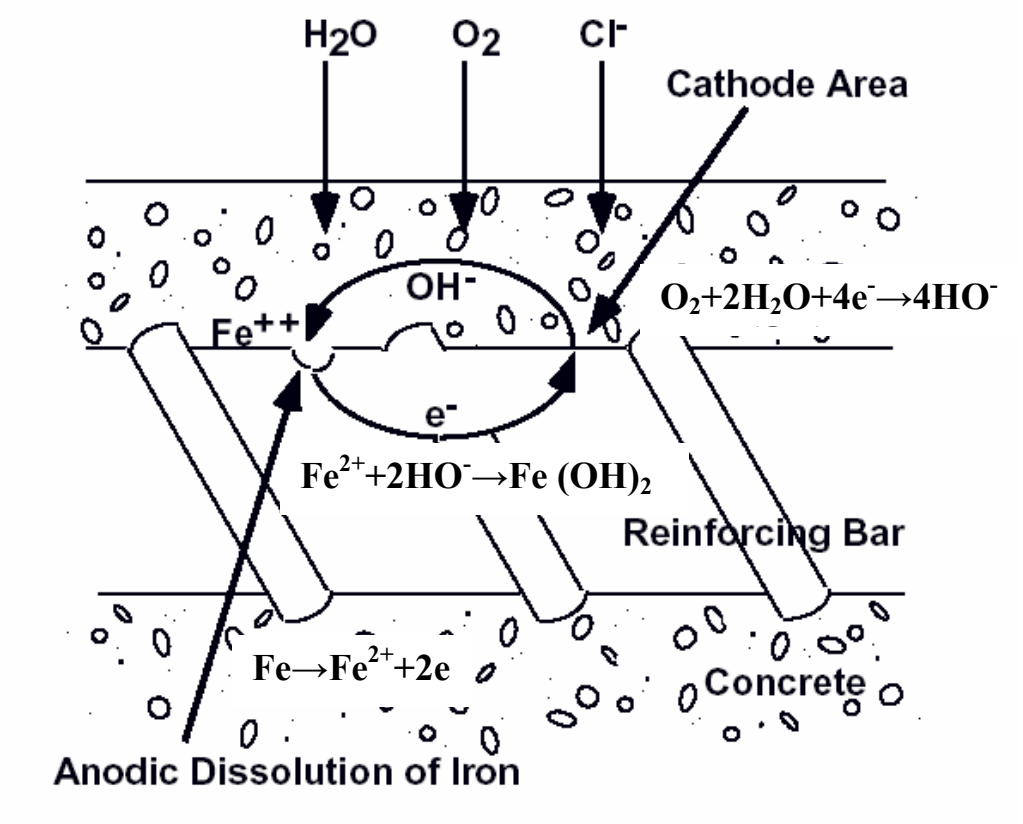

Figure 2.1: Schematic representation of the mechanics of reinforcement corrosion.

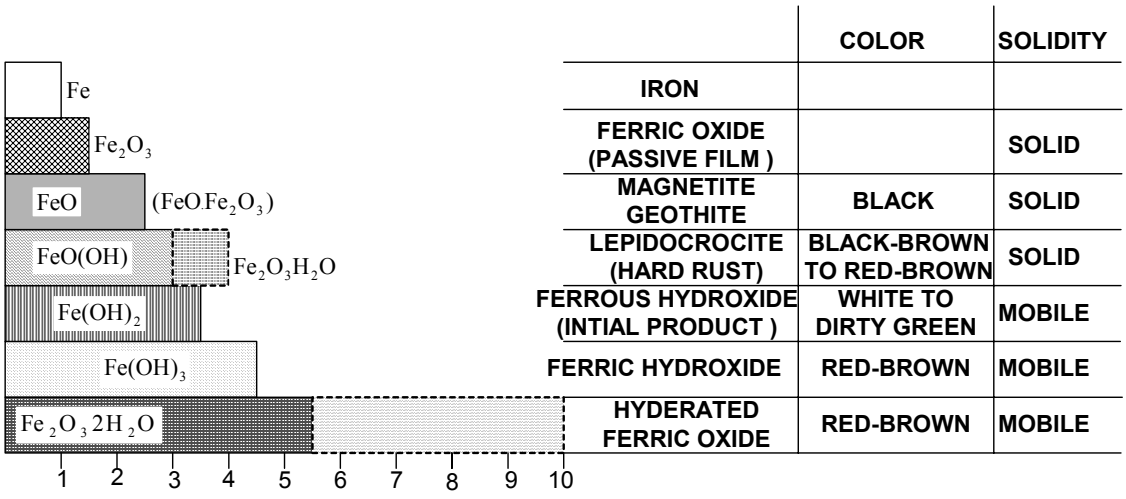

	COLOR	SOLIDITY
IRON		
FERRIC OXIDE (PASSIVE FILM)		SOLID
MAGNETITE GEOTHITE	BLACK	SOLID
LEPIDOCROCITE (HARD RUST)	BLACK-BROWN TO RED-BROWN	SOLID
FERROUS HYDROXIDE (INTIAL PRODUCT)	WHITE TO DIRTY GREEN	MOBILE
FERRIC HYDROXIDE	RED-BROWN	MOBILE
HYDERATED FERRIC OXIDE	RED-BROWN	MOBILE

Figure 2.2: Volume of various oxides formed due to corrosion of iron

the concrete cover to crack leading to its eventual spalling off at an advanced stage of the corrosion process, leading to a reduction in the cross-sectional area of the structural member. Hence, it can be noted that oxygen and moisture are the two most important ingredients for reinforcement corrosion to occur and the ingress of these elements through the concrete must be controlled to avoid corrosion.

2.1.2 Chloride Induced Reinforcement Corrosion

The role of chloride ions in inducing reinforcement corrosion is not very well understood. Chloride ions enter into the concrete from the service environments. Alternative sources include: chloride containing admixtures which are used to accelerate curing, contaminated aggregates, mixing water, air born salts, salts in ground water, and salts in chemicals that are applied to the concrete surface. The chloride ions from these sources slowly penetrate into the concrete, mostly through the pores in the hydrated cement paste. The chloride ions will eventually reach the steel and at a certain concentration level the protective film is destroyed and the steel begins to corrode, when oxygen and moisture are present at the steel-concrete interface.

Almost all researchers believes that corrosion of steel in concrete proceeds at a far greater rate in the presence of chloride ions, they act as an essential catalyst in the corrosion reaction. The chloride ions initiate the corrosion reaction by depassivating the natural oxide film on the steel surface, allowing the iron to dissolve into solution. On reaching the iron substrate, the chloride ions oxidize the iron to form $FeCl_3$ and that draws its unstable ferrous ion into solution, where it

reacts with the available hydroxyl ions to form $Fe(OH)_2$. This releases the Cl^- back into the solution and consumes the hydroxyl ions, as seen in the following reactions:

$$2Fe + 6Cl^- \rightarrow 2FeCl_3^- + 4e^- \quad (2.4)$$

$$2H_2 + O_2 + 4e^- \rightarrow 4OH^- \quad (2.5)$$

$$FeCl_3^- + 2OH^- \rightarrow Fe(OH)_2 + 3Cl^- \quad (2.6)$$

The electrons released in the oxidation reaction, as shown in Equation 2.4, flow through the steel to the cathode. This process results in an increase in the concentration of the chloride ions and a reduction of the pH at the points of corrosion initiation, probably accounting for the process of pitting corrosion. Equation 2.6 indicates that three chloride ions are released as a by-product of steel corrosion indicating that once the chloride ions reach the metal surface, no further chloride ions are required and depending on the electrical resistivity of concrete either general or local corrosion proceeds. It can be noted that for the chloride-induced reinforcement corrosion to proceed, the presence of moisture and oxygen is necessary.

Further, concrete acting as a conducting medium has a wide variation in the electrical resistivity. The resistivity values ranging from about 10 to 10,000 k.Ω.cm have been reported by researchers studying concrete with different moisture contents. An increase in temperature, moisture and ions, such as chloride ions results in a large drop in the resistivity. High water-cement ratio, chloride-bearing

saturated concrete provides the lowest resistivity to corrosion current, while low water-cement ratio, well-cured, dry concrete provides the highest. Chloride ions also cause a shift of potential of the steel. Non-uniform penetration of chloride ions to the level of the steel produces differences in potential and leads to the formation of “macro” corrosion cells. Non-uniform penetration is a general occurrence, and results from such factors as variations in concrete cover and local differences in concrete quality.

Another form of chemical protection provided by cement to reinforcing steel is its ability to bind chlorides. The chemical compound that is primarily responsible for chloride binding is tricalcium aluminate (C_3A). The chloride ions react with tricalcium aluminate in cement paste to form tricalcium chloroaluminate ($C_3A.CaCl_2.10H_2O$) also known as “Friedels salt”.

The chloride ions play a dominant role in the initiation of reinforcement corrosion. From this perspective, ACI 318 limits the water-soluble chlorides to 0.15% by weight of cement. ACI Committee 224, adopting a more conservative approach, has suggested that the acid-soluble chloride content should not be more than 0.2% by weight of cement. The British Standard, BS 8110 allows a maximum total chloride content of 0.4%. Rasheeduzzafar et al. [11] indicated that the chloride threshold limits for cements with up to 8% C_3A agree very well with the ACI 318 limit of 0.15% water-soluble chlorides. However, they reported that the ACI, BS and Australian code limits are conservative for concrete prepared with high C_3A cements.

Recent research findings have shown that cement alkalinity also significantly influences the chloride binding and hence the volume of free chlorides [12-15]. Taking into account the parallel effect of chlorides and alkalinity, Hausmann [16] suggested that the critical Cl^-/OH^- ratio is about 0.6. Gouda [17] indicated that the Cl^-/OH^- ratio was 0.3 based on the pH values of the electrolyte representative of the concrete pore solution.

Mangat and Moloy [18] indicated that a universal threshold Cl^-/OH^- ratio is not applicable to different cement concretes. In their investigations, reinforcing steel corrosion was observed in the control matrix when the pore fluid Cl^-/OH^- was 13. Al-Amoudi et al. [19] reported minimal reinforcement corrosion in silica fume and blast furnace slag cement mortar specimens placed in the aggressive environment of sabkha, even at Cl^-/OH^- ratios of 3.3 and 6.5, respectively.

2.1.3 Effect of Sulfate Ions on Reinforcement Corrosion

The effect of sulfate salts on the corrosion of reinforcement has not been adequately investigated. In marine environment and sabkha soils, chlorides and sulfate salts are present together and considerably affect concrete durability. Studies conducted by Holden et al. [20] on the pore solution composition of pastes prepared with fixed quantities of chlorides and sulfates indicates an increase in the OH^- ion concentration due to inclusion of sulfates as compared to the alkalinity of pore solution of cement contaminated with similar quantities of chloride salts alone. Their results showed substantial decrease in the chloride-binding capacity of

cements in which sodium chloride and sodium sulfate were mixed. These results reflect the tendency of sulfates ions to reacts preferentially with the C_3A phase, thus inhibiting the formation of Friedel′s salt. Thus, corrosion risk is likely to be significantly increased in circumstances where concrete is subjected to both chloride and sulfate salts.

Al-Amoudi and Maslehuddin [21] investigated reinforcement corrosion in cement paste specimens immersed in chloride, sulfate, and chloride plus sulfate environments. The results of this study indicated that while the sulfate ions are hardly able to induce reinforcement corrosion, considerable corrosion activity was observed in the concrete specimens immersed in chloride plus sulfate solution. The reinforcement corrosion increased when the sulfate concentration in the 15.7% chloride solution was increased from 0.55 to 2.10%. An extension of this study the plain and blended cement concrete specimens indicated a similar trend [22]. The effect of sulfate concentration, associated with fixed chloride level, was observed to be more pronounced on the corrosion rate, while no systematic trend was observed on the time to initiation of reinforcement corrosion.

Dehwah et al. [23] conducted an experimental investigation to study the combined effect of sulfate and chloride on reinforcement corrosion. They [23] reported an increase in reinforcement corrosion in the concrete contaminated with sodium chloride plus sodium sulfate in comparison to those contaminated with only sodium chloride only. They [23] reported that the presence of sulphate ions in the chloride solution increased the corrosion current density, but no significant effect on the time to initiation of reinforcement corrosion. Further, the corrosion current

density increased with increasing the sulfate concentration and the period of exposure. The corrosion current density on steel in the blended cement concrete specimens was much less than that in the plain cement concrete specimens, indicating that the corrosion resistance of blended cements was much better than that of plain cements.

2.1.4 Carbonation-Induced Corrosion

Carbonation is the result of interaction of carbon dioxide gas in the atmosphere with the alkaline hydroxides in the concrete. Like many other gases, carbon dioxide dissolves in water to form acid, as shown in Equation 2.7. Unlike most other acids the carbonic acid does not attack the cement paste, but just neutralizes the alkalis in the pore water, mainly forming calcium carbonate as in equation 2.8. There is a lot more calcium hydroxide in the concrete pores that can be dissolved in the pores water. This helps maintain the pH at its usual level of around 12. The presence of alkaline materials such as K^{++}, Na^{++} increases the pH of the pore solution to more than 13.5. However, as the carbonation reaction occurs eventually all the locally available calcium hydroxide reacts with CO_2, precipitating the calcium carbonate and allowing the pH to fall to a level where steel will corrode.

$$CO_2 + H_2O \rightarrow H_2CO_3 \quad (2.7)$$

$$H_2CO_3 + Ca(OH)_2 \rightarrow CaCO_3 + 2H_2O \quad (2.8)$$

In concrete of reasonable quality, that is properly consolidated and has no cracking, the expected rate of carbonation is very low. The rate of carbonation in concrete is directly dependent on the water/cement ratio (w/c) of the concrete, i.e., the higher the ratio the greater is the depth of carbonation in the concrete. For example, in concrete with w/c of 0.45 and concrete cover 25 mm (1 in.), it will require more than 100 years for carbonation to reach the concrete immediately surrounding the steel. Carbonation of moderate to good quality concrete is a slow process, and becomes significant in structures that are many decades of age, or exposed to environments containing high concentrations of carbon dioxide.

Carbonation damage occurs most rapidly when there is little concrete cover over reinforcing steel. Carbonation can occur even when the cover depth to reinforcing steel is high, this may be due to a very open pore structure where pores are well connected together and allow rapid carbon dioxide ingress. It may also happen when alkaline reserves in the pores are low. These problems occur when there is low cement content, high water cement ratio and poor curing conditions.

The carbonation induced reinforcement corrosion is less prevalent than chloride-induced reinforcement corrosion in the Arabian Gulf. Carbonation of concrete to an advance stage, sometime to the rebar level, is not uncommon due to the environmental conditions of the Arabian Gulf which is marked by the elevated ambient temperature (40 °C and above) and relative humidity (50 to 80%). These temperatures and humidity regimes are particularly suitable to accelerate corrosion process. There is a general agreement that carbonation is maximum at a relative humidity between 50 and 70%.

Carbonation of the hardened cement paste in which bound chlorides are present has similar effect of freeing the bound chlorides and thus increasing the risk of corrosion. The harmful effect of carbonation is in addition to the lowering of the pH value of the pore water so that severe corrosion may well follow. It has also been found in the laboratory testes that the presence of even small amount of chlorides in the carbonated concrete enhances the rate of corrosion induce by the low alkalinity of the carbonated concrete. Maslehuddin et al. [24] evaluated carbonation in plain and blended cements contaminated with chloride and sulfate salts. The data indicates higher carbonation in the contaminated specimens than in the uncontaminated specimens.

Hobbs [25] conducted as investigation into the influence of 35% replacement of one normal Portland cement by two fly ashes. He concluded that both water retention and strength development characteristics of fly ash concrete might be adversely affected by short-term curing than those of normal Portland cement concretes. He further concluded that the depth of carbonation in concretes of similar water-binder ratio or similar binder content could be higher in fly ash concrete than in normal Portland cement concretes.

2.1.5 Source of Chlorides

Chlorides ions are often unintentionally inducted into concrete through the constituent materials, such as salt-contaminated aggregate or mixing and curing water and admixtures utilized to modify the properties of the fresh or hardened concrete. Marine structures are exposed to seawater that invariably contains

chloride ions. Bridge decks, roads, parking garages are exposed to deicing salts that contribute the chloride ions. Chloride salts may also be present in ground water or in the soils.

The ingress of chlorides into concrete requires a continuous network of the capillary pore system, the coarse pore system of the aggregate/matrix interface and microcracks provide the path along which the transport of ions occurs. The diffusion of chlorides into the concrete occurs by different physical mechanism such as, the permeation of the salt solution, the capillary absorption of chloride-containing liquids, and the diffusion of the free chloride ions. Moreover, they may diffuse the hardened concrete when exposed to aggressive environment.

2.2 IMPROVING CONCRETE QUALITY

Concrete durability can be improved by many options such as: application of coating over concrete, use of concrete inhibitors, coated reinforcement and utilizing good quality concrete. The option of utilizing quality concrete is the cheapest compared to other measures. By using appropriate mix design, good consolidation and curing, quality and grading of aggregates, and reducing the water/cement ratio, a good quality or high performance concrete can be produced.

A significant reduction in the area of cross-section of a member is possible due to the use of high strength concrete. However, it should be realized that an increase in concrete strength may not proportionately influence its durability.

Therefore, concrete is now specified in terms of water permeability and diffusion indices rather than strength alone.

The use of the new generation concrete “high performance concrete” (HPC) has already gained wide importance all over the world. In HPC, not only there is a reduction in water to cement ratio (using of high range water reducers, etc.), but also the use of pozzolans, such as silica fume or ultra fine fly ash, results in the formation of a dense micro-structure and reduction in the relatively weak transition zone between the aggregate surface and hydrated cement paste that normally prevails in any cement concrete. Significant improvements in durability through the use of such materials will result in structures with longer life and lower maintenance costs.

High-performance concrete involves many ingredients that must be properly proportioned and mixed if the desired benefits are to be obtained. Mixture proportioning is a complex process requiring knowledge of the interaction of cements, natural pozzolans, slag, fly ash, silica fume, air-entraining admixtures, and high-range water-reducing admixtures; for the desired workability, strength, durability and finish.

2.3 ROLE OF AGGREGATE QUALITY ON REINFORCEMENT CORROSION

The aggregate characteristics play a major role in determining the properties of hardened concrete particularly the HPC. Aggregates occupy about 70% to 80% of concrete by volume [26], therefore, it’s not surprising that its quality is of

considerable importance. Aggregates were originally viewed as inert materials. In fact, aggregate is not truly inert and its physical, thermal and sometimes chemical properties influence the performance of concrete, as aggregates with undesirable properties cannot produce strong concrete.

Aggregates are cheaper than cement and it is economical to put into the mix as much of the aggregates and little of cement as possible. But economy is not the only reason for using aggregates; it confers considerable technical advantages to concrete, which has a higher volume stability and better durability than hydrated cement paste.

Aggregates must conform to certain standards for optimum engineering use. They must be clean, hard, strong, durable, free of absorbed chemicals, coating of clay and other fine materials in amounts that could affect hydration and bond with the cement paste. Aggregate particles that are friable or capable of being split are undesirable. The essential requirement of an aggregate for concrete is that it remains stable within the concrete and in the particular environment throughout the design life of the concrete.

Classification of aggregates can be made into normal weight, light weight and high density aggregates. High density aggregates are used for the production of concrete in high radiation areas where massive structures are needed. Light weight aggregates are always characterized by a high porosity, which results in a low apparent density. Light weight aggregate can be classified into natural and artificial

categories. The structural concrete made of light weight aggregate is approximately 20% lighter than the normal concrete.

Aggregate characteristics can be divided into two groups: physical features (particle size and shape and texture) and quality features (strength, density, porosity, hardness, elastic moduli, chemical and mineral composition, etc.) smaller size aggregates produce high strength concrete, and the particle shape and texture affect the workability of fresh concrete and the strength of hardened concrete. Properties, such as the particle size and shape, which are influenced by selective crushing and the use of the appropriate type of crusher for the particular rock type, as well as the cleanliness in terms of fines and clay content, have great influence on the water requirement of the concrete. The strength and durability properties of hardened concrete may also be affected by any change in the water demand.

The aggregate in concrete mainly affect its workability, unit weight, elasticity and strength to a large extent, these properties depend on the grading and the proportions of fine and coarse aggregates. The chemical or mineralogical characteristics of the aggregates are less important than the physical characteristics, such as shape and size of particles, and distribution of voids within a particle. With regard to concrete durability and reinforcement corrosion, the behavior of the interface between concrete and aggregate is of major concern.

Micro-cracks are likely to initiate between the coarse aggregate particles and cement paste zone. As a consequence, the interfacial zone has a much higher porosity than the hydrated cement paste. It is a vital contributing factor to concrete

permeability. Thus, theoretically, owing to different binding capacity at aggregate and cement paste interface, physical characteristics, such as size, shape and surface roughness, have a great effect on concrete durability and reinforcement corrosion. Aggregate with strong physical and chemical bonds with Portland cement paste while having similar thermal expansion would contribute to better durability.

Weathering due to wetting and drying can also affect the durability of aggregates. The expansion and contraction coefficients of aggregates vary with temperature and moisture content. If alternate wetting and drying occurs, severe strain develops in some aggregates, and with certain types of rock, this can cause a permanent increase in volume of the concrete and eventual breakdown (e.g., clay lumps, shale). Quartz and feldspar aggregate along with limestone, dolomite, and granite are considered low-shrinkage aggregates; and aggregates with sandstone, shale, slate, hornblende, and greywacke are often associated with high shrinkage in concrete

The effect of coarse aggregate characteristics on the properties of concrete has been studied by many researchers [27-29]. The relevant characteristics studied are: cleanliness, grain size, gradation, shape, texture and chemical reactivity. Also, the effects of mineralogical characteristics on concrete properties were investigated. Zhang and Gjorv [30] investigated the effect of four coarse aggregate types, available in North California, on the compressive strength and elastic behavior of a very high strength concrete mixture. Durability and mechanical properties such as, compressive strength, tensile strength, modulus of elasticity and stress-strain

behavior, of high strength of concrete made using local aggregate was studied by Beshr [31].

2.4 ROLE OF BLENDED CEMENTS ON REINFORCEMENT CORROSION

Pozzolanic materials, such as fly ash, silica fume, blast furnace slag, are often used as a partial replacement of cement or fine aggregate in concrete mixtures. A pozzolan is defined as a siliceous or siliceous and aluminous material which in itself possesses little or no cementing property, but which will, in a finely divided form and in the presence of moisture, chemically react with calcium hydroxide at ordinary temperatures to form compounds possessing cementitious properties [4].

Pozzolanic materials are often industrial by-products and are generally less expensive than cement. Their use in concrete is beneficial from an economic point of view and from an environmental perspective. In addition, the use of pozzolans as a partial replacement for cement improves the durability characteristics of the concrete. This is accomplished through an overall pore size refinement and a densification of the transition zone between the cement paste and the coarse aggregate. This results in less micro-cracking and a less permeable concrete.

Hardened concrete consists of solid phases and voids. Solid phases include hydrated cement paste (HCP), aggregate, and transition zone - a layer between the aggregate and cement paste. The transition zone is about 20 μmm thick and is characterized by a higher void content than the bulk paste. Among the solid constituents of concrete, it is the transition zone that has the greatest influence on

concrete strength, elastic modulus, durability and permeability. At early ages, ettringite and calcium hydroxide form in the transition zone making this layer weak and porous. If mineral admixtures are incorporated into concrete, calcium hydroxide further reacts with the supplementary materials and forms calcium silicate hydrate (C-S-H), which reduces the transition zone thickness, makes it denser, and thus less permeable.

In Portland cement concrete, the high alkalinity of the pore solution affords protection to embedded reinforcing steel by the formation of a protective passive layer. In addition, calcium hydroxide, a hydration product of Portland cement, acts as a buffer maintaining the high alkalinity in the pore solution, thus preserving the passivation on the reinforcing steel. Low permeability of the concrete restricts chloride ingress and carbonation, either of which will depasivate embedded steel and lead to corrosion. Blended cements may be used to decrease the permeability of the concrete without compromising pore solution alkalinity.

Durability of concrete to aggressive environment is generally a direct function of its permeability. Manmohan and Mehta [32] observed that highly reactive pozzolans, such as rice husk, silica fume, are able to reduce the size of voids in hydrated cement pastes, thus making them almost impermeable even at an early age. Mehta and Gjorv [33] confirmed the pore-refining capability of silica fume when present in normal concrete. Hustad and Loland [34] investigated the permeability of concrete containing condense silica fume and concluded that there is a significant effect on permeability.

Corrosion of steel in concrete is an electrochemical process requiring the presence of electrolyte moisture and air. In the presence of chlorides, when the passive film somehow gets disrupted, the electrical resistivity of the concrete plays an important role in protecting the steel from further corrosion. Gjorv [35] showed that the Ohmic resistance of concrete substantially increased by increasing the silica fume dosage. Al-Amoudi et al. [36] studied the performance of blended cements in resisting reinforcement corrosion when exposed to chloride-sulfate environments. They showed that the corrosion current density on the steel in fly ash, blast furnace slag and silica fume cement concrete specimens was 3,13, and 120 times lower than that in the ordinary Portland cement concrete specimens.

Byfors [37] conducted investigation into the chloride diffusion characteristics of paste samples prepared from silica fume and fly ash cement blends. He found that silica fume and fly ash inclusion considerably reduces the chloride diffusion rate. By conducting measurement of pH in extracted pore solution, he concluded that although mineral addition reduced the pH, the addition of silica fume or fly ash in appropriate quantities could significantly extend the chloride diffusion and chloride-initiated reinforcement corrosion.

2.5 ROLE OF FIBERS IN IMPROVING CORROSION-RESISTANCE OF CONCRETE

High performance concrete is a brittle material when compared with normal concrete. To overcome this drawback, fibers are normally included in concrete to improve its ductility. Fiber-reinforced concrete (FRC) is made primarily of

hydraulic cements, aggregates, and discrete fibers. The role of the randomly oriented, discrete, discontinuous fibers is to reduce the cracks that develop in concrete either at the time it is loaded or as it is subjected to environmental changes. If the fibers are strong enough, are appropriately bonded to the matrix, and are there in sufficient quantity, they will help keep the crack widths small and permit the concrete to carry significant stresses over a relatively large strain capacity in the post-cracking stage. The addition of steel fibers to the high performance concrete matrix changes the basic characteristics of its stress-strain behavior [38]. Compared with normal strength concrete, the slope of the descending part of the stress-strain curve lengthens with increasing the fiber content. With the addition of a reasonable amount of fibers to concrete, higher ductility and toughness can be achieved.

The fibers will not improve the strength of the concrete in any significant way. Moreover, the fibers cannot compensate for deficiencies in the concrete mix design or in the curing procedures. Fibers cannot, in general, be used to simply replace the conventional steel reinforcement. Steel bars are placed at specific locations in the structural members, to withstand the design tensile, shear or compressive loads. Fibers are not very effective in this regard, since they are randomly distributed throughout the matrix. The prime function of the fibers is to control matrix cracking, and to enhance the bond between the FRC and the conventional steel reinforcement, if used together. Thus, fibers and steel reinforcement should be seen as complementary, rather than competing materials.

Compressive strength is little influenced by the steel fiber addition with observed increases ranging from 0 to 15 percent for up to 1.5 volume percent of fibers [39]. The tensile strength increases after cracking, if steel fibers are added. When using steel fibers in concrete, attention has to be given to the corrosion of fibers. As the steel volume locally is very small when fibers are used, only limited expansion forces develop due to corrosion and normally no spalling occurs. Steel fibers in the immediate surface layer rapidly corrode to the depth of surface carbonation, which might however give aesthetical defects in the form of rust colored surfaces. Steel fibers are less susceptible to corrosion than conventional reinforcing bars, as they are electrically discontinuous.

2.6 SERVICE LIFE PREDICTION MODELS

2.6.1 Stages in Reinforcement Corrosion

Corrosion of steel in concrete takes place in three distinct stages namely; initiation stage (depassivation), activation stage (propagation), and final stage (deterioration) [40], as schematically shown in Figures 2.3 and 2.4. Depassivation is the loss of oxide (passive) layer over the rebar, which is initially formed due to the high alkalinity of concrete. The process of depassivation takes an initiation period, t_p, which is the time from construction to the time of initiation of corrosion (depassivation).

The propagation phase starts from the time of depassivation, t_p, to the final state**,** is reached at a critical time, t_{cr}, at which corrosion would produce spalling of

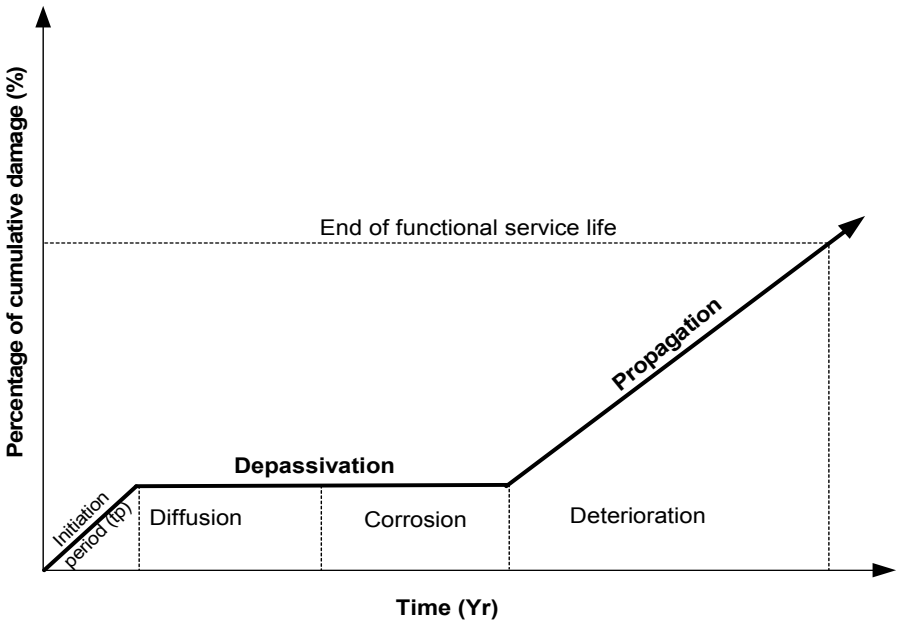

Figure 2.3: Deterioration processes of a concrete element

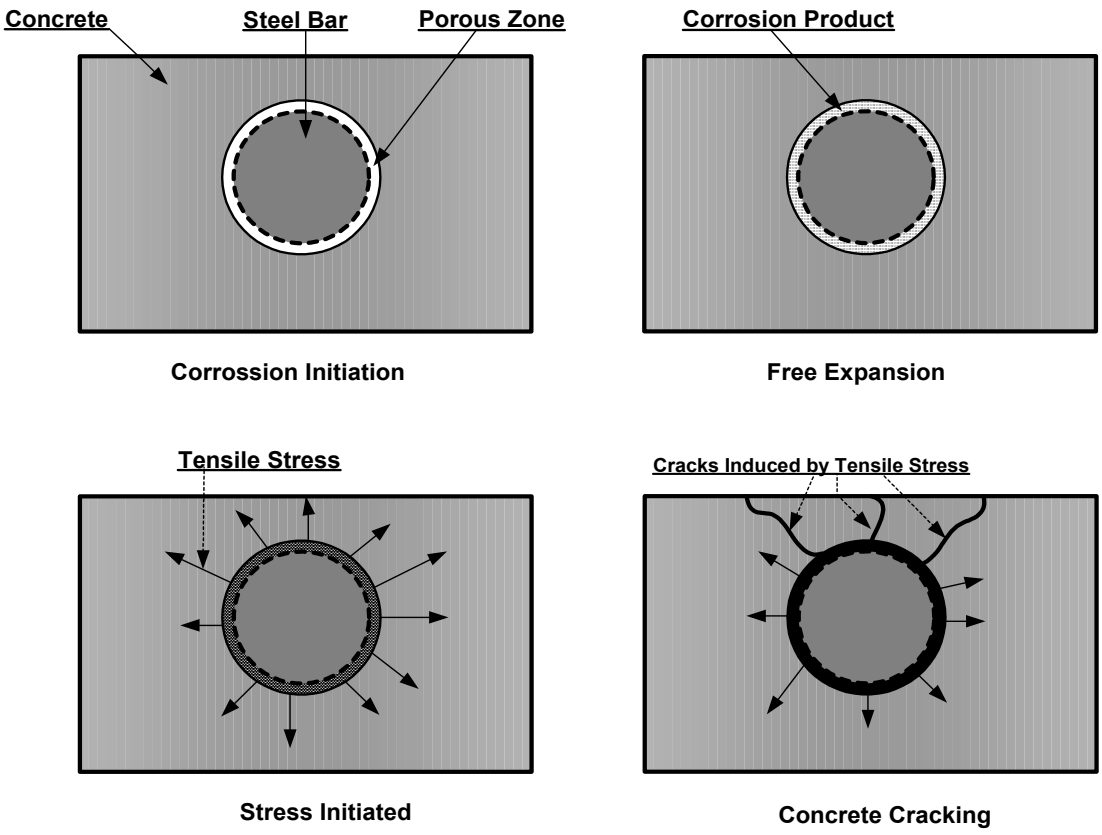

Figure 2.4: Schematic diagram of corrosion cracking processes

concrete cover or cracking through the whole of concrete cover. During the propagation period, i.e., corrosion period, t_{cor}, which begins at the moment of depassivation, the rebar corrosion rate is usually assumed to be in a steady-state.

2.6.2 Deterioration Modeling

The service life of a structure is determined largely by its durability properties and existing environmental conditions. Every structure is to be designed for dead, live and special loads so that its load-carrying capacity is not exceeded. Poor condition of numerous existing offshore and under-water structures points out to a requirement for developing a design procedure that will consider environmental and durability conditions. Environmental loads can be included in the existing design procedures and thus have an effect on the material and geometrical properties to insure an adequate service-life of the structure. Environmental loads are those that initiate or accelerate the deterioration processes of materials, especially the corrosion of steel in concrete. Besides cracking and spalling of the concrete cover, environmental loads cause reduction of the cross sectional area of a reinforcement bar which can result in a loss of the section bearing capacity.

The average service-life of bridges in the United States, including rehabilitation and the component replacement, was estimated to be 70 years. Major rehabilitation of a bridge takes place when the structure is about 35 years old [41]. The design life for buildings and other structures in Europe is 50 years, while bridges are expected to last 120 years [42]. Under these conditions, predicting the

service life of concrete structures became an important subject in making the most cost-effective decisions concerning future management of these structures.

There are several ways of predicting service life due to the corrosion damage of reinforcement in concrete using different deterioration models. Several researchers have documented the processes of diffusion of chloride, oxygen and moisture through concrete, and their effects on corrosion initiation and subsequent rate of concrete deterioration [43]. Cady and Weyers [44], based on field and laboratory data, have developed a model to estimate the time to rehabilitate concrete bridge decks. Tuutti [45] has presented conceptual models for predicting the effective service life of reinforced concrete members, when chloride-related corrosion is considered as the primary deterioration mechanism. Bazant [46] has developed a mathematical model of predicting reinforcement corrosion. Empirical equation for predicting the time to cracking has been suggested by Morinaga [47]. Wang and Zhao [48] have suggested a method using finite element analysis to determine the thickness of corrosion product. Dagher and Kulendran [49] have also carried out finite element modeling of corrosion damage in concrete structures. Ahmad et al. [50] suggested an experimental methodology for service life prediction based on cumulative damage theory.

Due to the complexity of the corrosion process in concrete, the observed data from the field and laboratory deviate significantly from existing models. The quantitative prediction of the time to cracking is useful for establishing the overall deterioration model to predict the service life. It is necessary to establish the quantitative relationships among those factors that control the time to cracking, and

thus the time to corrosion cracking of the cover concrete in reinforced concrete can be better predicted.

2.6.3 Bazant's Mathematical Models for Time to Cracking

Bazant [46] proposed a simplified mathematical model for predicting time-to-cracking of concrete cover for corrosion of reinforcement exposed to seawater. The model considered various chemical and physical phenomena regarding chloride-induced reinforcement corrosion, the basic assumptions of Bazant's model are as following:

- one-dimensional oxygen and chloride transport through concrete cover
- steady-state corrosion and rust production after depassivation
- density of original steel versus the rust product

Thus, Bazant [46] defined the time-to-cracking as a function of:

- electrochemical properties: corrosion rate
- dimensional properties: cover depth, bar spacing
- physical properties: density of steel, density of rust product
- mechanical properties of concrete: tensile strength, modulus of elasticity, Poisson's ratio, and creep coefficient.

The Bazant's [46] formula is a follows:

$$t_{cor} = \rho_{cor} \frac{D\Delta D}{pJ_r} \tag{2.9}$$

$$\text{and} \quad \rho_{cor} = \left[\frac{1}{\rho_r} - \frac{0.583}{\rho_{st}} \right]^{-1} \frac{\pi}{2} = 3.6\, gm/cm^3 \tag{2.10}$$

Where ***p*** is the perimeter of bar, ***D*** is the diameter of the bar, **Δ*D*** is the change in diameter of the bar, $\mathbf{J_r}$ is the rate of rust production, and $\boldsymbol{\rho_{cor}}$ is a function of the mass densities of steel and rust given by equation 2.10.

Equation 2.9 gives the simplified mathematical model for predicting time-to-cracking of concrete cover for corrosion of reinforcement exposed to seawater by Bazant. The value of ΔD can be obtained through number of techniques, it is here where various models differ. Bazant [46] has suggested a simple method, based on estimation of the pressure required at the surface of the bar to expand a cylindrical hole of diameter D by ΔD. The pressure required at the surface of the hole for homogeneous concrete to expand the diameter of hole by ΔD, has been assumed to be the average of the pressure required for a hole in an infinite medium and that required for a thick-wall cylinder of diameter $D+2C_v$, where C_v is the cover thickness to rebar. ΔD can be expressed as $\delta_{pp}p_r$. Where δ_{pp} is bar hole flexibility and p_r is the pressure at the surface of the bar. The value of δ_{pp} is taken as the average of the two bar hole flexibilities as given below.

$$\delta_{pp}^{o} = (1+\nu) D / E_{ef} \tag{2.11}$$

$$\delta_{pp} = \left[1 + \nu + \frac{D^2}{2C_v\left(C_v + D\right)}\right] D / E_{ef} \tag{2.12}$$

$$E_{ef} = E/\left(1 + \phi_{cr}\right) \tag{2.13}$$

Using the average bar hole flexibility, δ_{pp} and from the equilibrium conditions at failure which required that the average tensile stress on the crack surface, generated by the pressure equals to the tensile strength of concrete f_t, the critical value of ΔD that produces inclined cracks or cover spalling is given by:

$$\Delta D = 2 f_t^t \frac{C_v}{D} \delta_{pp} \quad \text{(for inclined cracks)} \tag{2.14}$$

$$\Delta D = f_t^t \left(\frac{s}{D} - 1\right) \delta_{pp} \quad \text{(for cover spalling)} \tag{2.15}$$

According to Bazant's model, the time to cracking is a function of corrosion rate, cover depth, spacing, and certain mechanical properties of concrete such as tensile strength, modulus of elasticity, Poisson's ratio and creep coefficient. A sensitivity analysis of Bazant's theoretical equations demonstrates that for these parameters, corrosion rate is the most significant parameter in determining the time to cracking of the cover concrete. Unfortunately, Bazant's model has never been validated experimentally.

2.6.4 Morinaga's Model

Based on field and laboratory data, the empirical equations suggested by Morinaga [47] can be used for predicting the time to cracking. It is assumed that

cracking of concrete will first occur when there is a certain quantity of corrosion product that is formed on the reinforcement. The amount is given by:

$$Q_{cr} = 0.602\left(1+\frac{2C_v}{D}\right)^{0.85} D \tag{2.16}$$

Where: Q_{cr} is the critical mass of corrosion products (10^{-4} g/cm^2);

Cv is the cover to the reinforcement (mm)

D is the diameter of reinforcing bar (mm).

The time for cracking to take place is given by:

$$t_{cor} = \frac{Q_{cr}}{J_r} \tag{2.17}$$

$$J_r = \left(\frac{W}{F}\right) I_{corr} \tag{2.18}$$

Where J_r (gm/cm^2/day) is the instantaneous corrosion rate. The electrochemically measured value of I_{corr} can be converted to the instantaneous corrosion rate, J_r, through Faraday's law equation 2.18. W is the equivalent weight of steel (27.925 gm) and F is Faraday's constant (96487 Coulombs (or Amp-sec)). According to Morinaga's equations, the time to cracking is a function of the corrosion rate, concrete cover and bar size. Therefore, the time to cracking can be easily predicted.

The two models presented above i.e., Bazant's mathematical model and Morinaga's empirical equation is based on the steady state corrosion process to calculate the time to cracking. It should be noted that the corrosion process is a dynamic process and electrochemical process, and is strongly dependent on the environmental factors (temperature, relative humidity, etc) and properties of

concrete structure. These factors act simultaneously on the corrosion process in the service conditions. The influences of these factors on the corrosion process should be considered as an interaction among them. The interaction model for corrosion has not been sufficiently studied due to the lack of the long-term corrosion data in the field. Most of the research work on accelerated corrosion tests is limited to the effects of the individual variables. In fact, these factors can not be separated or isolated from each other in the service conditions. The actual metal loss required to cause cracking of concrete has been a subject of disagreement among the researchers for years. A wide range of cracking criteria has been presented for different situations and conditions.

2.6.5 Experimental Method of Service Life Prediction

An experimental methodology, suggested by Ahmad et al. [50], for service life prediction based on cumulative damage theory is described below: If a reinforced concrete specimen is allowed to corrode for a time duration, L_c, at its natural corrosion rate, I_{corr}, from the time of depassivation, t_p, onward and then the same is subjected to an impressed anodic current, I_a, up to the time of cracking, t_{cor}, of cover concrete, then according to the cumulative damage theory, one can write the following equation:

$$\frac{L_c}{L_t} + \frac{L_a}{L_l} = 1 \qquad (2.19)$$

Where:

$\frac{L_c}{L_t}$ = fraction of damage due to the natural corrosion

$\frac{L_a}{L_l}$ = fraction of damage due to externally applied current

L_a = the time taken by the specimen for its complete damage under the effect of external current being applied after the natural corrosion that had already taken place;

L_l = the time taken by the specimen for its complete damage under applied current alone excluding the effect of natural corrosion;

L_c = duration of the natural corrosion, starting from the time of depassivation of rebar to the date of application of external current; and

L_t = the total life of specimen against corrosion cracking of cover concrete.

The values of L_a and L_l may be obtained through an accelerated corrosion test by applying anodic current to rebar of a core-shaped corroding reinforced concrete specimen, either cast in laboratory or obtained from a corroding structure. The failure tensile stress of concrete, F_0, of the reinforced concrete specimen under splitting, is determined.

After applying the anodic current, I_a, for a time period of T, the failure tensile stress of concrete, F_T, of the reinforced concrete specimen under splitting, is to be determined. Then the value of L_a may be determined using the following equation, derived by Ahmad et al. [50]:

$$L_a = \frac{F_c \quad f\left(\frac{C_v}{D}\right)}{E.\ I_a\ K_1} \tag{2.20}$$

Where:

$f(C_v/D)$ = a function of the ratio of cover thickness, C_v, to the rebar diameter, D

The above ratio function is given as:

$$f\left(\frac{C_v}{D}\right)=\frac{4.72\left(\frac{C_v}{D}\right)^2+4.72\left(\frac{C_v}{D}\right)+1}{\left(\frac{C_v}{D}\right)+1} \tag{2.21}$$

E = modulus of elasticity of concrete,

K_1 = a constant, which may be determined through the best fit of the following equation:

$$\frac{F_r}{F_o}=1-K_1\left(\frac{E\ T\ I_a}{F_a\ f\left(\frac{C_v}{D}\right)}\right) \tag{2.22}$$

Then the value of L_l may be determined using the following equation, derived by Ahmad et al. [50]:

$$L_l=\frac{1}{K_2} \tag{2.23}$$

K_2 = a constant, which may be determined through the best fit of the following equation;

$$\frac{1}{L_a}=K_2+K_3*NCF \tag{2.24}$$

Where:

K_3 = a constant

NFC = natural corrosion factor, which is given by the following equation:

$$NCF = \frac{E\ L_c\ I_{corr}}{f_t^{/}\quad f\left(\frac{C_v}{D}\right)} \tag{2.25}$$

Where:

f'_t = cylindrical tensile strength of concrete

I_{corr} = corrosion rate of rebar in reinforced concrete specimen before the application of I_a

Substituting the above expressions of L_a and L_l in Eq. 2.19, the final expression for L_t may be obtained as:

$$L_t = L_c \Big/ \left[1 - \left(\frac{K_2}{K_1}\right)\left\{\frac{F_o f(C_v/D)}{E\ I_a}\right\}\right] \tag{2.26}$$

CHAPTER 3

METHODOLOGY OF RESEARCH

3.1 EXPERIMENTAL PROGRAM

The objective of this study is to evaluate the effect of the quality of local aggregates on the strength and reinforcement corrosion of concrete. To meet these objectives, selected aggregates were evaluated for strength characteristics by measuring the tensile strength and reinforcement corrosion characteristics were evaluated by measuring the chloride diffusion, corrosion potentials, corrosion current density and time to cracking due to accelerated corrosion. The other objective of this study was to evaluate the effect of silica fume and steel fibers in enhancing the properties of concrete and the effect of thermal variations on the strength and reinforcement corrosion.

The experimental program was thus designed to evaluate the above-mentioned objectives. Figure 3.1 shows the experimental variables adapted to evaluate the effect of aggregate quality on the properties of concrete.

3.2 MATERIALS

The following three types of aggregates were utilized to prepare concrete specimens required for this study.

1. Limestone aggregates from quarries in Abu-Hadriyah,
2. Limestone aggregates from quarries on Riyadh road, and
3. Steel slag aggregates.

Table 3.1 shows the absorption and specific gravity of the selected coarse aggregates. The gradation of the coarse aggregate based on ASTM C 33 is shown in Table 3.2. Dune sand was used as the fine aggregate. Table 3.3 shows the absorption and specific gravity of the fine aggregates.

ASTM C150 Type I Portland cement was utilized in preparing the concrete specimens. Silica fume (8% by weight of the cementitious material) and steel fibers (1% by volume of concrete) were used to enhance the strength and durability of concrete. Table 3.4 shows the chemical composition of the Portland cement and silica fume.

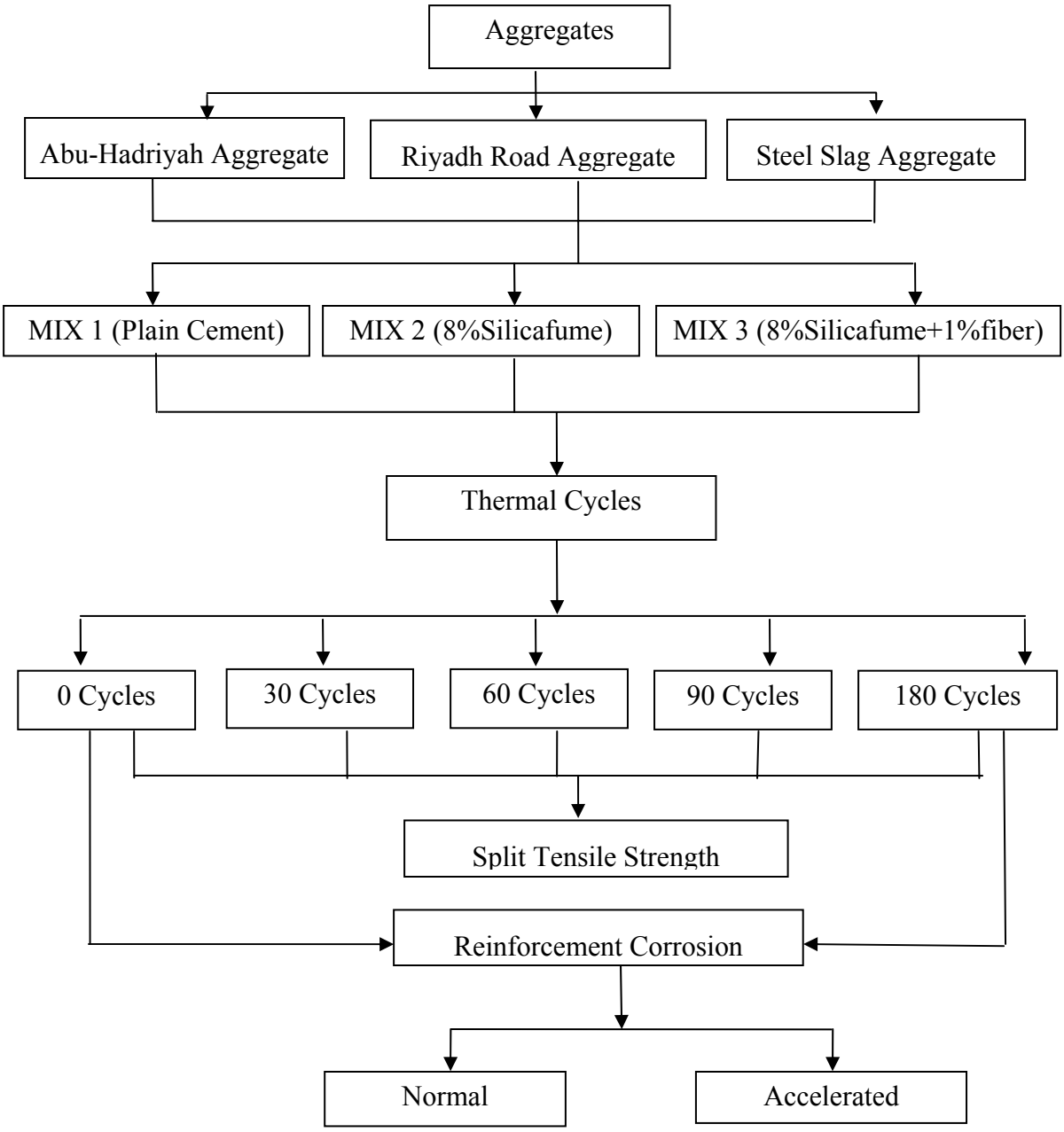

Figure 3.1: Flow chart showing the experimental program

Table 3.1: Absorption and specific gravity of coarse aggregates

Aggregates	Absorption (%)	Bulk Specific Gravity
Lime Stone (Abu-Hadriyah)	2.20	2.54
Lime Stone (Riyadh Road)	1.6	2.70
Steel Slag	0.85	3.51

Table 3.2: Grading of the coarse aggregates used in the preparing concrete specimens

Size	Percentage Passing
3/4”	100
1/2”	50
3/8”	30
3/16”	10
3/32”	0

Table 3.3: Absorption and specific gravity of fine aggregates

Absorption (%)	Bulk Specific Gravity
0.653	2.54

Table 3.4: Chemical composition of Portland cement and silica fume

Constituents (wt %)	Type I cement	Silica fume
SiO_2	19.92	98.7
Al_2O_3	6.54	0.21
Fe_2O_3	2.09	0.046
CaO	64.70	0.024
MgO	1.84	-
SO_3	2.61	0.015
K_2O	0.56	0.048
Na_2O	0.28	0.085
C_3S	55.9	-
C_2S	19	-
C_3A	7.5	-
C_4AF	9.8	-

3.3 CONCRETE SPECIMENS

Two types of concrete specimens were utilized to evaluate the effect of aggregate quality on reinforcement corrosion. Concrete cylinders measuring 75 mm in diameter and 150 mm high were used to evaluate the tensile strength and chloride diffusion. While reinforced concrete cylinders of 75 mm in diameter and 150 mm high with centrally placed steel bars of 12 mm diameter, were used to evaluate reinforcement corrosion. Epoxy paint was applied to the bar at the end of the bar and at the interface between the concrete to avoid the initiation of corrosion at those critical locations, as shown in Figure 3.2.

3.4 PREPRATION OF CONCRETE SPECIMEN

3.4.1 Concrete Mix Specification

Concrete mixes were designed according to absolute volume method, and proportioning of materials was carried out on weight basis. A concrete mix with cementitious materials content of 450 kg/m^3, effective water to cementitious materials ratio of 0.35 and, coarse to fine aggregate ratio of 1.63 were utilized in all the concrete mixtures. All the above-mentioned parameters were kept constant in all the concrete mixtures. Superplasticizer was used to improve the workability of the concrete mixes, as the water to cementitious ratio was low. Table 3.5 shows the dosages of superplasticizer Gleinum 51, utilized to attain the slump of 75±25 for this study.

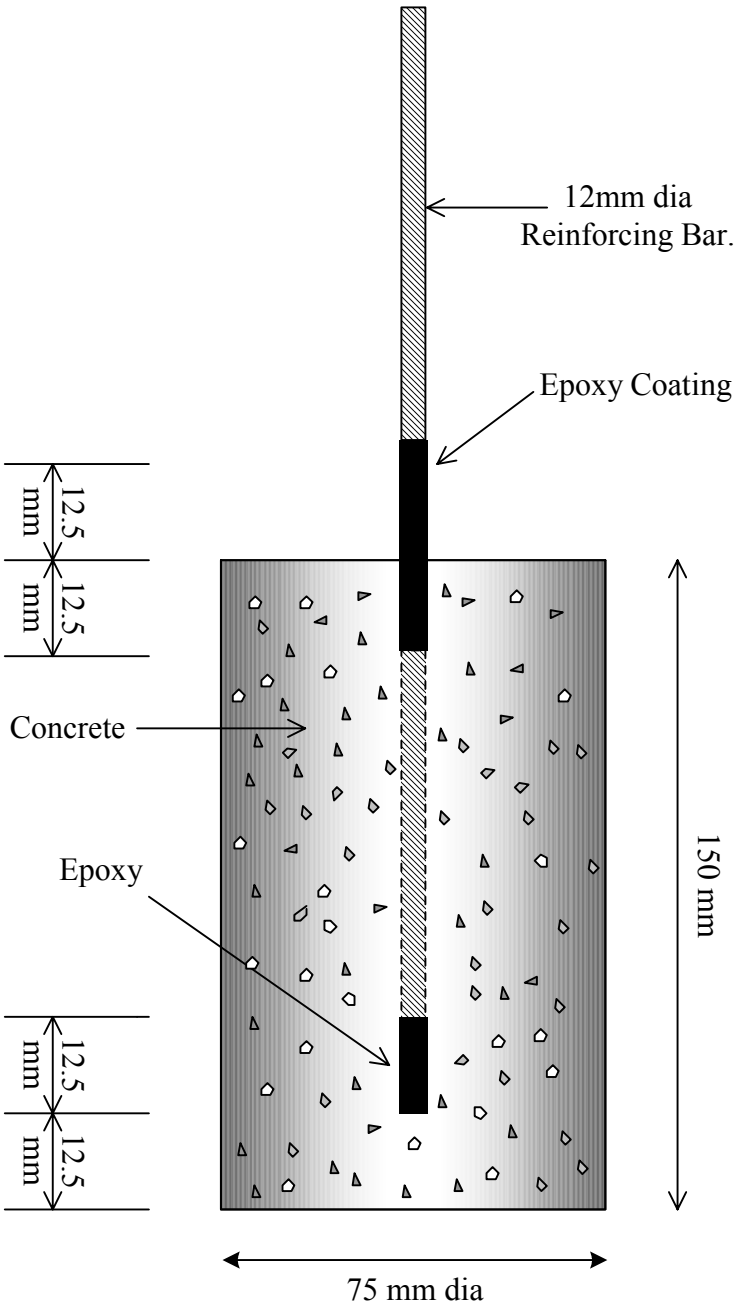

Figure 3.2: Concrete specimen to be utilized to evaluate reinforcement corrosion

Table 3.5: Mix proportioning of concrete mixes

Mix type	Cement (kg/m^3)	Silica fume (kg/m^3)	Coarse aggregates (kg/m^3)	Fine aggregates (kg/m^3)	Steel fibers (kg/m^3)	Water (kg/m^3)	Superplasticizer (kg/m^3)
Abu-Hadriyah (Plain)	450	0	1140	699	0	181	0.20
Abu-Hadriyah (Silica fume)	414	36	1151	705	0	181	0.24
Abu-Hadriyah (Silica fume +fibers)	414	36	1069	650	78	181	0.35
Riyadh (Plain)	450	0	1140	699	0	173	0.31
Riyadh (Silica fume)	414	36	1151	705	0	173	0.35
Riyadh (Silica fume +fibers)	414	36	1069	650	78	173	0.40
Steel Slag (Plain)	450	0	1361	834	0	172	0.38
Steel Slag (Silica fume)	414	36	1374	843	0	172	0.38
Steel Slag(Silica fume +fibers)	414	36	1334	817	78	172	0.40

3.4.2 Mixing of Concrete and Specimen Casting

The concrete constituents were mixed in a revolving drum type mixer for approximately three to five minutes to obtain uniform consistency. Additional mixing time of two to five minutes was provided to silica fume cement concrete mixes to disperse the silica fume uniformly. After mixing, concrete was filled in cylindrical moulds in three layers and the moulds were vibrated over a vibrating table to remove entrapped air.

3.4.3 Curing

After casting, the concrete specimens were cured for 28 days in a curing tank under laboratory conditions. Following the curing period, some of the specimens were kept in an oven, while the other specimens were tested to evaluate reinforcement corrosion, tensile strength and chloride diffusion.

3.5 EXPERIMENTAL TECHNIQUES

3.5.1 Split Tensile Strength

The tensile strength of the concrete can be determined experimentally by the following three methods: (1) uniaxial tensile strength, (2) split cylinder test; and (3) beam test in flexure. The first method of obtaining the tensile strength is referred as a direct test for determining the tensile strength, while the second and third methods are indirect tests. The second method of obtaining the tensile strength was used to evaluate the effect of aggregate on tensile properties of concrete.

In the direct test, the specimen is gripped at its ends and pulled apart in tension, the tensile strength is the failure load divided by the area experiencing tension. It is very difficult to apply pure tension force, free from eccentricity. it is also difficult to avoid secondary stresses such as those induced by grips or by embedded studs. The flexure test (modulus of rupture test) and the splitting tensile test are the indirect methods of determining the tensile strength. In the flexure test, a rectangular beam is loaded at the center or at the third point till the beam fails in bending, and the computed tensile stress at failure load is called the modulus of rupture. The modulus of rupture test gives a higher value of strength than the direct tension test made on the same concrete. In flexure test, the maximum fiber stress reached may be higher than that in direct tension because the propagation of a crack is blocked by less-stressed material nearer to the neutral

The indirect method of applying tension in the form of splitting was suggested by a Brazilian engineer [51], and the test is often referred to as the Brazilian test, although it was also developed independently in Japan. In this test, a concrete cylinder, of the type used for compression test, is placed with its axis horizontal between the plates of the testing machine and it is loaded in the compression on the plane between the loaded sides, and the specimens fails in tension an the plane between the loaded sides along the vertical diameter of the specimen. Any element on this vertical diameter is subjected to vertical compressive stress and the split tensile strength is calculated as follows.

$f_{sp}= 2P/ \pi LD$

Where f_{sp}= split tensile strength, N/mm^2

P= compressive load, N

L= length of the specimen, mm

D= diameter of the specimen, mm.

However, immediately under the load, a high compressive stress would be induced so a narrow strip of a packing material, such as plywood, or thin steel rod is used are placed between the cylinder and the plates of testing machine. Without packing strips, the recorded strength is lower, typically by 8 percent.

The split tensile strength is a more reliable technique to evaluate tensile strength of concrete (lower coefficient of variation) compared to other methods [51]. The most important advantage of this test is the approximated uniformity of the tensile stress over the diametral area of the cylinder and the simplicity of the test which affords the opportunity to test economically a large number of specimens. The split tensile strength of 75 mm diameter and 150 mm high concrete cylindrical specimens was determined according to ASTM C 496 to assess the effect of aggregate type, silica fume and fiber content on the tensile properties of the concrete. Figure 3.3 shows the experimental setup used for the split tensile test. The close-up view of the concrete specimen under split tensile testing is shown in Figure 3.4.

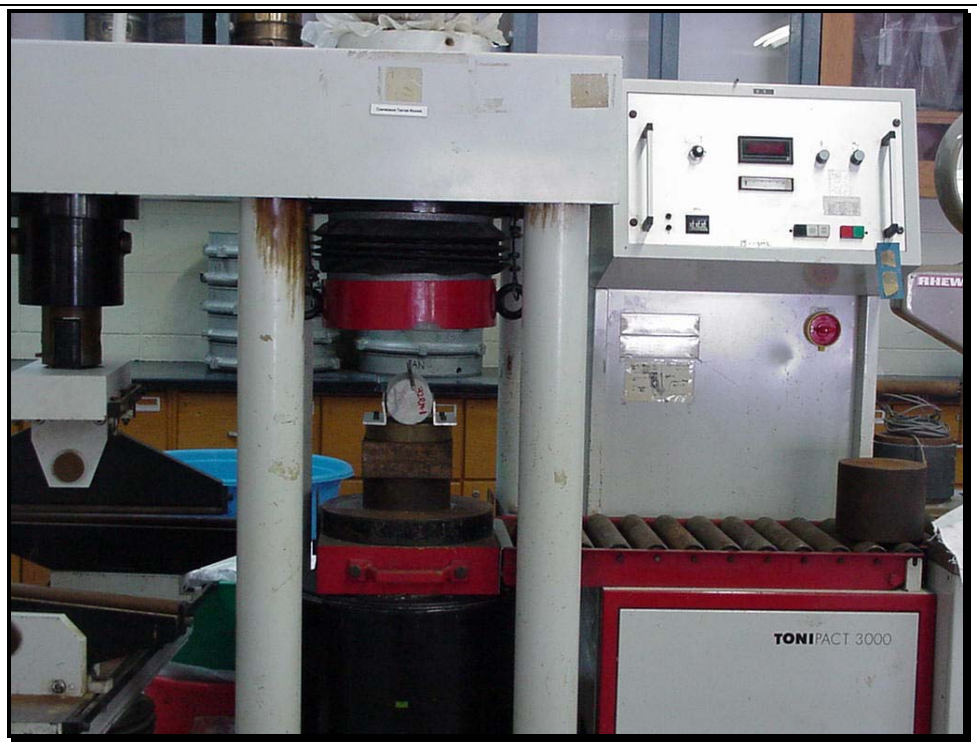

Figure 3.3: General view of split tensile test setup

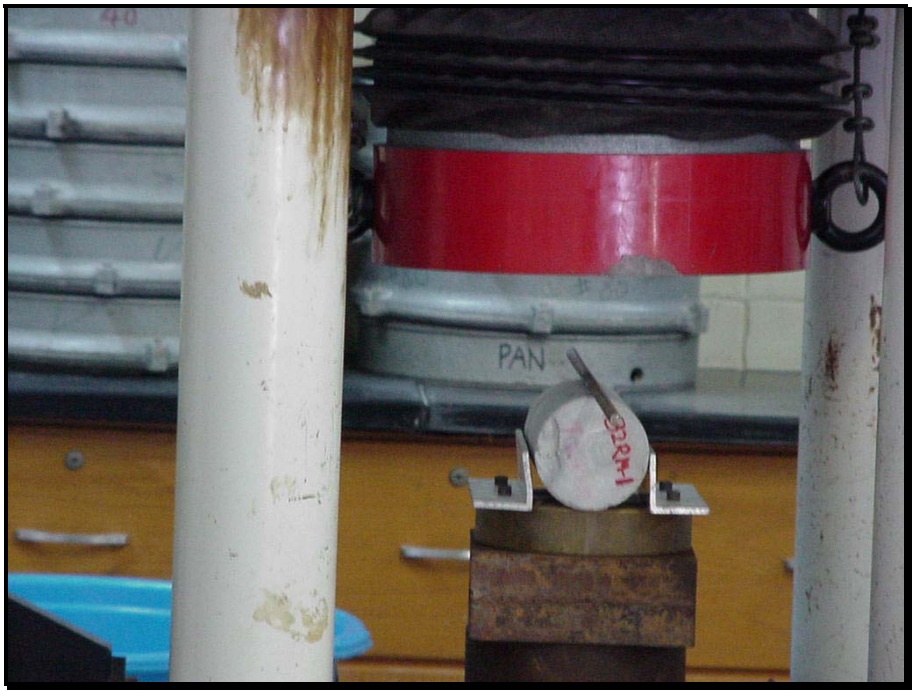

Figure 3.4: Close-up view of the split tensile strength test

3.5.2 Chloride Diffusion

The effect of aggregate quality on chloride diffusion in concrete was evaluated on cylindrical specimens. An epoxy coating was applied on the curved surface and on one face of 75 mm ϕ and 150 mm high cylinders. The other face was left uncoated, to ensure unidirectional flow of chloride ions and then they were immersed in 5% sodium chloride (NaCl) solution for three months, as shown in Figure 3.5. After this period, the specimens were removed and cleaned and concrete discs of 5 mm thickness were obtained at depths of 5, 20, 50, 75 and 100 mm. These discs were crushed to obtain concrete powder passing ASTM # 100 sieve. Five grams of the powder was placed in a beaker to which 50 ml of hot distilled water was added. The beaker was covered and the contents were allowed to cool for 24 hours. The mixture was then filtered into a flask and the filtrate was made up to 150 ml by adding more distilled water. 0.2 ml of this solution was added to 9.8 ml of distilled water using a pipette tip. Then, 2ml of 0.25 M ferric ammonium sulfate and 2 ml of mercuric thiocyanate were added to it. This solution was then poured into a test tube and the test tube was placed in spectrophotometer to measure the absorbance. A blank solution was prepared and its absorbance was also measured. The chloride concentration was calculated using the chloride calibration curve prepared earlier utilizing a chloride solution of known concentration.

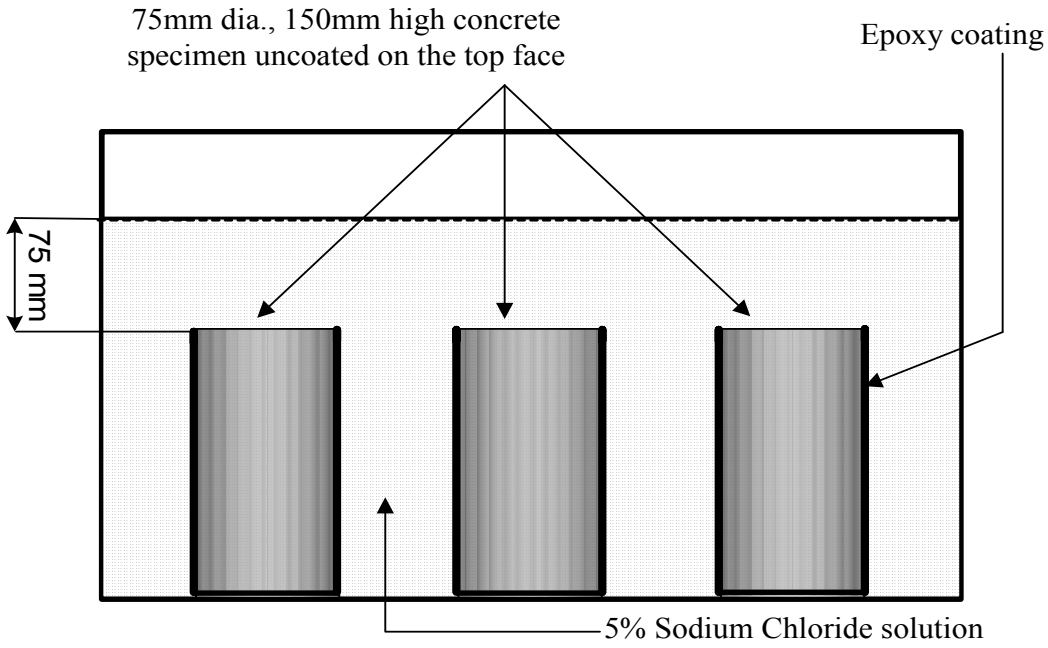

Figure 3.5: Setup for chloride diffusion testing

The chloride concentration was then plotted against depth. The coefficient of chloride diffusion in each of the selected specimens was determined from the chloride profile by solving Fick's second law of diffusion [52], as shown below.

$$\frac{C_x}{C_s} = 1 - \text{erf}\left\{\frac{x}{2\sqrt{D_e t}}\right\} \qquad (3.1)$$

where: C_x is the chloride concentration at depth x, %.
Cs is the chloride concentration at the concrete surface, %.
x is the depth from concrete surface, cm.
t is the time in seconds, and
D_e is the effective chloride difusion coefficient, cm^2/s.

3.5.3 Corrosion Potentials

Corrosion is an electrochemical process as described in Section 2.1.1. The process of corrosion causes electrical potentials to be generated and the half-cell provides a method of detecting and categorizing these electrical potentials. The method and equipment are presented in ASTM C 876 [53]. The measurement of the free corrosion potential of the reinforcement consists of determination of the voltage difference between the steel and reference electrode in contact with the concrete.

A good contact between the reference electrode and the concrete was ensured in order to minimize the Ohmic drops and avoid errors. The more negative the reading, the greater is the probability of corrosion. The significance of half-cell

readings and their relationship to potential for corrosion is well documented. The reference electrode used in this study was a Saturated Calomel Electrode (SCE).

3.5.4 Corrosion Current Density

Linear polarization resistance technique is used to measure the rate of corrosion of steel reinforcement [54, 55]. The test procedure is based on the Stern-Geary characterization of the typical polarization curve for the corroding metal. Here, a liner relationship is described mathematically for a region on the polarization curve in which slight changes in the current applied to the corroding metal in an ionic solution causes corresponding changes in the potentials of the metal. In other words, if a large current is required to change the potentials by an given amount, the corrosion rate is high and on the other hand, if only a small current is required, the corrosion rate is low [56].

In this test, three electrodes were used to measure the resistance to polarization (R_p) using a potentiostat\galvanostat. The steel rod is connected to the working electrode terminal while a steel plate and reference electrode are connected to the respective terminals of the potentiostat. The steel is polarized by applying a potential of ±10mV of the open circuit potential and the resulting current between the counter and working electrodes are measured. Figure 3.6 shows the schematic representation of set-up used to measure the corrosion current density. Figure 3.7 shows the general view of experimental setup and Figure 3.8 shows the close up view of test setup. The potentials are changed at a rate of 6 mV/min. and the resulting current is measured.

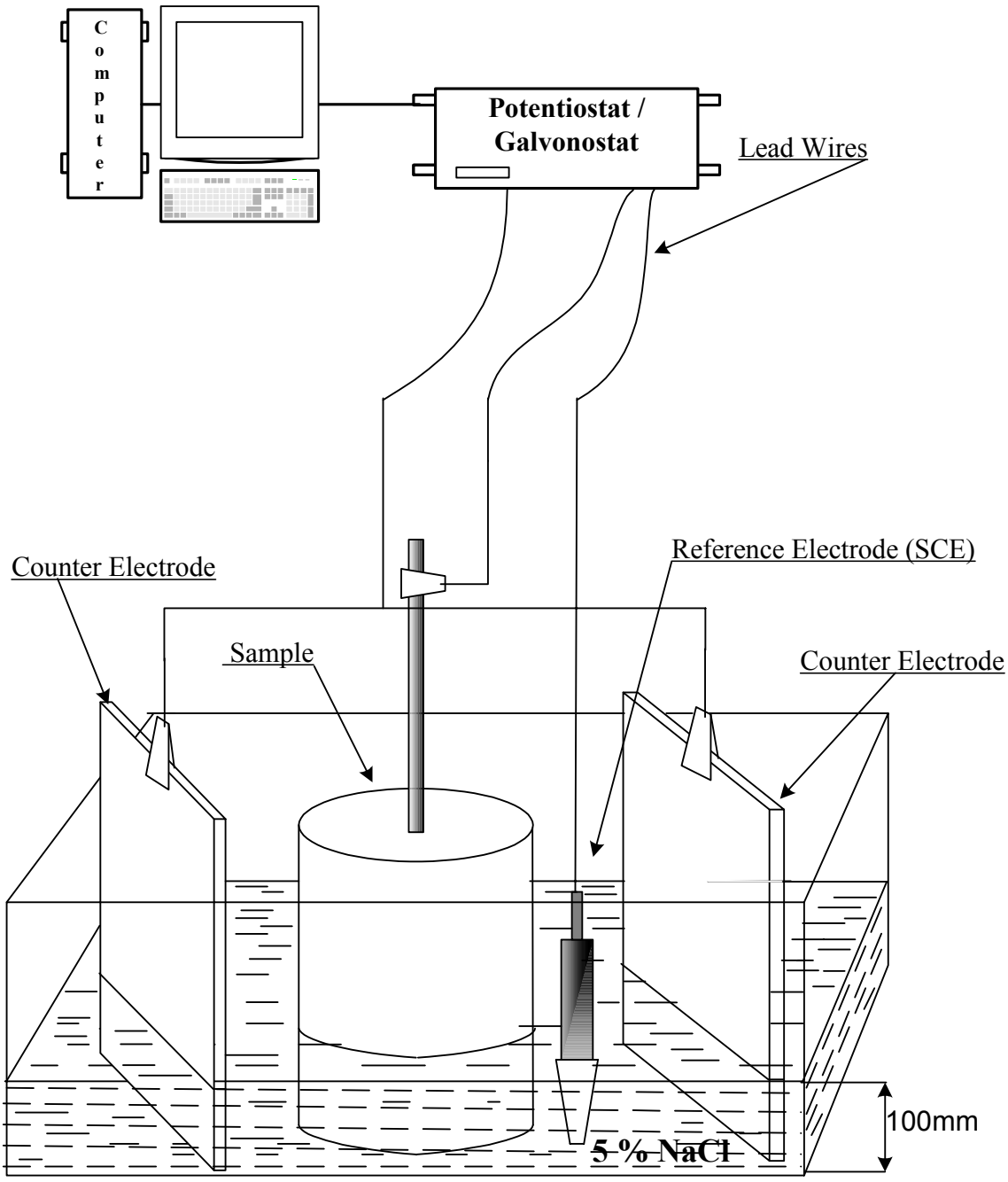

Figure 3.6: Schematic representation of the experimental setup used for corrosion current density measurements

Figure 3.7: General view of experimental setup for corrosion current density measurements

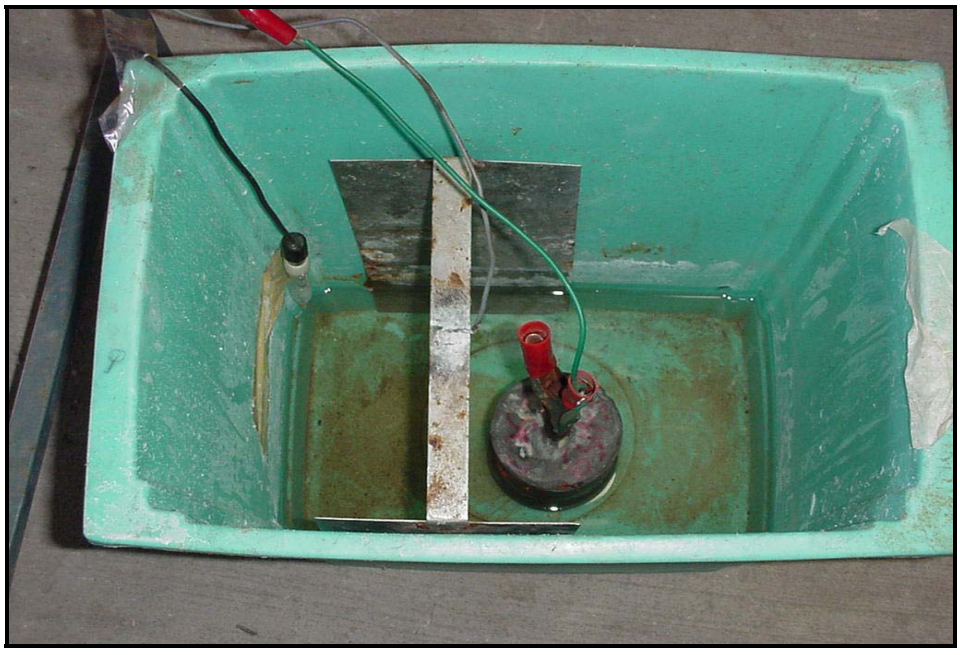

Figure 3.8: Close up view of corrosion current density test

The slope of the potential-current curve is Rp polarization. The corrosion current density is then calculated using the following relationship [57]:

$$I_{corr} = \frac{B}{Rp}$$

Where, I_{corr} = the corrosion current density, $\mu A/cm^2$

R_p = the linear polarization resistance, $\frac{\Delta E}{\Delta I}$ Ωcm^2

$$B = \frac{\beta_a \beta_c}{2.3(\beta_a + \beta_c)}$$

β_a = the anodic tafel constant

β_c = the cathodic tafel constant.

The Tafel constants can be determined by polarizing the steel to ±250 mV of the corrosion potential. In the absence of sufficient data on tafel constants, a value of 100 mV is to be used for steel in a highly resistant medium [58]. A good correlation between the weight loss determined by gravimetric methods and linear polarization technique was observed by Gonzalez et al [59] by using a B=26 mV for steel in the active state and B=52 mV in the passive state. In our investigation, $\beta_a = \beta_c = 120$ mV was used throughout, which corresponds to B=26 mV. Such values have been found to be useful in the corrosion experiments conducted at KFUPM.

3.5.5 Accelerated Corrosion

Cylindrical concrete specimens 75 mm in diameter and 150 mm high with embedded steel bars were cast. Epoxy paint was applied to the end of the bar and at the interface of concrete and air to avoid the initiation of corrosion at those critical locations. These specimens were then exposed to an accelerated corrosion environment by impressing an anodic potential of 2.5 Volts. For this purpose, the bars in the concrete specimens were connected to the positive terminal of a DC power supply, while a stainless steel plate was connected to its negative terminal. The current supplied to each of the specimen, due to the application of a potential difference of +2.5V, was monitored at 4 hours interval by measuring the potential drop over a 1 Ohm resistor. The two leads of the resistor were connected to a data acquisition system for monitoring the current. Figure 3.9 is a schematic representation of the experimental setup utilized to evaluate the corrosion resistance of concrete specimens and Figure 3.10 shows the test setup. The current supplied to each of the specimens was plotted against time and the time–current curves were utilized to evaluate the time to cracking of concrete due to reinforcement corrosion [60].

3.5.6 Thermal Variation

The temperature variation has significant effect on the durability of concrete. The thermal coefficient of concrete is a function of two main components i.e., thermal coefficient of aggregate and thermal coefficient of cement paste, both of

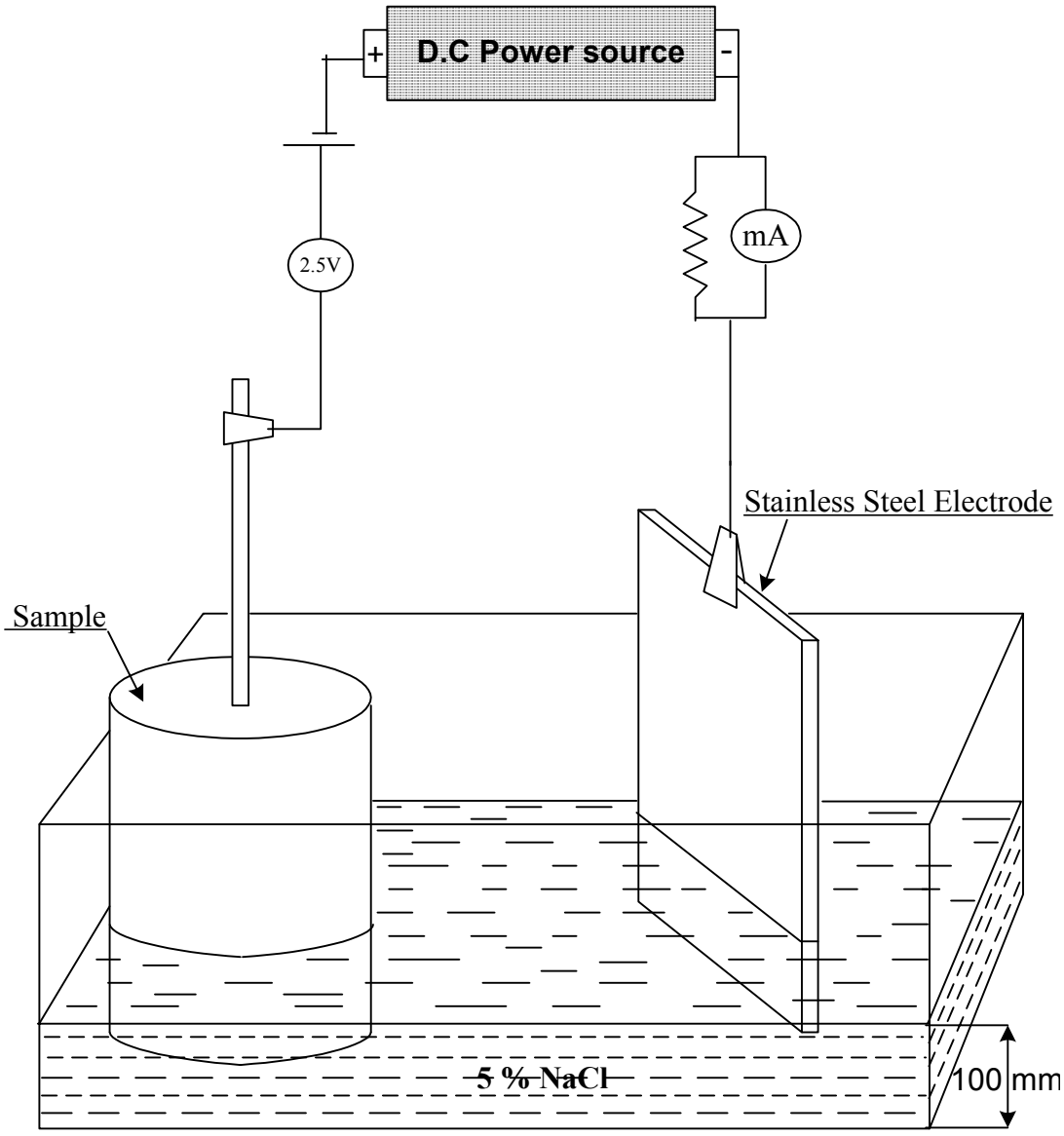

Figure 3.9: Schematic representation of the experimental setup utilized to accelerated reinforcement corrosion

Figure 3.10: Experimental setup utilized to accelerate reinforcement corrosion

these components have different thermal expansion coefficients. The significance of the difference in the coefficient would result in cracking of concrete and access to deleterious agents.

In order to evaluate the effect of thermal variation on the strength and durability of concrete made using the selected aggregate, the reinforced and plain concrete specimens were exposed to temperature variation. The concrete specimens were divided into two sets. One set of specimens was exposed to controlled laboratory conditions at room temperature, while the other set was stored in an oven, as shown in Figure 3.11, maintained at a temperature of 70 °C for 8 hours and then left for cooling for 16 hours.

After 30, 60, 90, and 180 cycles, the unreinforced specimens were removed and tested to study the effect of thermal variation on split tensile strength. The reinforced samples were removed after 120 cycles and divided into two sets. The first set was tested for normal corrosion by measuring the corrosion potentials and corrosion current density. The second set was tested for accelerated corrosion by applying the impressed anodic current.

Figure 3.11: Shows specimens exposed to thermal cycling

CHAPTER 4

RESULTS AND DISCUSSIONS

The selected local aggregates were utilized to prepare plain and reinforced concrete specimens. The plain concrete specimens were utilized to assess the effect of type of aggregate, silica fume and silica fume plus steel fibers on split tensile strength and chloride diffusion in concrete. Reinforced concrete specimens were utilized to evaluate the effect of aforesaid factors on reinforcement corrosion. The results obtained from the experiments conducted in this study are discussed in the following sections.

4.1 EFFECT OF AGGREGATE QUALITY ON THE TENSILE STRENGTH OF CONCRETE

The effect of aggregate quality on the split tensile strength of concrete was determined on 75 mm diameter and 150 mm high cylindrical concrete specimens after 28 days of curing under laboratory conditions. Figure 4.1 shows the effect of aggregate quality on the split tensile strength of plain cement concrete. The highest

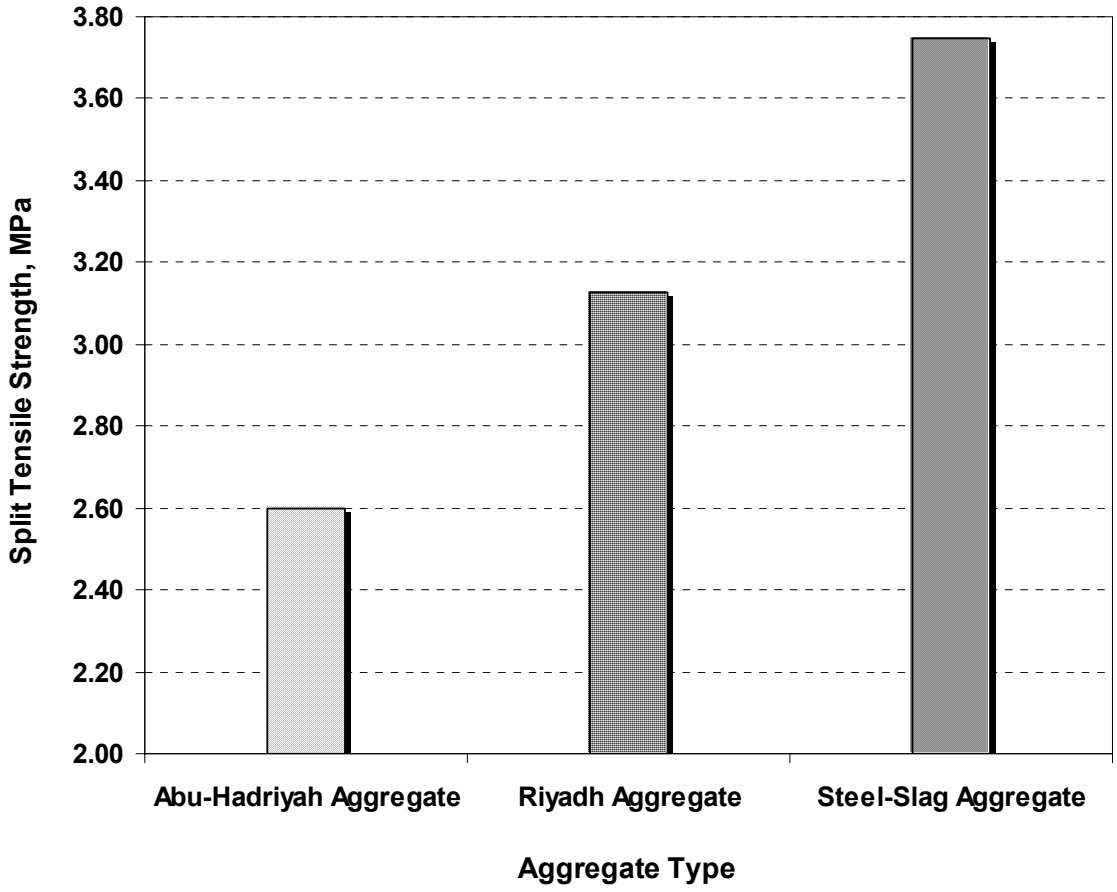

Figure 4.1: Effect of aggregate quality on the split tensile strength of plain cement concrete specimens.

split tensile strength of 3.75 MPa was noted in the steel slag aggregate concrete. The split tensile strength of Riyadh aggregate concrete was more than that of Abu-Hadriyah aggregate concrete; the values of split tensile strength in these concrete specimens were 3.12 and 2.60 MPa, respectively.

Figure 4.2 shows the effect of silica fume addition on the split tensile strength of concrete specimens prepared with the selected aggregates. In this case also, the split tensile strength of steel slag aggregate concrete was more than that of the concrete specimens prepared with the other two aggregates. Further, the split tensile strength of Riyadh aggregate concrete was better than that of Abu-Hadriyah aggregate concrete. The split tensile strength of concrete specimens prepared with steel slag aggregate, Riyadh aggregate and Abu-Hadriyah aggregate was 3.86, 3.14 and 2.75 MPa, respectively.

Figure 4.3 shows the split tensile strength of concrete specimens prepared with the selected aggregates and incorporating silica fume plus steel fibers. The addition of 1% steel fibers to the silica fume cement concrete has improved the split tensile strength of the concrete specimens prepared with the selected aggregates. The tensile strength of steel slag aggregate concrete was more than that of Abu-Hadriyah and Riyadh aggregate concretes. The split tensile strength of concrete specimens prepared with Abu-Hadriyah, Riyadh and steel slag aggregates was 3.16, 3.39 and 4.04 MPa, respectively.

The data in Figures 4.1 through 4.3 show that the quality of coarse aggregate significantly influences the tensile strength of concrete. This trend was noted in

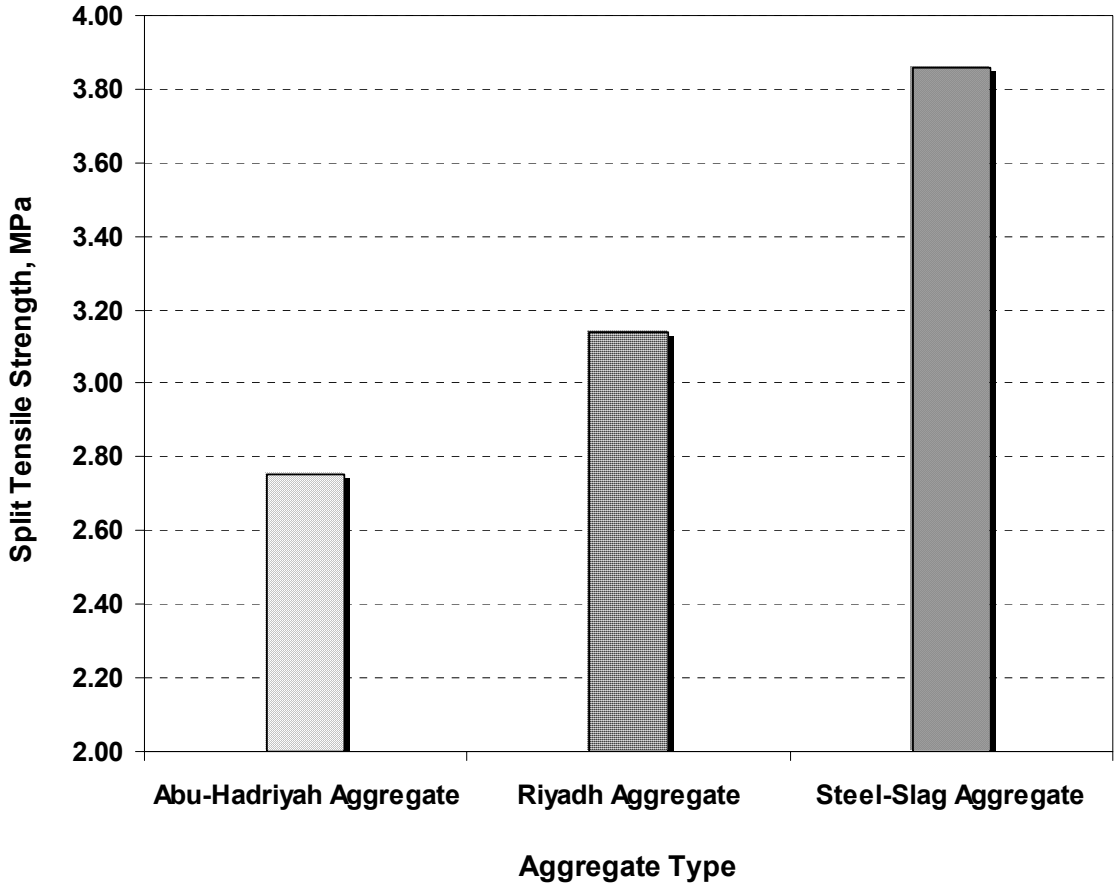

Figure 4.2: Effect of aggregate quality on the split tensile strength of silica fume cement concrete specimens.

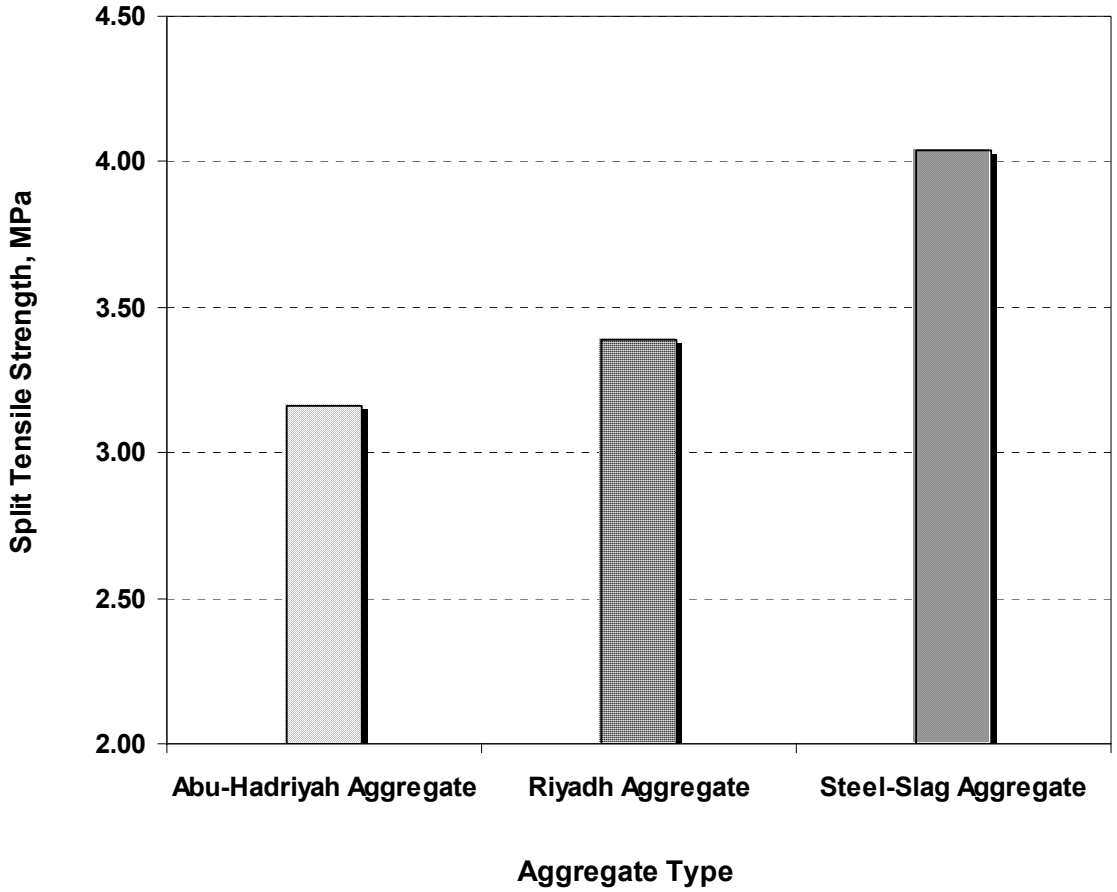

Figure 4.3: Effect of aggregate quality on the split tensile strength of concrete specimens prepared with silica fume plus steel fibers

plain, silica fume and steel fiber reinforced concrete. The percentage improvement in the split tensile strength of plain cement concrete when Riyadh and steel slag aggregates were used in lieu of Abu-Hadriyah aggregate was 20 and 44%, respectively. The percentage improvement in the split tensile strength of silica fume cement concrete specimens when concrete was prepared with Riyadh and steel slag aggregates instead of aggregates from Abu-Hadriyah was 14 and 40%, respectively. The percentage improvement in split tensile strength of the steel fiber cement concrete when Abu-Hadriyah aggregate was replaced by Riyadh aggregates or steel slag aggregates was 7 and 28%, respectively. The summarization of the percentage improvement in the split tensile strength when Riyadh and steel slag aggregate was used in place of Abu-Hadriyah aggregate is presented in Table 4.1.

When concrete is subjected to tensile stress, failure takes place at one or more of the following locations: (i) at the paste-aggregate interface, (ii) within the paste matrix or (iii) within the aggregate. In rich concrete mix, as the one utilized in this study, the possibility of failure within the paste matrix alone is very rare, since this phase is very strong due to the high cement content and low water to cement ratio. Therefore, the failure plain has to pass through either the paste-aggregate interface or through the aggregate. In both modes of failure, the quality of aggregate significantly influences the mode of failure of concrete under tension.

The higher tensile strength of concrete prepared with steel slag and Riyadh aggregates, compared to the concrete specimens prepared with Abu-Hadriyah aggregate, may be attributed to the quality of the aggregate. The limestone from

Table 4.1: Percentage improvement in the split tensile strength of concrete due to replacement of Abu-Hadriyah aggregate with Riyadh and steel slag aggregate

Mix Type	Aggregate Type	f_{sp} (MPa)	% Improvement
Plain Cement	Abu-Hadriyah	2.60	—
	Riyadh	3.12	20
	Steel Slag	3.75	44
Silica Fume Cement	Abu-Hadriyah	2.75	—
	Riyadh	3.14	14
	Steel Slag	3.86	40
Silica fume + Steel fibers	Abu-Hadriyah	3.16	—
	Riyadh	3.39	7
	Steel Slag	4.04	28

Abu-Hadriyah is capable of absorbing significant amount of water due to its porous structure. Hence, the cement-aggregate bond in this aggregate is better than that in the Riyadh and steel slag aggregate concretes. Thus, the failure of concrete prepared with aggregates from Abu-Hadriyah is supposed to be within the aggregate. In a study conducted on three different coarse aggregate in the concrete produced with a water to cement ratio of 0.24, Aitcin et al. [61] found that the aggregate-cement paste was stronger in the limestone concrete than in the gravel concrete due to the interfacial reaction effect.

Wu [62] investigated the effect of four different types of coarse aggregates on the split tensile strength of concrete and concluded that the impact of the type of coarse aggregate on the strength of concrete is more significant in the high strength concrete. In high-strength concretes investigated in his study [62], about 10 to 20% higher compressive and splitting tensile strength was obtained with crushed quartzite compared to marble aggregate. The results of split tensile test showed that the split tensile strength of concrete is influenced by the tensile strength of aggregates, particularly in high strength concrete. He [62] suggested that high strength concrete with lower brittleness can be prepared by selecting high-strength aggregate with low brittleness.

Figure 4.4 shows the effect of admixtures on the split tensile strength of concrete specimens prepared with limestone aggregate from Abu-Hadriyah. The split tensile strength of steel fiber reinforced concrete specimens was more than that of silica fume and plain cement concretes. The improvement in the split tensile strength of plain cement concrete prepared with Abu-Hadriyah aggregate due to

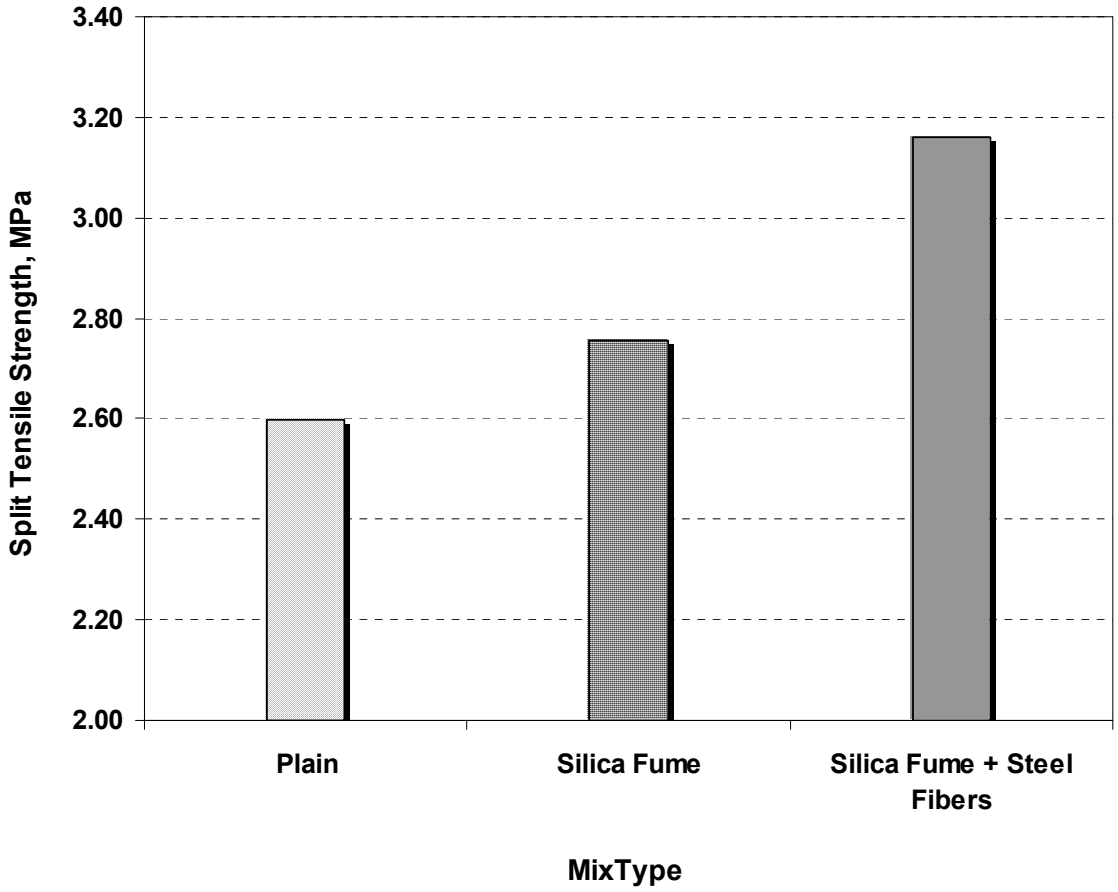

Figure 4.4: Split tensile strength of concrete specimens prepared with coarse aggregate from Abu-Hadriyah.

the addition of silica fume was 6% while it was 22% due to the addition of silica fume plus steel fibers.

Figure 4.5 shows the variation in the split tensile strength of concrete specimens prepared with Riyadh aggregate. The split tensile strength of silica fume and fiber reinforced cement concrete was more than that of plain cement concrete. The improvement in the split tensile strength of plain cement concrete prepared with Riyadh aggregate due to the addition of silica fume was negligible while it was 9% in the case of the steel fiber plus silica fume cement concrete.

The split tensile strength of concrete specimens prepared with steel slag aggregates is shown in Figure 4.6. The highest split tensile strength was noted in the steel fiber silica-fume cement concrete specimens. The split tensile strength did not improve significantly in the concrete specimens prepared with steel fiber silica-fume cement concrete. The improvement in the split tensile strength due to the addition of silica fume was 3% and it was 8% in the specimens prepared with the steel fiber silica-fume cement concrete.

The data depicted in the Figures 4.4 through 4.6 is summarized in Table 4.2, which indicate that the incorporation of silica fume and steel fibers to plain cement concrete improves its split tensile strength. The improvement in the split tensile strength of silica fume cement concrete may be related to the reaction between $Ca(OH)_2$ and silica fume. Silica fume reacts with $Ca(OH)_2$ in the presence of moisture to form additional C-S-H. This forms a basis for improvement of both the strength and durability of concrete. The higher split tensile strength of silica fume

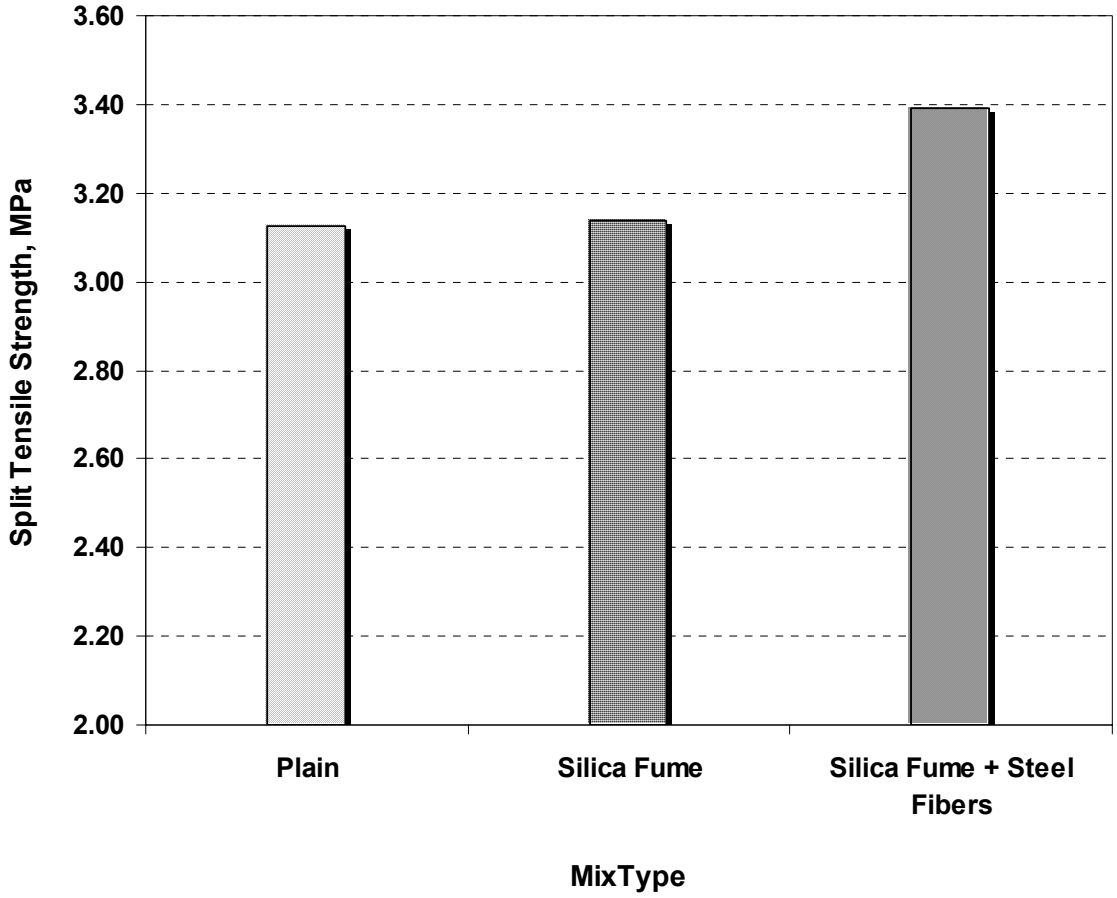

Figure 4.5: Split tensile strength of concrete specimens prepared with coarse aggregates from Riyadh road.

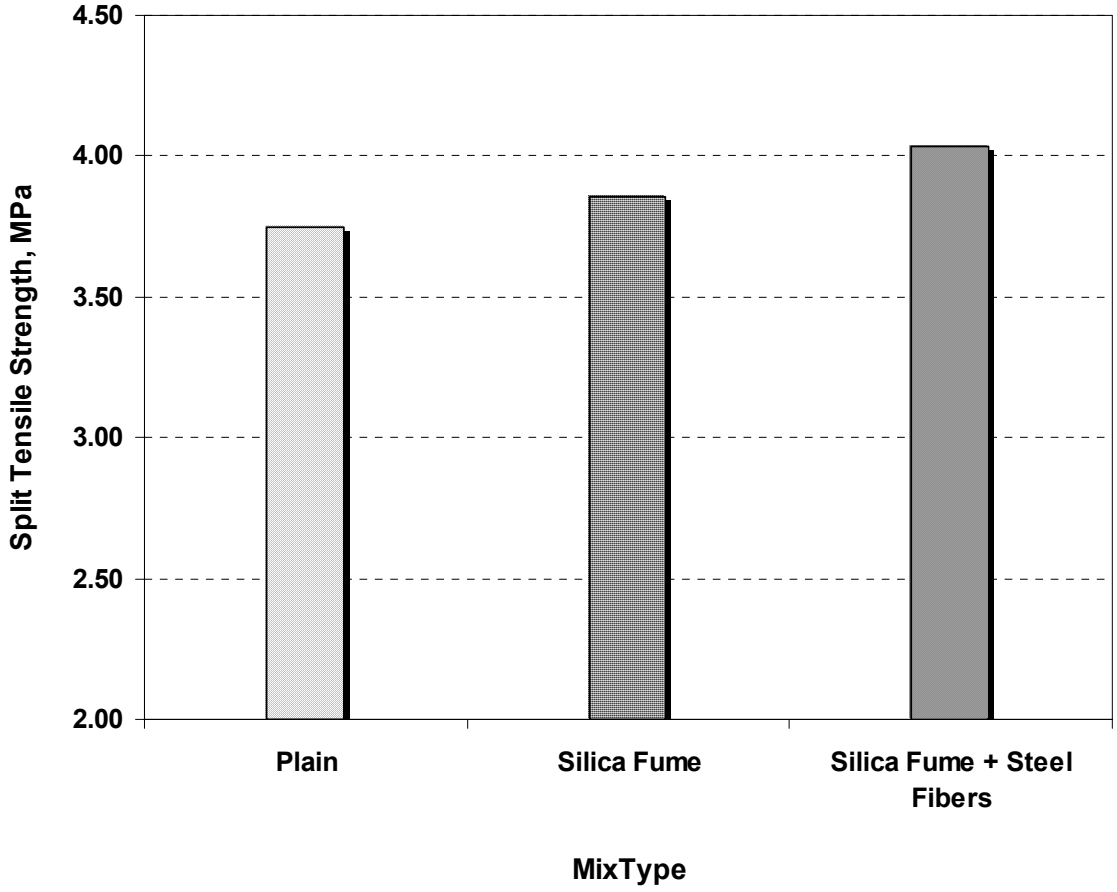

Figure 4.6: Split tensile strength of concrete specimens prepared with steel slag aggregates.

Table 4.2: Percentage improvement in split tensile strength of concrete due to addition of silica fume and steel fiber to plain cement concrete

Aggregate Type	Mix Type	f_{sp} (MPa)	% Improvement
Abu-Hadriyah	Plain Cement	2.60	—
	Silica Fume Cement	2.75	6
	Silica Fume + Steel Fibers	3.16	22
Riyadh	Plain	3.12	—
	Silica Fume	3.14	1
	Silica Fume + Steel Fibers	3.39	9
Steel Slag	Plain	3.75	—
	Silica Fume	3.86	3
	Silica Fume + Steel Fibers	4.04	8

cement concrete compared to plain cement concrete has been reported by several researchers [31, 63, 64, 65].

The split tensile strength of concrete incorporating steel fibers was more than that of silica fume cement concrete. This may be attributed to the fact that incorporation of steel fibers in concrete delays the growth of splitting crack, and consequently increases the ductility. The improvement was particularly true for concrete prepared with crushed limestone aggregates from Abu-Hadriyah. The split tensile strength of fiber reinforced concrete prepared with aggregates from Abu-Hadriyah was more than that of plain cement concrete prepared with Riyadh aggregate. The values of split tensile strength of fiber reinforced concrete prepared with Abu-Hadriyah aggregate and plain cement concrete prepared with Riyadh aggregate were 3.16 and 3.12 MPa, respectively. These results agree with the those obtained by Beshr [31], who reported a significant improvement in the split tensile strength of concrete prepared with crushed limestone from Abu-Hadriyah when steel fibers were added.

4.2 EFFECT OFAGGREGATE QUALITY ON TIME TO INITIATION OF REINFORCEMENT CORROSION

Reinforced concrete specimens prepared with the selected aggregates were partially immersed in 5% sodium chloride solution and the corrosion potentials were measured periodically. The corrosion potential curves were utilized to assess the time to initiation of reinforcement corrosion. For this purpose, ASTM C 876 criterion was utilized. According to this criterion, if the corrosion potentials are

numerically less than -270 mV SCE, then there is 90% probability of reinforcement corrosion.

The corrosion potential curve for the plain cement concrete specimens prepared with limestone from Abu-Hadriyah is shown in Figure 4.7, and that of silica fume cement concrete specimens using Abu-Hadriyah aggregates is shown in Figure 4.8. The corrosion potential curve for fiber reinforced concrete specimens prepared with Abu-Hadriyah aggregates is shown in Figure 4.9.

Figures 4.10 through 4.12 show the corrosion potential curves for concrete specimens prepared with Riyadh aggregate. The corrosion potential curves for steel slag aggregate concrete specimens are shown in Figures 4.13 through 4.15.

The time–corrosion potential curves in the Figures 4.7 through 4.15 were evaluated to study the effect of aggregate and admixtures on the time to initiation of reinforcement corrosion. Figure 4.16 shows the effect of mix type on the time to initiation of reinforcement corrosion in the concrete specimens prepared with Abu-Hadriyah aggregate. The time to initiation of reinforcement corrosion in plain cement concrete and silica fume cement concrete was nearly the same; being 72 and 80 days, respectively, whereas in the fiber reinforced concrete specimens corrosion initiation was noted after 125 days.

The effect of mix type on the time to initiation of reinforcement corrosion in the concrete specimens prepared with Riyadh road aggregates is shown in Figure 4.17. The plain cement concrete was the least effective in delaying the corrosion

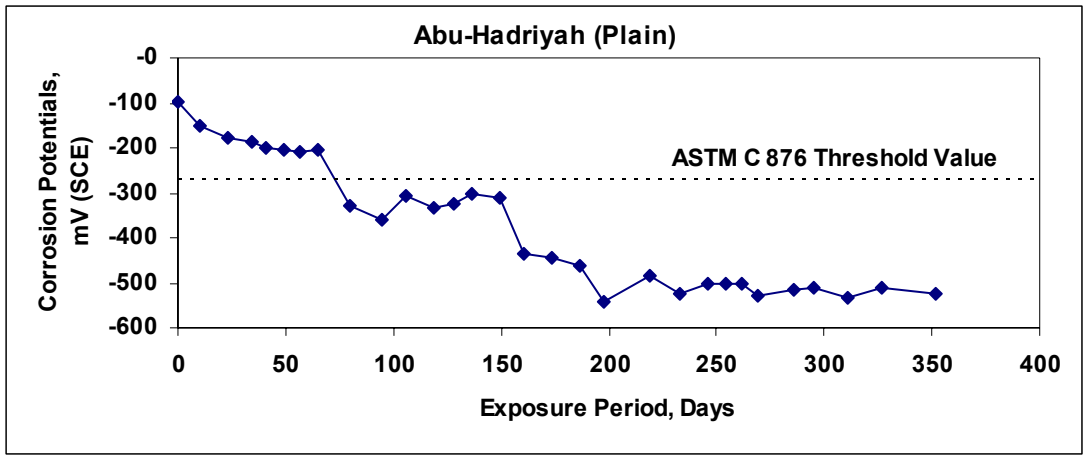

Figure 4.7: Variation of corrosion potentials on the steel in the plain cement concrete specimens prepared using Abu-Hadriyah aggregate.

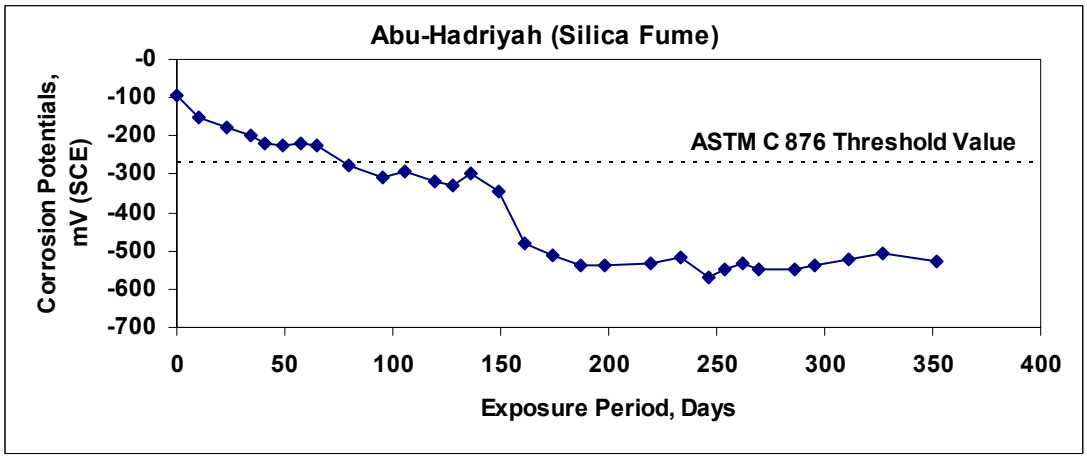

Figure 4.8: Variation of corrosion potentials on the steel in the silica fume concrete specimens prepared using Abu-Hadriyah aggregate.

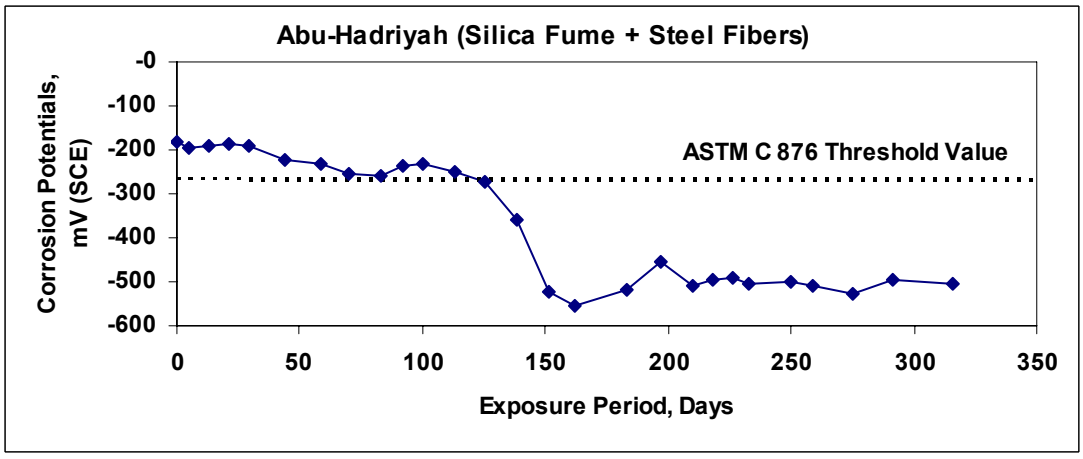

Figure 4.9: Variation of corrosion potentials on the steel in the fiber reinforced concrete specimens prepared using Abu-Hadriyah aggregate.

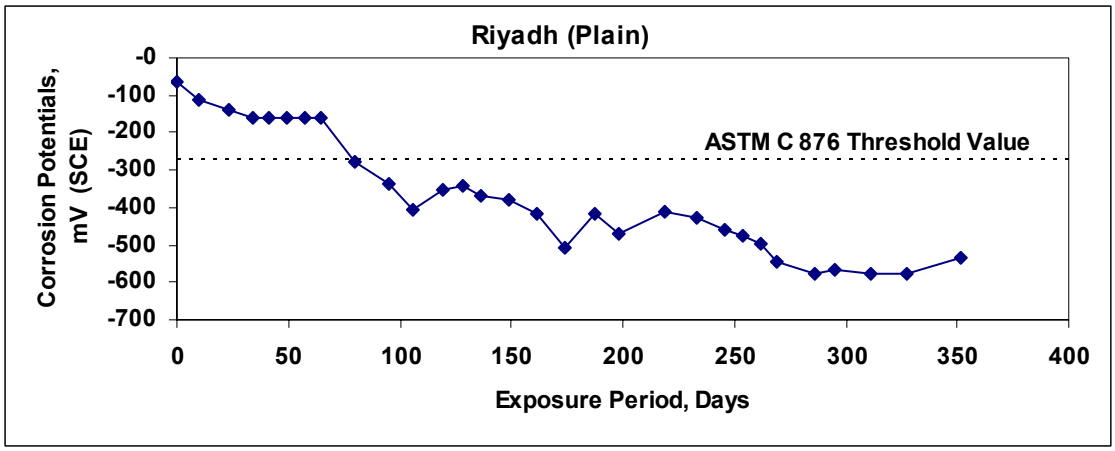

Figure 4.10: Variation of corrosion potentials on the steel in the plain cement concrete specimens prepared using Riyadh aggregate.

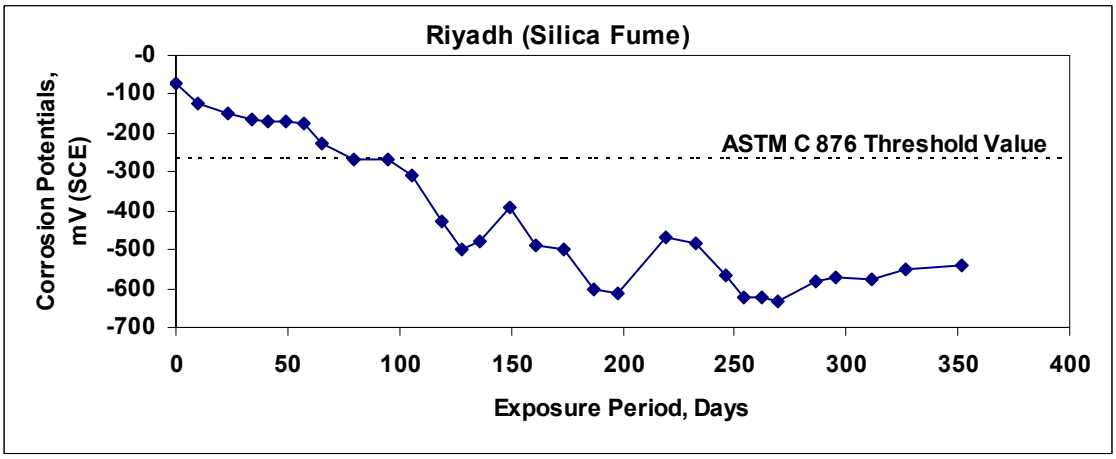

Figure 4.11: Variation of corrosion potentials on the steel in the silica fume concrete specimens prepared with Riyadh aggregate.

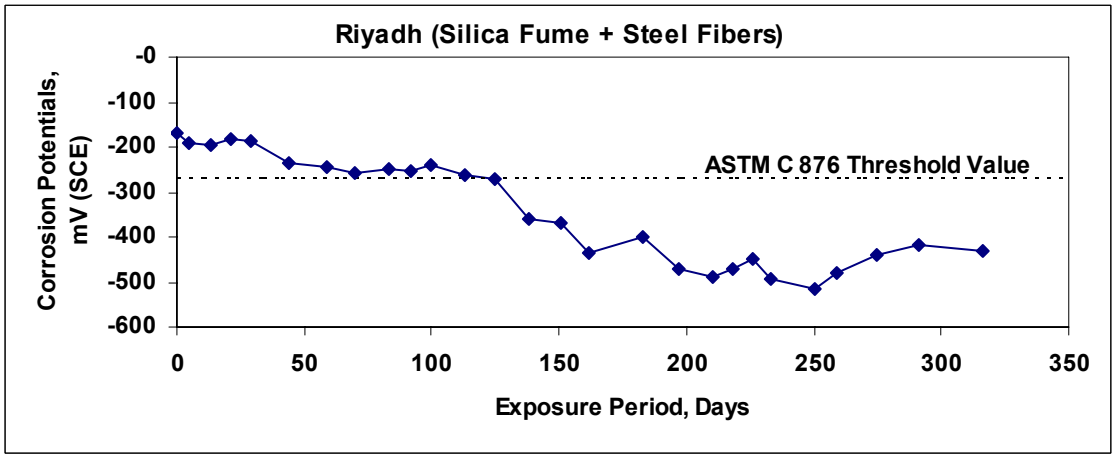

Figure 4.12: Variation of corrosion potentials on the steel in the fiber reinforced concrete specimens prepared with Riyadh aggregate.

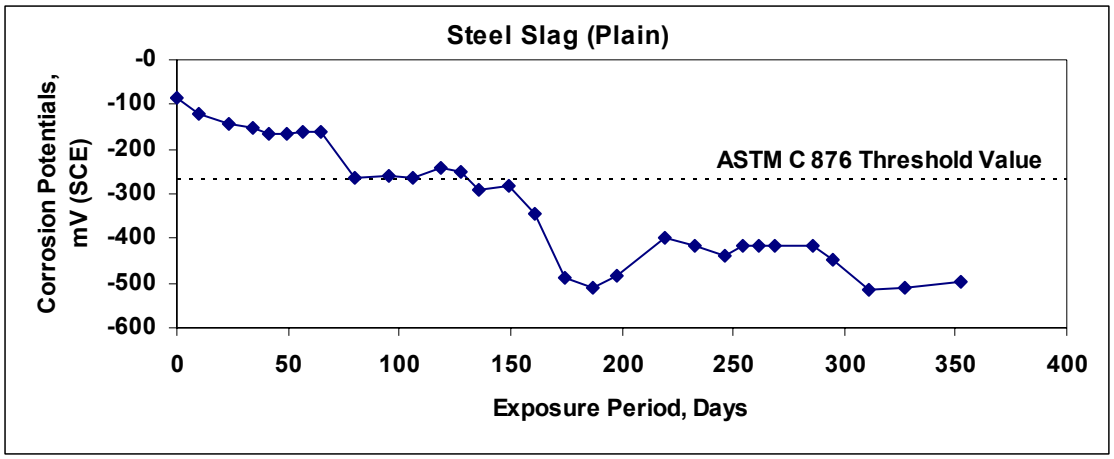

Figure 4.13: Variation of corrosion potentials on the steel in the plain cement concrete specimens prepared with steel slag aggregate.

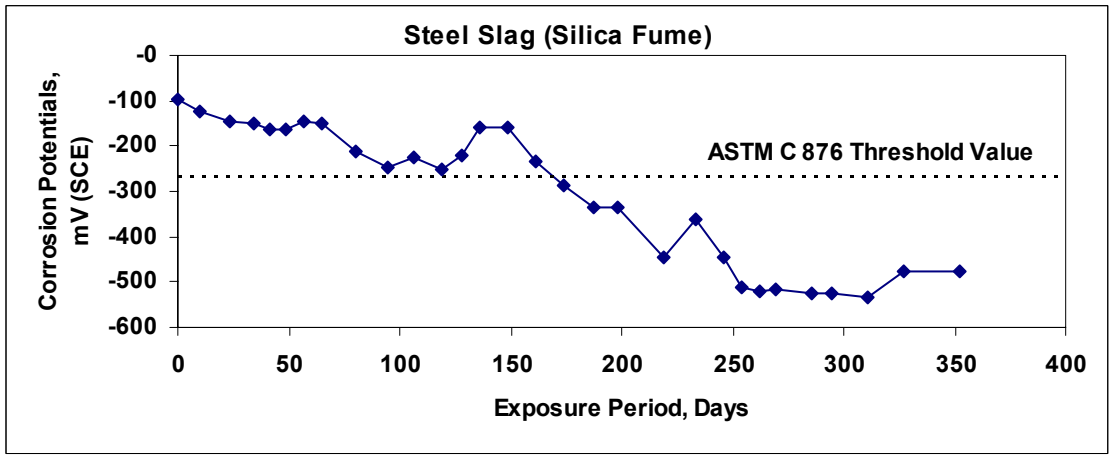

Figure 4.14: Variation of corrosion potentials on the steel in the silica fume concrete specimens prepared with steel slag aggregate.

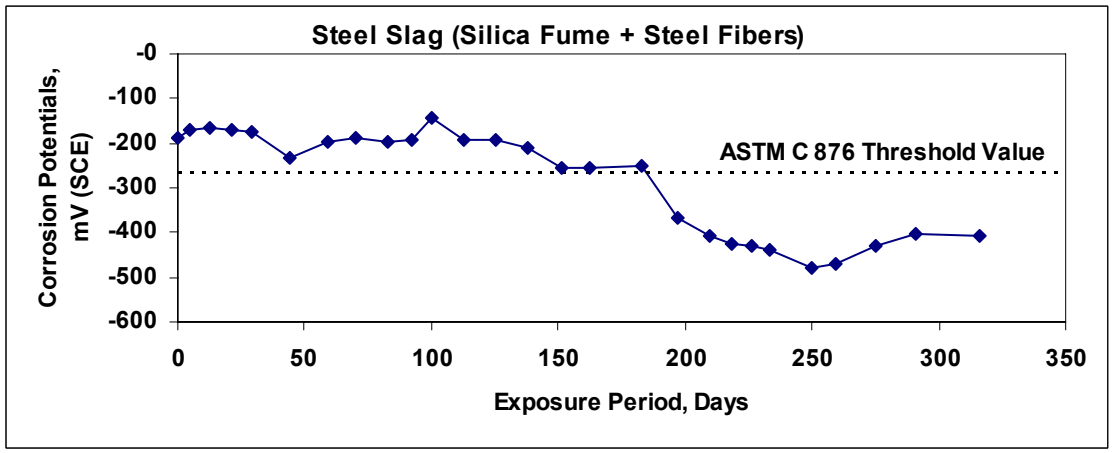

Figure 4.15: Variation of corrosion potentials on the steel in the fiber reinforced concrete specimens prepared with steel slag aggregate.

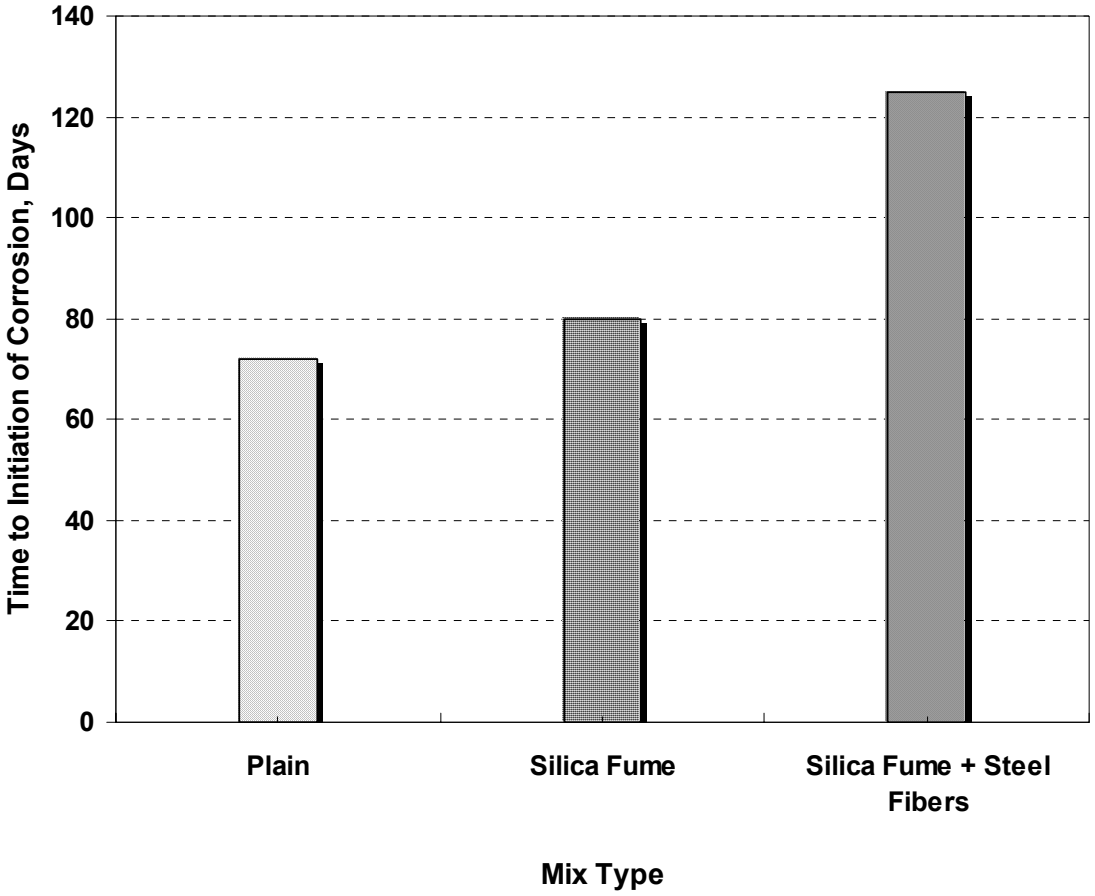

Figure 4.16: Time to initiation of reinforcement corrosion in the concrete specimens prepared with Abu-Hadriyah aggregate.

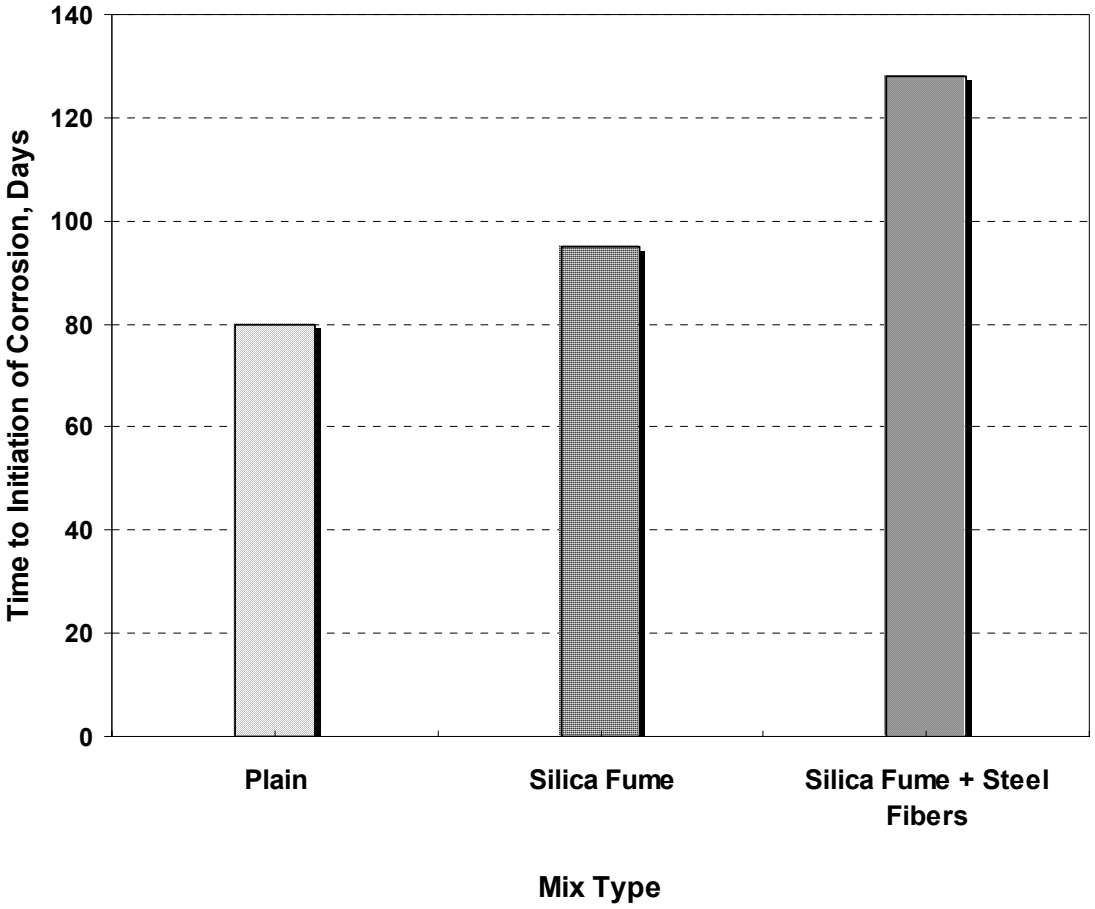

Figure 4.17: Time to initiation of reinforcement corrosion in the concrete specimens prepared with Riyadh Road aggregate.

initiation, as it took 80 days for chlorides to depassivate the protective layer on reinforcement. The time to initiation of reinforcement corrosion in the silica fume and fiber reinforced concrete was 95 and 128 days, respectively.

Figure 4.18 shows the effect of admixture on the time to initiation of reinforcement corrosion in the concrete specimens prepared with steel slag aggregates. The effect of discreet random steel fibers in delaying the time to initiation of reinforcement corrosion was observed in the steel slag aggregate concrete also. However, the beneficial effect of fiber addition on delaying corrosion in this group of specimens was not that significant compared to that noted in the concrete specimens prepared with the other aggregates, as the time to initiation of reinforcement corrosion in fiber reinforced concrete specimens was slightly more than that in the silica fume cement concrete specimens, the values being 189 and 174 days, respectively.

The data in Figures 4.16 through 4.18 indicate that, the incorporation of steel fibers to concrete had considerably delayed the time to initiation of reinforcement corrosion in all the three types of aggregates. Table 4.3 shows the percentage improvement in the time to initiation of reinforcement corrosion due to the addition of silica fume and steel fiber to the concrete. In general, the improvement in the time the to initiation of corrosion due to addition of steel fiber plus silica fume was more than that due to the addition of silica fume alone. The average improvement due to the addition of fibers was in the range of 45 to 75%, while in the silica fume concrete it was in the range of 10 to 35%. The reason for this delay in the time to initiation of reinforcement corrosion due to incorporation of fibers can be

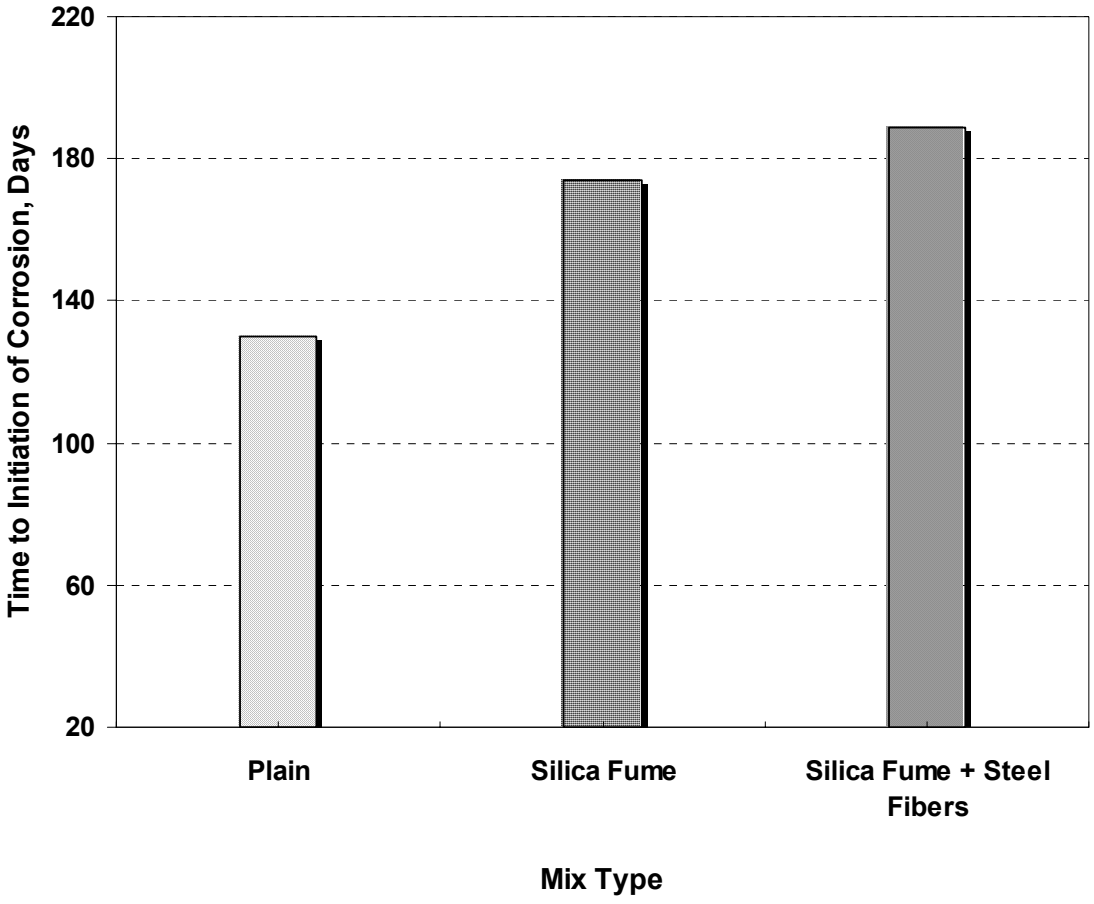

Figure 4.18: Time to initiation of reinforcement corrosion in the concrete specimens prepared with steel slag aggregate.

Table 4.3: Percentage improvement in time to initiation of reinforcement corrosion due to addition of silica fume and steel fibers to plain cement concrete

Aggregate Type	Mix Type	Time to Initiation of Corrosion (Days)	% Improvement
Abu-Hadriyah	Plain Cement	72	—
	Silica Fume Cement	80	11
	Silica Fume + Steel Fibers	125	74
Riyadh	Plain	80	—
	Silica Fume	95	19
	Silica Fume + Steel Fibers	128	56
Steel Slag	Plain	130	—
	Silica Fume	174	34
	Silica Fume + Steel Fibers	189	45

attributed to its prime function of controlling matrix cracking in concrete, thereby reducing its water-retaining capability, thereby retarding the diffusion of chlorides ion to the steel surface.

The data in Figures 4.19 through 4.21 indicate the effect of aggregate quality on the time to initiation of reinforcement corrosion. Figure 4.19 shows the effect of aggregate quality on the time to initiation of corrosion in the plain cement concrete. The time to initiation of reinforcement corrosion in the concrete specimens prepared with Abu-Hadriyah, Riyadh and steel slag aggregates was 72, 80 and 130 days, respectively.

Figure 4.20 shows the effect of aggregate quality on the time to initiation of corrosion in the silica fume cement concrete. The time to initiation of reinforcement corrosion in the Abu-Hadriyah, Riyadh and steel slag aggregate was 80, 90 and 174 days, respectively. These data also depict the beneficial effect of steel slag aggregate in delaying the corrosion process.

Figure 4.21 compares the effect of aggregate quality on the time to initiation of reinforcement corrosion in the fiber reinforced concrete specimens. There was a minor difference in the time to initiation of reinforcement corrosion in the concrete specimens prepared with Abu-Hadriyah and Riyadh aggregates, the values being 125 and 128 days, respectively. In the steel slag aggregate concrete specimens, the corrosion initiation was noted after an exposure period of 189 days.

The data in Figures 4.19 through 4.21 indicate that the quality of aggregates has a considerable effect on the time to initiation of reinforcement corrosion. The

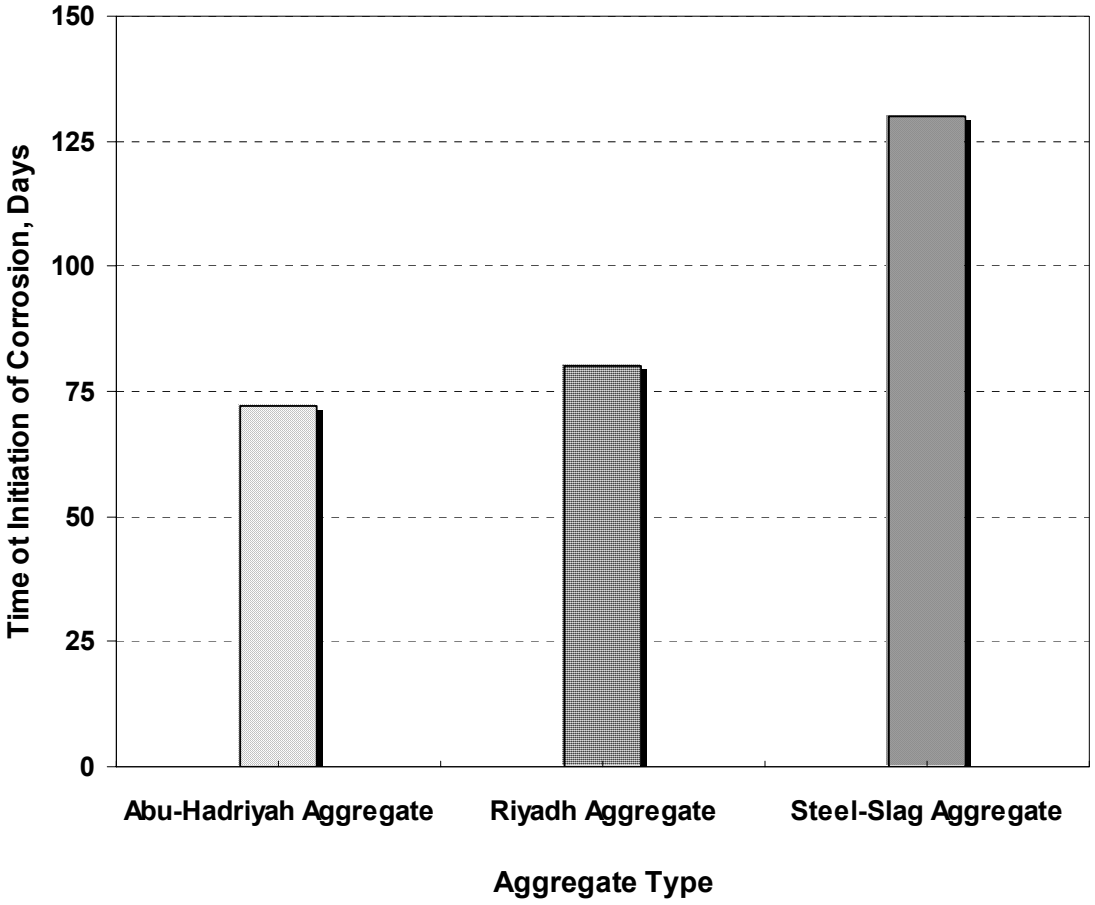

Figure 4.19: Effect of aggregate on the time to initiation of reinforcement corrosion in the plain cement concrete specimens.

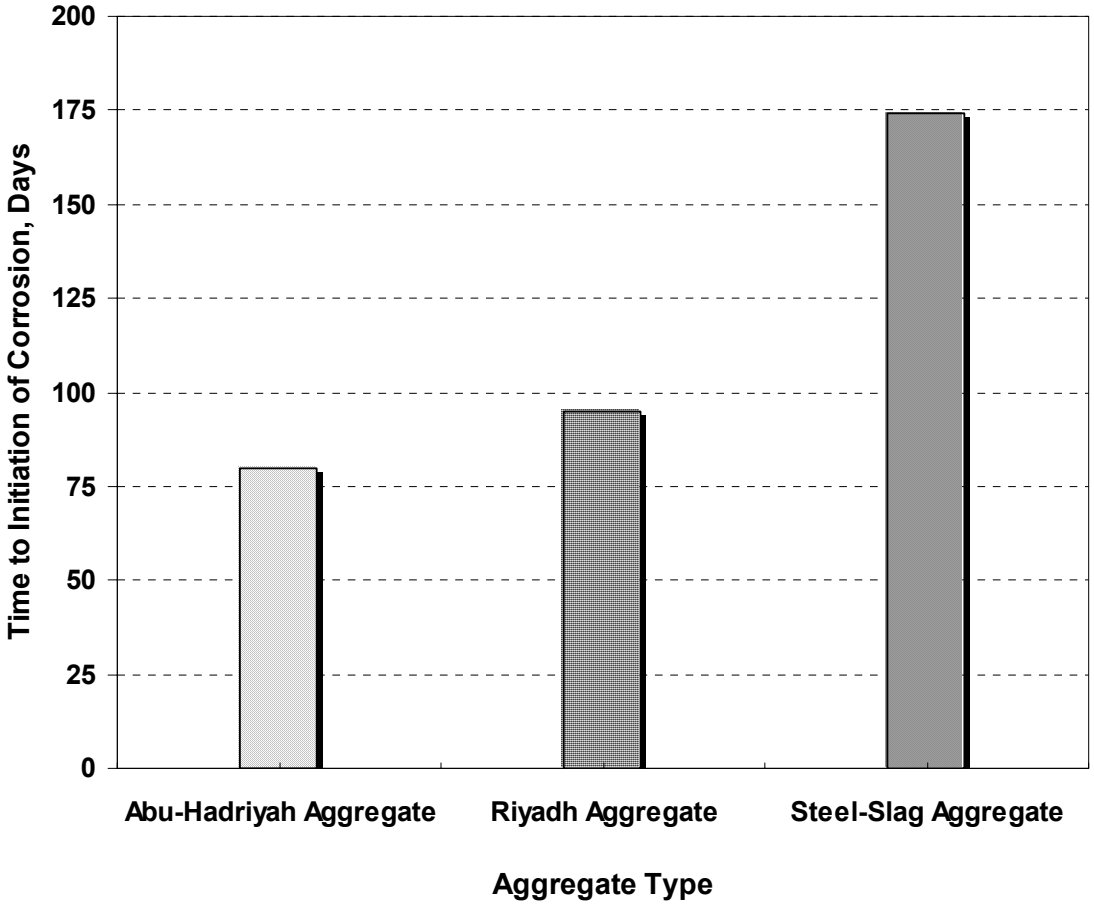

Figure 4.20: Effect of aggregate on the time to initiation of reinforcement corrosion in the silica fume cement concrete specimens

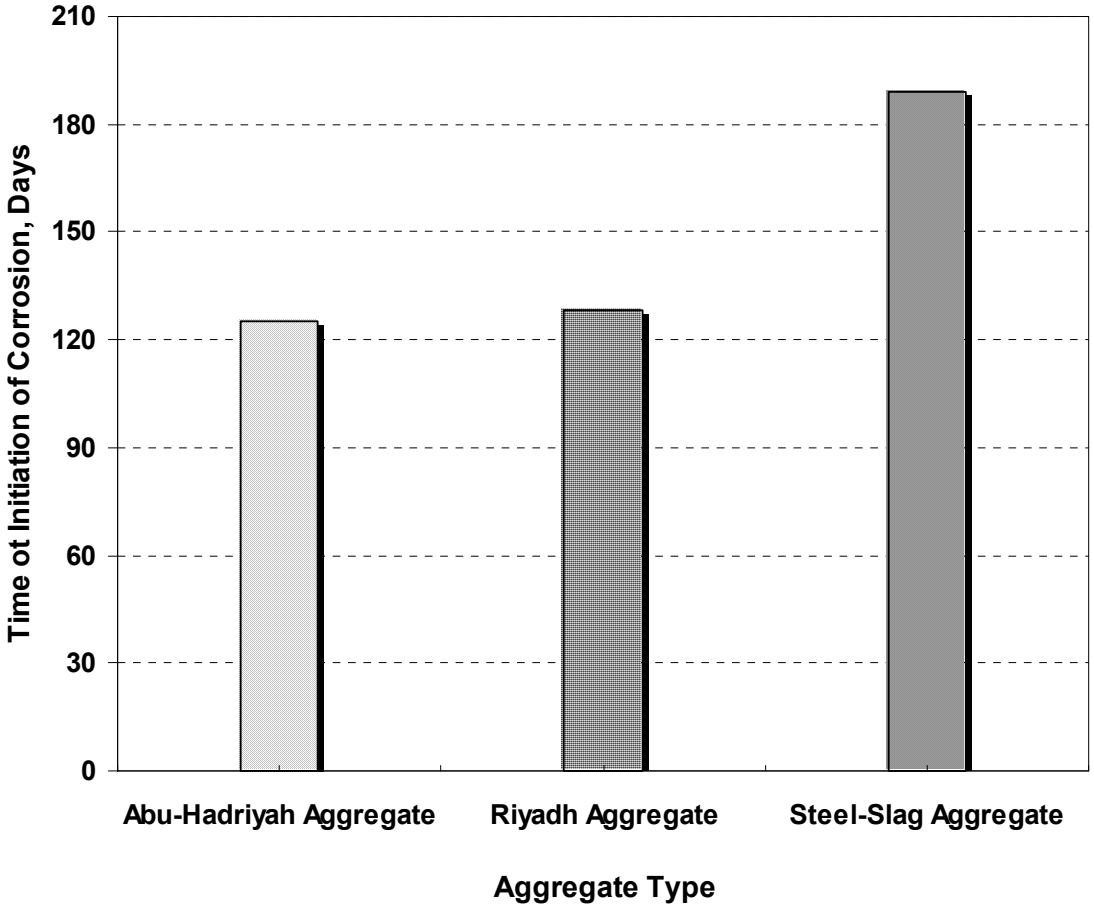

Figure 4.21: Effect of aggregate on the time to initiation of reinforcement corrosion in the fiber reinforced concrete specimens.

time to initiation of reinforcement corrosion significantly increase when steel slag aggregate was used. The limestone from Abu-Hadriyah was less effective in delaying corrosion initiation. This may be due to the porous structure of the Abu-Hadriyah aggregate.

The percentage improvement in the time to initiation of reinforcement corrosion when Riyadh and steel slag aggregates were used instead of Abu-Hadriyah aggregate is summarized in Table 4.4. The concrete specimens prepared with the steel slag aggregate showed a significant improvement in the time to initiation of reinforcement corrosion in the range of 51 to 118% of that prepared with crushed limestone aggregate from Abu-Hadriyah. While the concrete specimens prepared with the coarse aggregates from Riyadh showed an improvement of about 2 to 20%. The reason for the improvement in the time to initiation of reinforcement corrosion in the concrete specimens prepared with steel slag aggregates can be attributed to its dense structure when compared to the other two aggregates used in this study. The dense structure of the steel slag aggregate probably delayed the diffusion of chloride ions to steel surface thereby delaying the process of reinforcement corrosion.

4.3 EFFECT OF AGGREGATE QUALITY ON CORROSION CURRENT DENSITY

The variation of corrosion current density (I_{corr}) with time in the concrete specimens exposed to 5% sodium chloride solution was plotted to study the effect of aggregate quality and the admixtures on the rate of reinforcement corrosion.

Table 4.4: Percentage improvement in time to initiation of reinforcement corrosion in concrete specimens due to use of Riyadh and steel slag aggregates in place of Abu-Hadriyah aggregate

Mix Type	Aggregate Type	Time to Initiation of Corrosion (Days)	% Improvement
Plain Cement	Abu-Hadriyah	72	—
	Riyadh	80	11
	Steel Slag	130	81
Silica Fume Cement	Abu-Hadriyah	80	—
	Riyadh	95	19
	Steel Slag	174	118
Silica fume + Steel fibers	Abu-Hadriyah	125	—
	Riyadh	128	2
	Steel Slag	189	51

Figure 4.22 depicts the variation of the corrosion current density (I_{corr}) in the plain, silica fume and fiber reinforced cement concrete specimens prepared with limestone from Abu-Hadriyah. Figure 4.23 shows the variation of I_{corr} in the plain cement, silica fume and fiber reinforced cement concrete specimens prepared with Riyadh aggregates. The variation of I_{corr} in the concrete specimens prepared with steel slag aggregate is shown in Figure 4.24.

The data in Figures 4.22 through 4.24 show that, in all the concrete specimens the I_{corr} values increased with time. In early period of exposure, i.e., 1 to 2 weeks, the I_{corr} in all the specimens was less than 0.05μA/cm^2. This indicates the passivity of steel in the initial period of exposure. The I_{corr} curves for the Riyadh and Abu-Hadriyah aggregate concretes were nearly the same as shown in Figures 4.22 and 4.23. The I_{corr} curves for steel slag aggregate were different with low corrosion current density values as shown in Figure 4.24. After 100 days of exposure, the I_{corr} values in the concrete specimens prepared with Abu-Hadriyah and Riyadh aggregates were more than 0.1μA/cm^2. This shows the depassivation of steel and start of corrosion activity. In the concrete specimens prepared with steel slag aggregates, the depassivation and corrosion initiation was recorded after about 170 days.

Figures 4.25 through 4.27 show the effect of aggregate quality on I_{corr} at different exposure periods i.e., 90, 180 and 270 days. The effect of aggregate quality on I_{corr} in the plain cement concrete is shown in Figure 4.25.

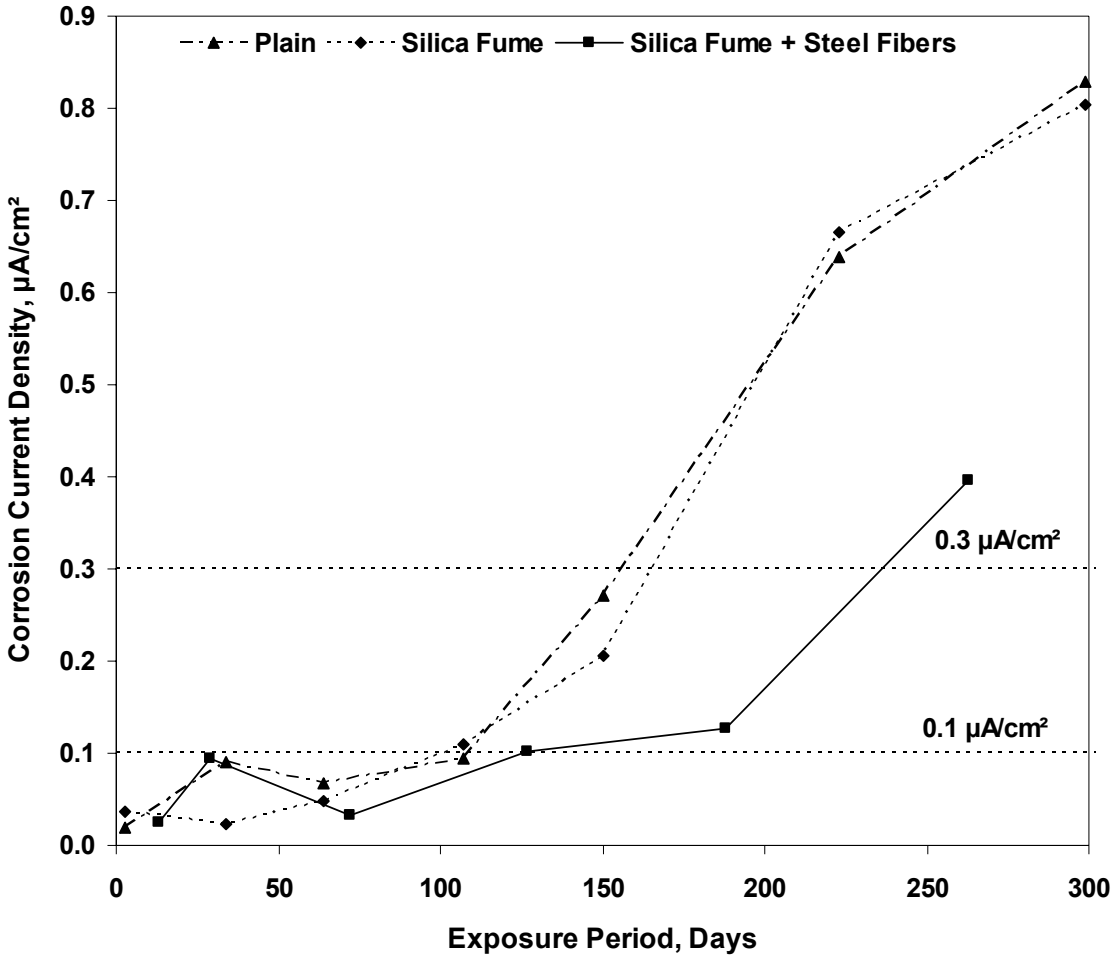

Figure 4.22: Variation of corrosion current density on the steel in the Abu-Hadriyah aggregate concrete specimens.

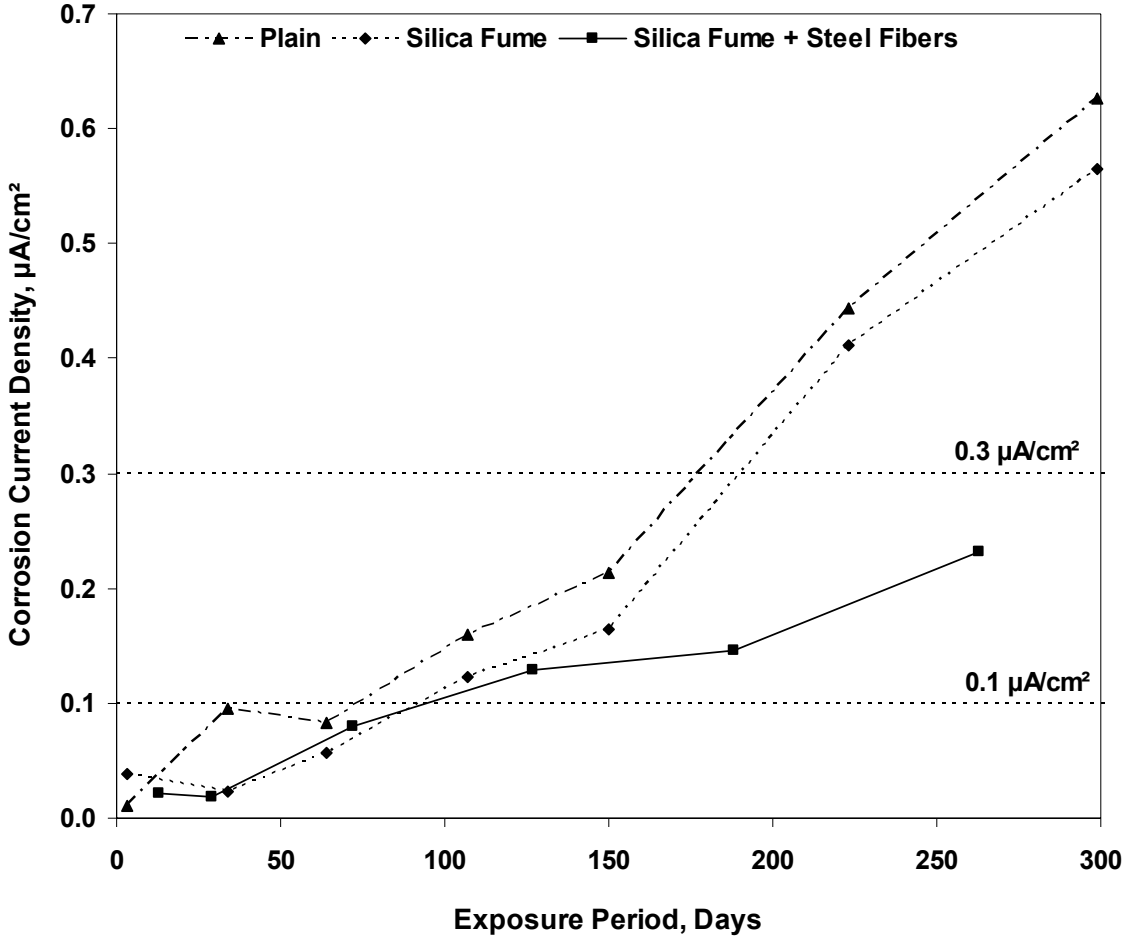

Figure 4.23: Variation of corrosion current density on steel in the Riyadh Road aggregate concrete specimens.

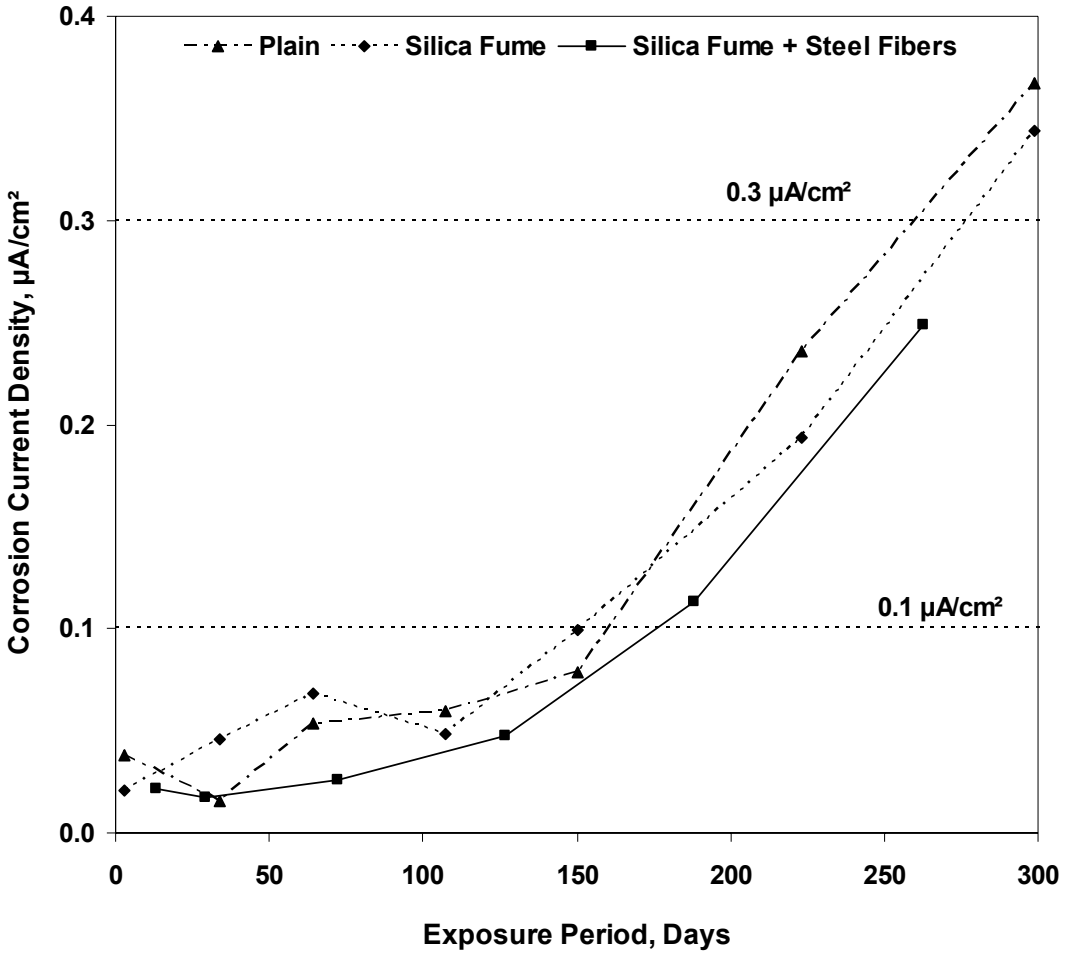

Figure 4.24: Variation of corrosion current density on steel in the steel slag aggregate concrete specimens.

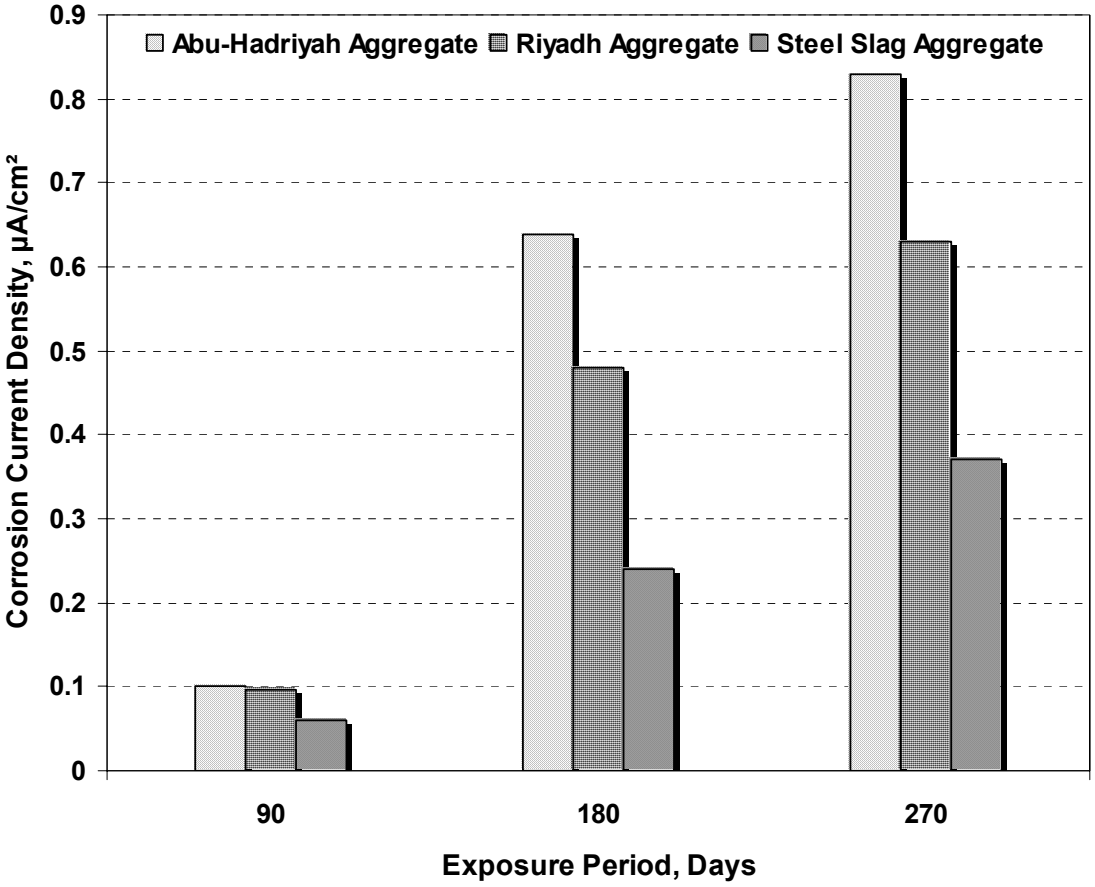

Figure 4.25: Effect of aggregate quality on I_{corr} in the plain cement concrete.

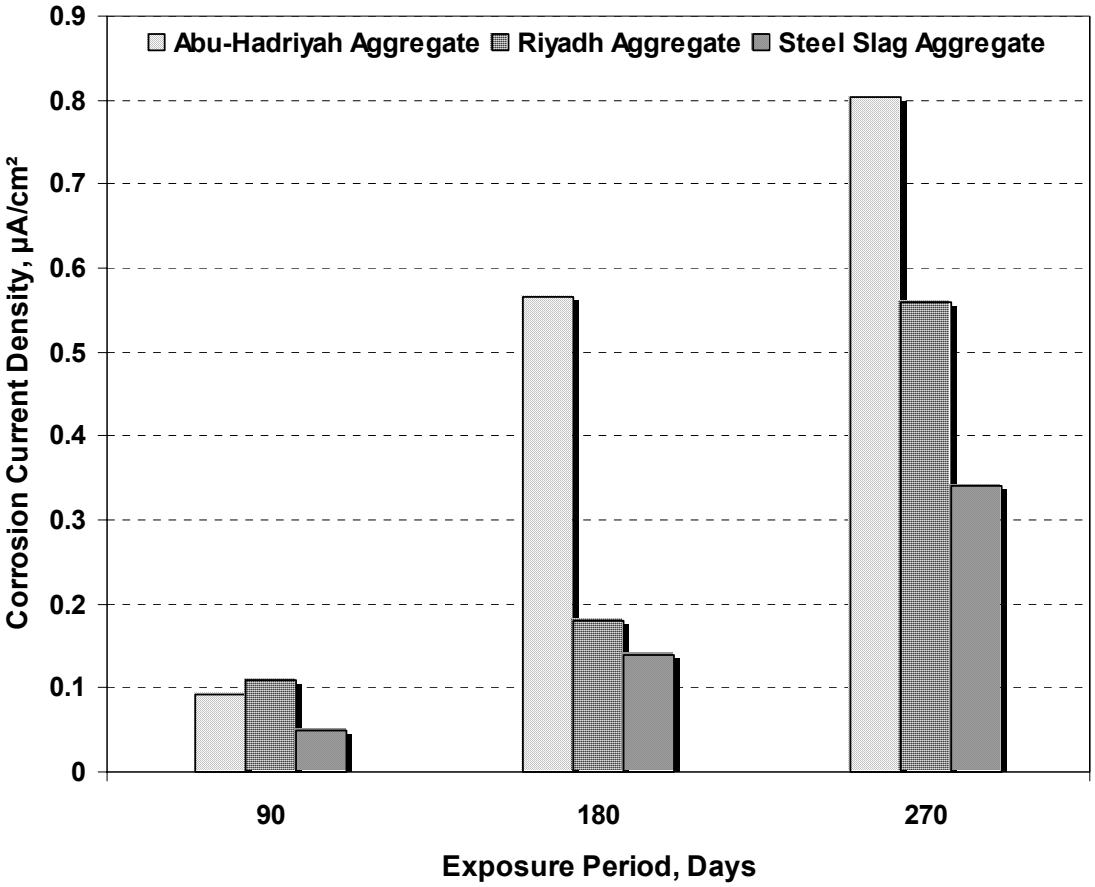

Figure 4.26: Effect of aggregate quality on I_{corr} in the silica fume cement concrete.

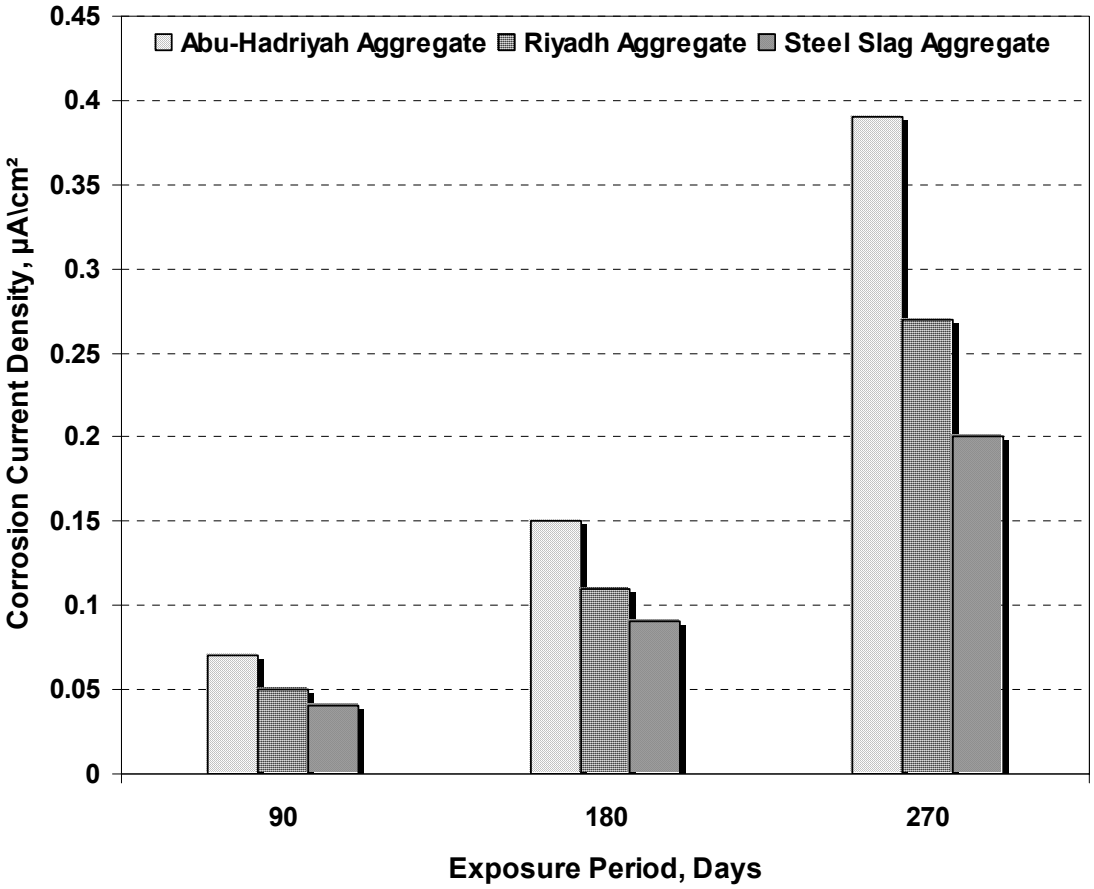

Figure 4.27: Effect of aggregate quality on I_{corr} in the fiber reinforced concrete.

The effect of aggregate quality on I_{corr} in silica fume cement concrete specimens is shown in Figure 4.26. The data in Figure 4.27 depict the effect of aggregate quality on I_{corr} in the concrete specimens prepared with steel fiber cement concrete.

It could be observed from the data in Figures 4.25 through 4.27 that, in the initial period of exposure, the I_{corr} values were not significantly affected by the quality of coarse aggregate. But in the later stages of exposure, the quality of aggregate has a significant effect on the I_{corr} values. The percentage decrease in the I_{corr} values in the Riyadh and steel slag aggregate concrete specimens with respect to Abu-Hadriyah aggregate concrete specimens is tabulated in Table 4.5.

The steel slag aggregate concrete showed consistently low I_{corr} values. The highest I_{corr} values were noted in the limestone aggregate from Abu-Hadriyah. The poor performance of Abu-Hadriyah aggregate concrete was due to the poor quality of the aggregate. Initially, the I_{corr} values were slightly higher in the concrete specimens prepared with Riyadh aggregates but in the later stages of exposure they tended to be less than those in the Abu-Hadriyah aggregate concrete.

Figures 4.28 through 4.30 show the effect of mix type on I_{corr} in the concrete specimens prepared with Abu-Hadriyah, Riyadh and steel slag aggregates, after 90, 180 and 270 days of exposure to 5% NaCl solution. The corrosion activity on steel bars in the fiber reinforced concrete specimens in all the three aggregate concrete was less than that of plain and silica fume cement concretes after the same exposure period.

Table 4.5: Percentage reduction in corrosion current density in the concrete specimens due to use of Riyadh and steel slag aggregates in place of Abu-Hadriyah aggregate

Mix Type	Aggregate Type / Days	Corrosion Current Density ($\mu A/cm^2$)			% Decrease in the Corrosion Current Density		
		90	**180**	**270**	**90**	**180**	**270**
Plain Cement	Abu-Hadriyah	0.1	0.639	0.829	—	—	—
	Riyadh	0.096	0.48	0.63	4	25	22
	Steel Slag	0.06	0.24	0.37	67	62	55
Silica Fume Cement	Abu-Hadriyah	0.093	0.566	0.803	—	—	—
	Riyadh	0.11	0.18	0.56	-18	68	30
	Steel Slag	0.05	0.14	0.34	46	75	58
Silica Fume +Steel Fibers	Abu-Hadriyah	0.07	0.15	0.39	—	—	—
	Riyadh	0.05	0.11	0.27	29	21	30
	Steel Slag	0.04	0.091	0.2	43	39	49

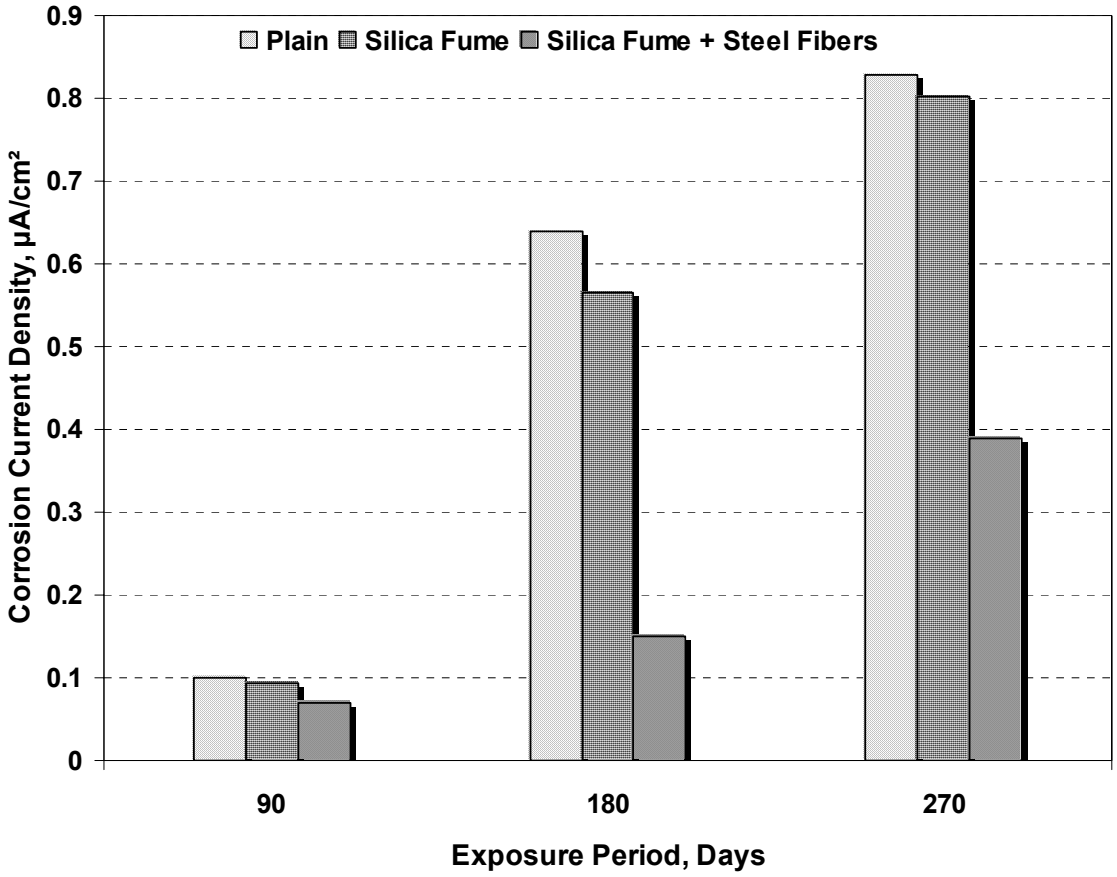

Figure 4.28: Effect of mix type on corrosion current density in the concrete specimens prepared with Abu-Hadriyah aggregates after different exposure periods.

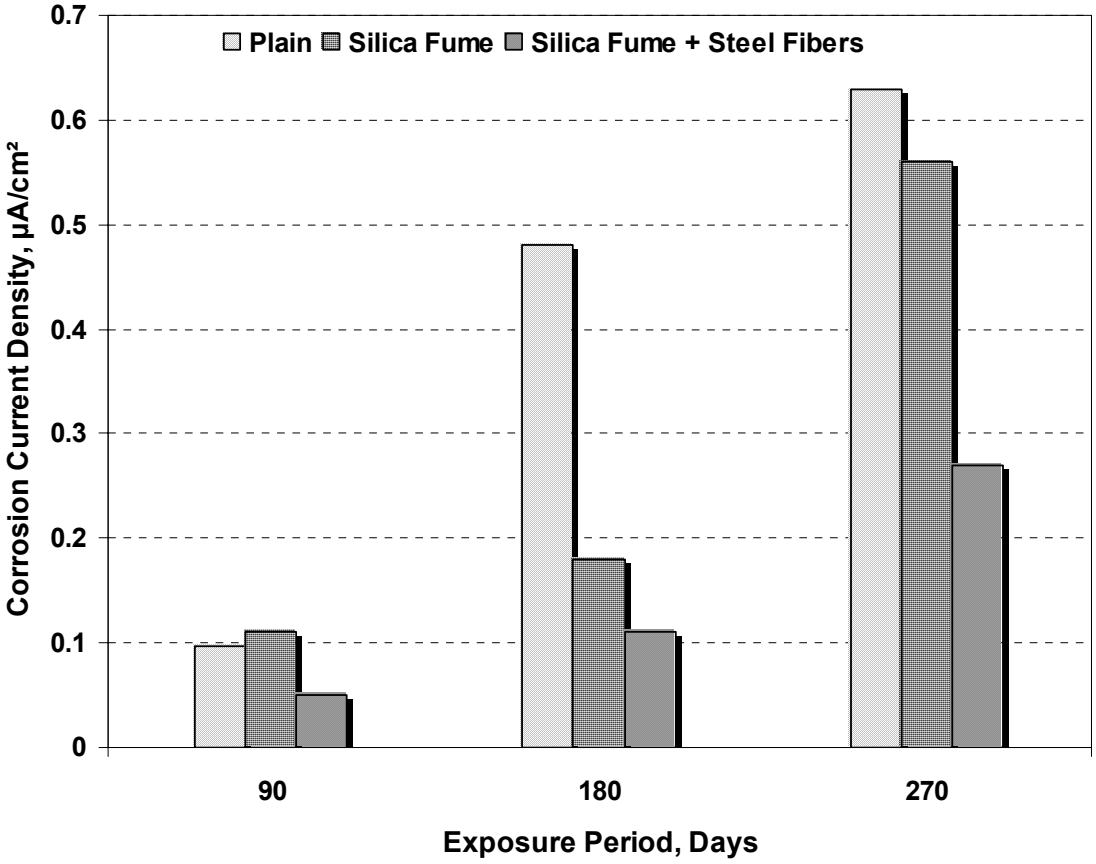

Figure 4.29: Effect of mix type on corrosion current density in the concrete specimens prepared with Riyadh road aggregates after different exposure periods

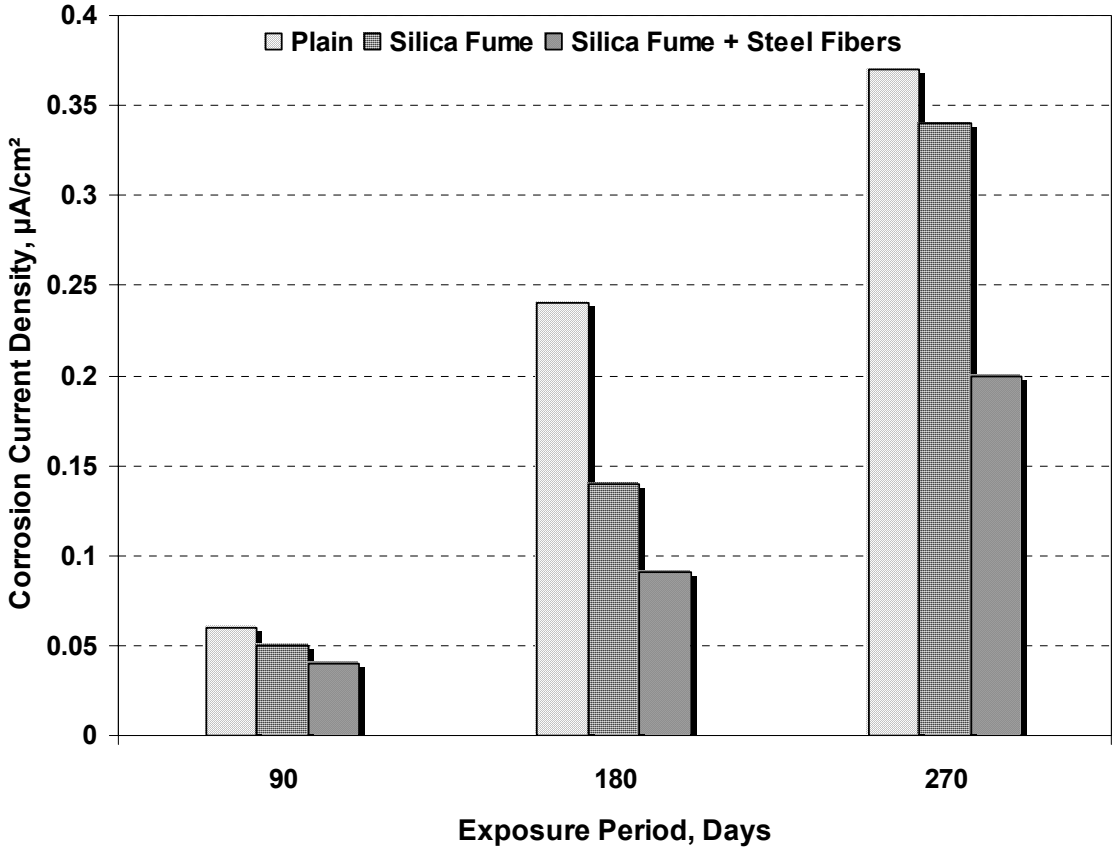

Figure 4.30: Effect of mix type on corrosion current density in the concrete specimens prepared with steel slag aggregates after different exposure periods.

Table 4.6 shows the decrease in the I_{corr} with respect to plain cement concrete specimens prepared with the selected aggregate when silica fume and silica fume plus steel fibers were added. The effect of silica fume alone in reducing I_{corr} was not significant, but when silica fume plus fiber were added to plain cement concrete, the corrosion current density was reduced significantly.

The superior performance of steel fiber cement concrete specimens in resisting reinforcement corrosion can be explained as follow: It is well known that silica fume reacts rapidly with calcium hydroxide liberated on the process of cement hydration, leading to a very dense and homogeneous pore structure, but at the same time that change in pore structure may also increase the brittleness of concrete due to the absence of large calcium hydroxide crystals, which play a role in the interruption and propagation of micro cracks. Steel fibers arrest the propagation of microcracks in the concrete matrix resulting in lower ingress of deleterious agents, such as oxygen, moisture etc., to the reinforcement surface which is needed for corrosion to take place, hence resulting in lower rate of reinforcement corrosion. Also, the electrical resistivity will be lower in the absence of micro cracks.

Table 4.6: Percentage reduction in corrosion current density in the concrete specimens due to use of silica fume and steel fiber in place of plain cement concrete

Aggregate Type	Mix Type / Days	Corrosion Current Density ($\mu A/cm^2$)			% Decrease in the Corrosion Current Density		
		90	180	270	90	180	270
Abu-Hadriyah	Plain Cement	0.1	0.639	0.829	--	--	--
	Silica Fume Cement	0.093	0.566	0.803	7	11	29
	Silica Fume +Steel Fibers	0.07	0.15	0.39	30	77	53
Riyadh	Plain Cement	0.096	0.48	0.63	--	--	--
	Silica Fume Cement	0.11	0.18	0.56	15	62	11
	Silica Fume +Steel Fibers	0.05	0.11	0.27	48	77	57
Steel Slag	Plain Cement	0.06	0.24	0.37	--	--	--
	Silica Fume Cement	0.05	0.14	0.34	17	71	8
	Silica Fume +Steel Fibers	0.04	0.091	0.2	33	62	46

4.4 EFFECT OF AGGREGATE QUALITY ON TIME TO CRACKING OF CONCRETE DUE TO ACCELERATED REINFORCEMET CORROSION

The time to cracking of concrete due to reinforcement corrosion was evaluated by impressing an anodic potential of 2.5 Volts. The current was measured by connecting the two leads of a resistor to a data acquisition system. The current flowing through each specimen was plotted against time as shown in Figures 4.31 through 4.39. The initial current requirement for maintaining an anodic potential of +2.5V in all the curves was below 2 mA. The lowest initial current requirement was noted in the concrete specimens prepared with steel slag aggregate, the initial current requirement in Abu-Hadriyah and Riyadh aggregate concrete was almost the same. The time-current curves were analyzed to evaluate the time to cracking of concrete due to accelerated reinforcement corrosion. The time to cracking of concrete, due to reinforcement corrosion, was taken as the point at which a rapid increase in current or a slope of the time-current curve was noted. The time required for cracking of concrete is summarized in Table 4.7.

Figure 4.40 shows the effect of admixtures on the time to cracking of concrete due to reinforcement corrosion. As expected, the plain cement concrete specimens were the first to show signs of cracking. The second to crack were the silica fume cement concrete specimens, while the fiber reinforced concrete specimens were the last to crack. The percentage improvement in the time to cracking of concrete due to reinforcement corrosion after addition of silica fume and fibers is summarized in Table 4.8.

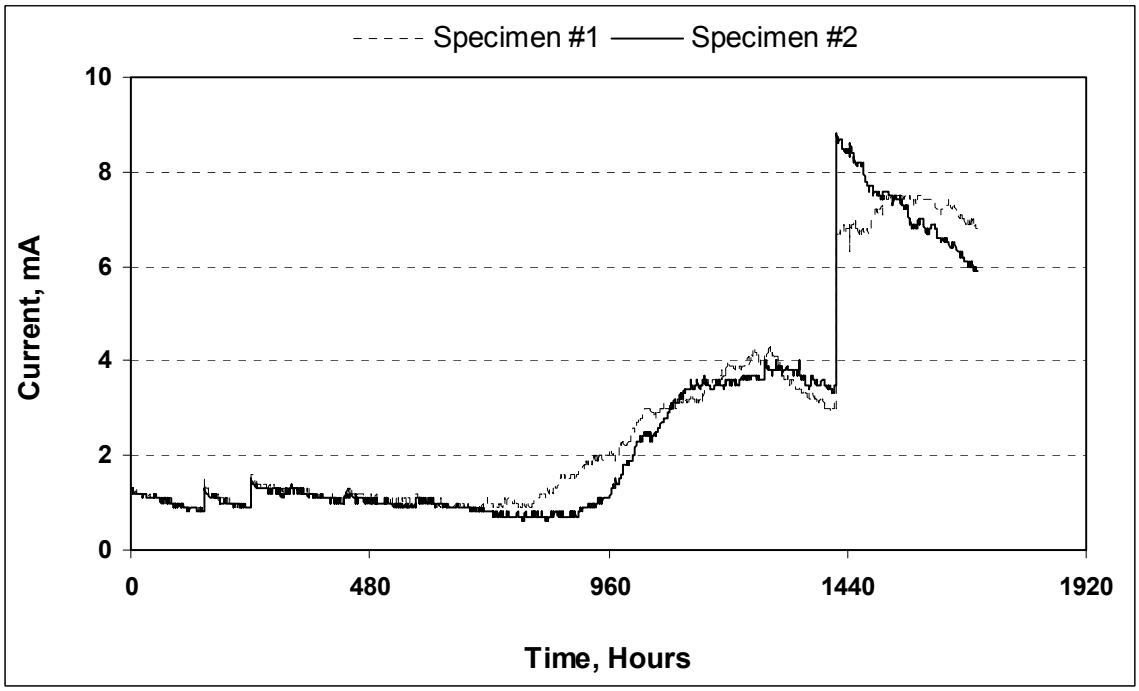

Figure 4.31: Variation of current with time in the plain cement concrete specimens prepared with Abu-Hadriyah aggregate.

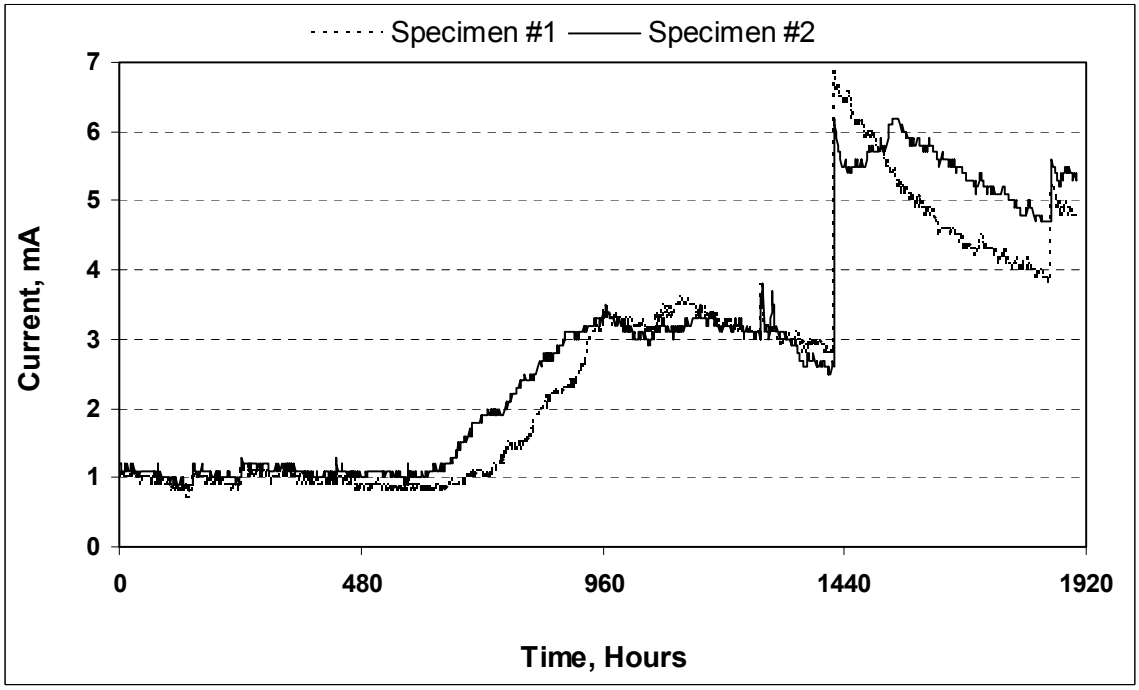

Figure 4.32: Variation of current with time in the silica fume cement concrete specimens prepared with Abu-Hadriyah aggregate.

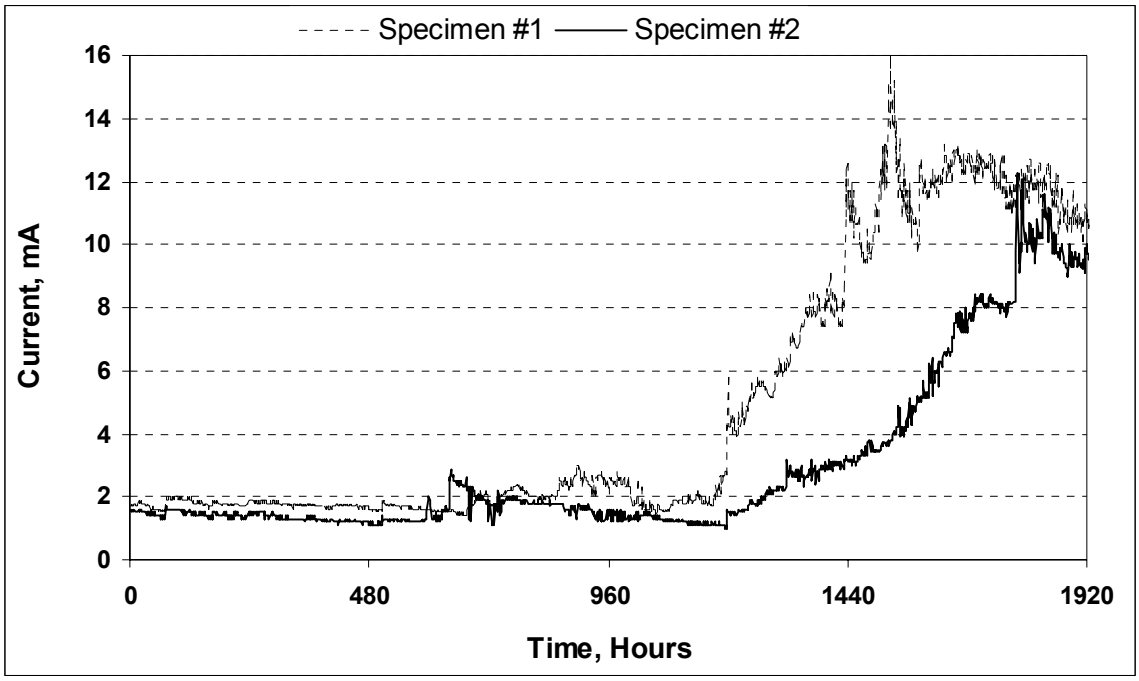

Figure 4.33: Variation of current with time in the fiber reinforced concrete specimens prepared with Abu-Hadriyah aggregate.

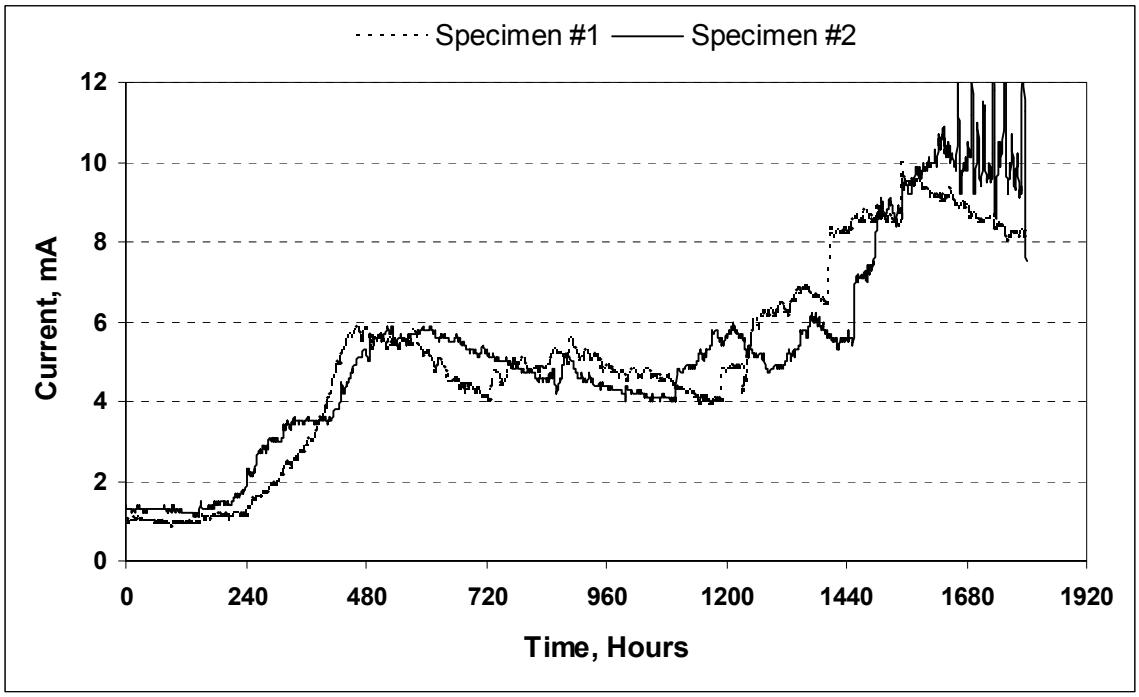

Figure 4.34: Variation of current with time in the plain cement concrete specimens prepared with Riyadh aggregate.

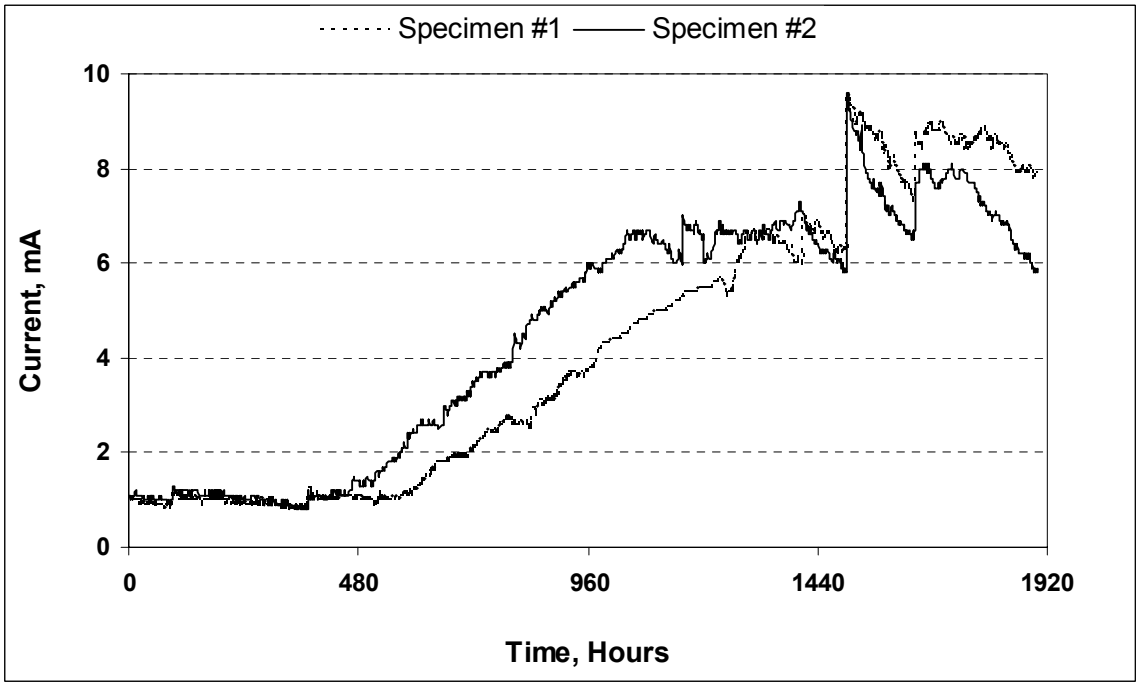

Figure 4.35: Variation of current with time in the silica fume cement concrete specimens prepared with Riyadh aggregate.

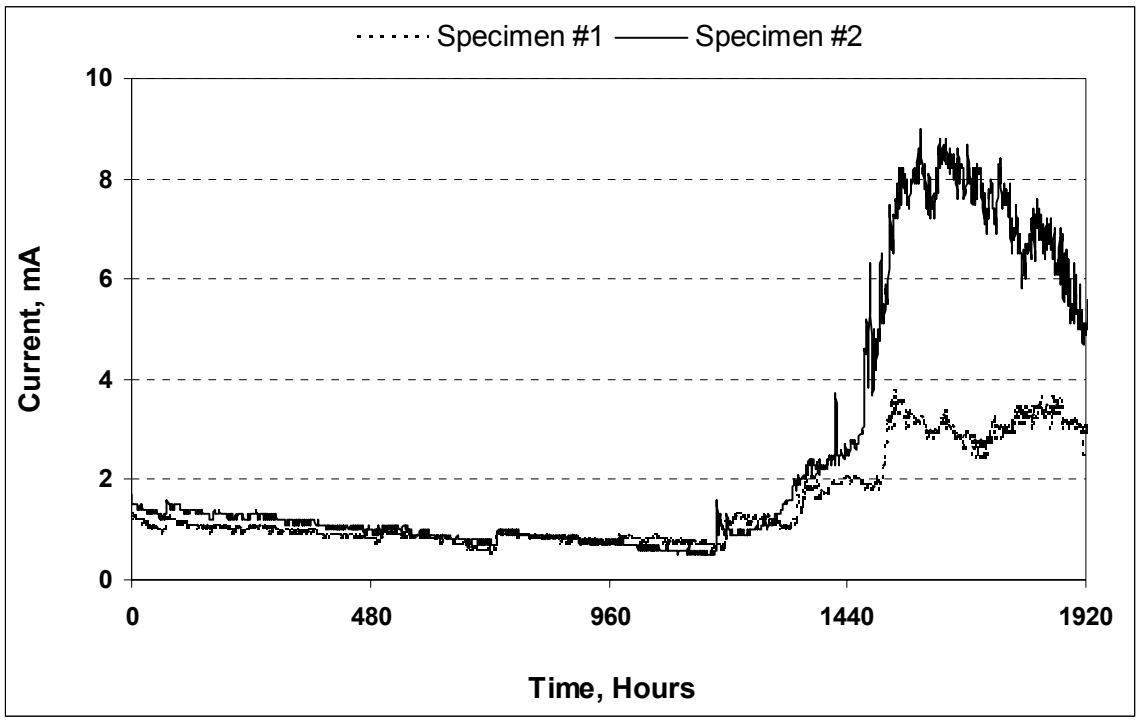

Figure 4.36: Variation of current with time in the fiber reinforced concrete specimens prepared with Riyadh aggregate.

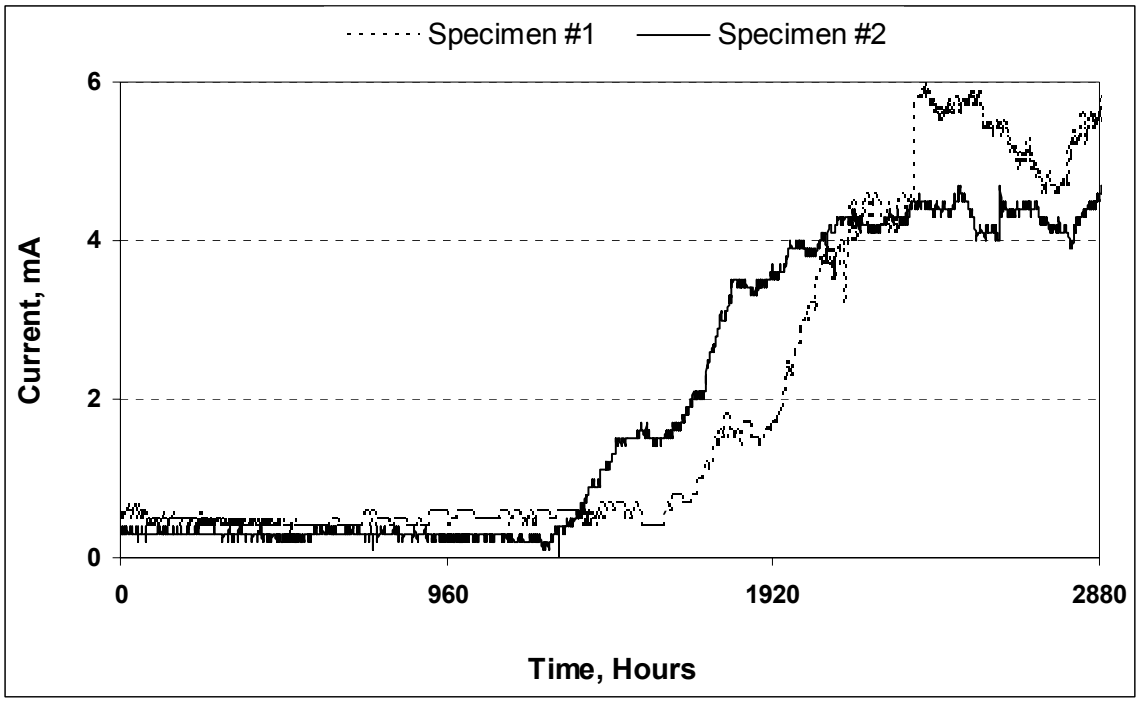

Figure 4.37: Variation of current with time in the plain cement concrete specimens prepared with steel slag aggregate.

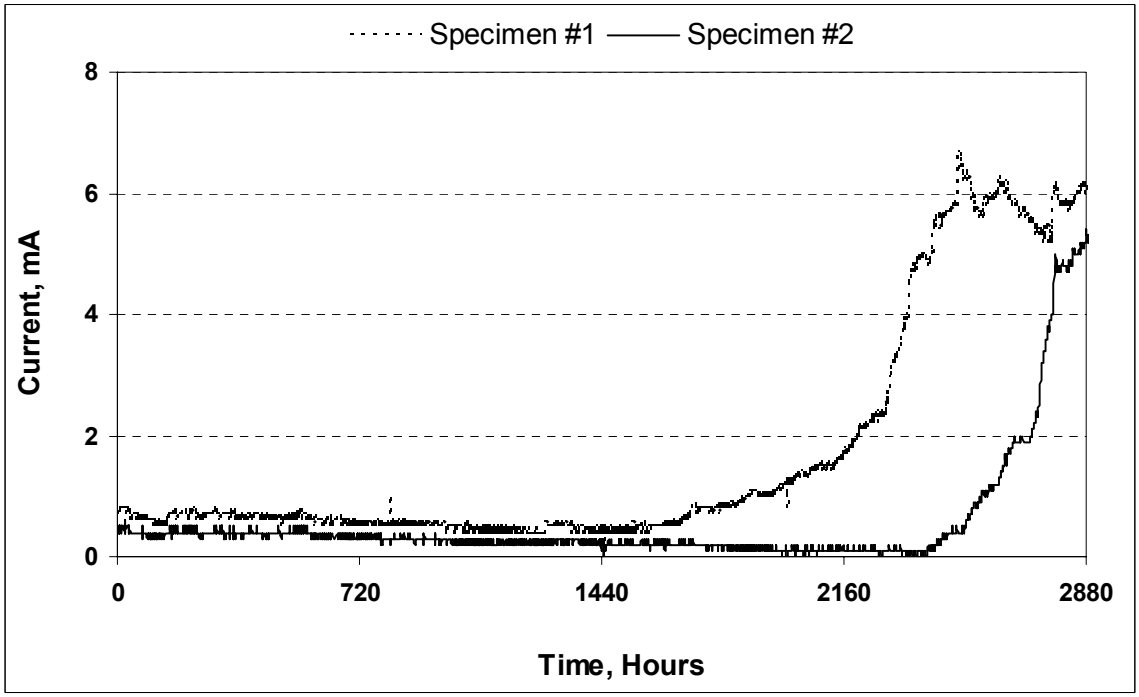

Figure 4.38: Variation of current with time in the silica fume cement concrete specimens prepared with steel slag aggregate.

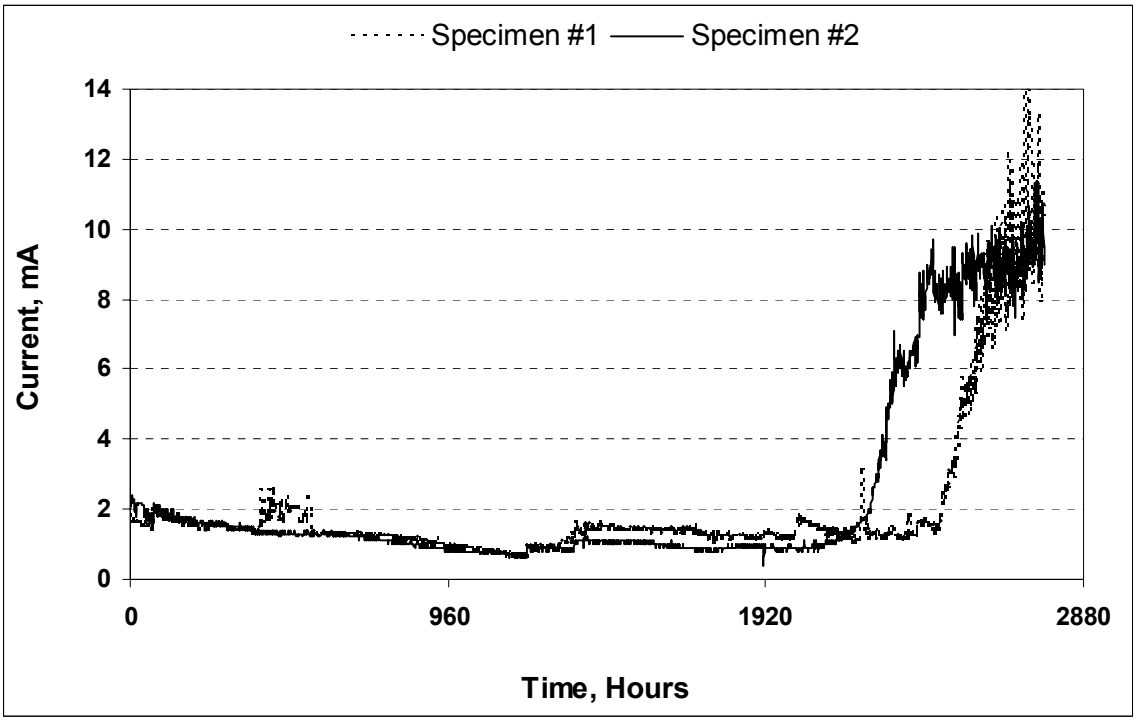

Figure 4.39: Variation of current with time in the fiber reinforced concrete specimens prepared with steel slag aggregate.

Table 4.7: Time to initiation of concrete cracking due to reinforcement corrosion

Aggregate Type / Mix Type	Time to Initiation of Cracking, Hours		
	Plain	Silica fume	Silica fume + Fibers
Abu-Hadriyah Aggregate	1350	1440	1550
Riyadh Aggregate	1400	1500	1600
Steel Slag Aggregate	1820	2340	2550

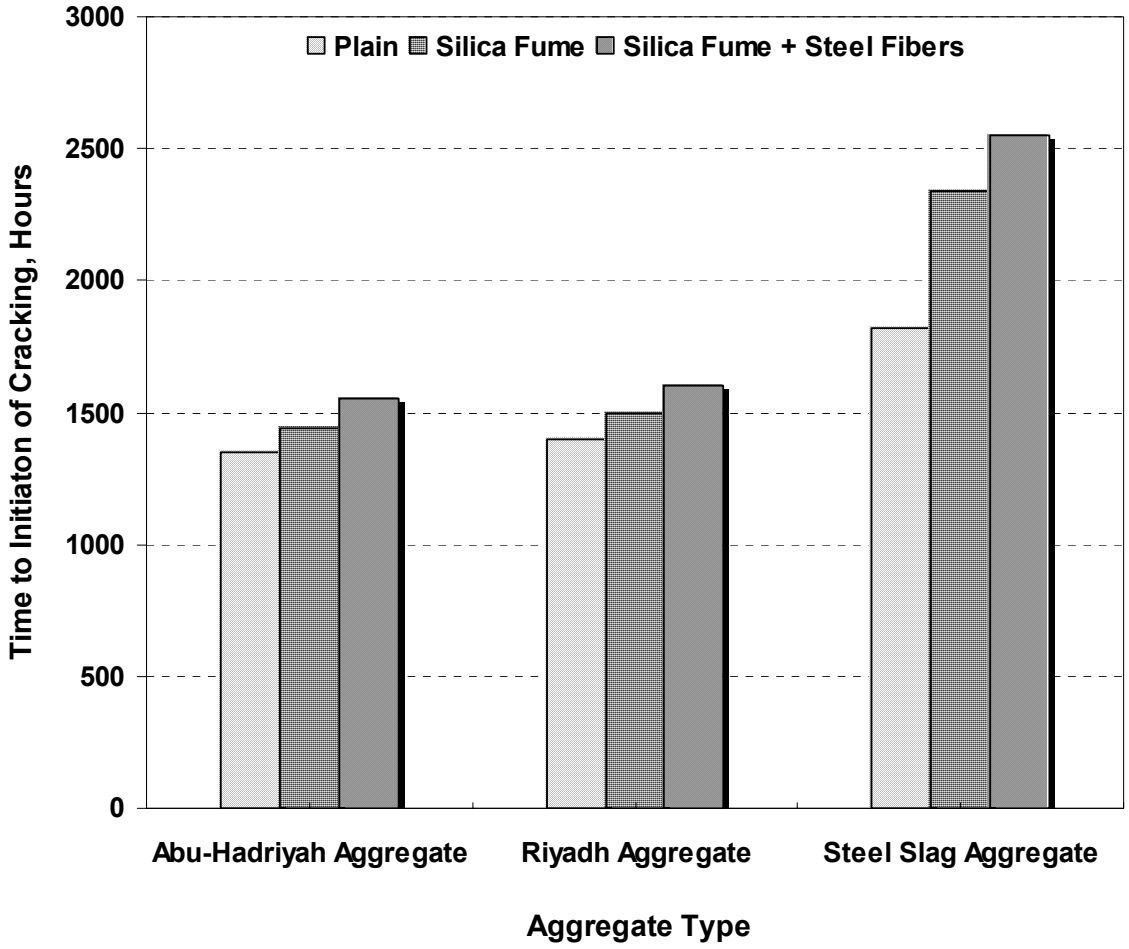

Figure 4.40: Effect of mix design on time to initiation of concrete cracking due to accelerated reinforcement corrosion.

Table 4.8: Percentage improvement in time to cracking of concrete due to reinforcement corrosion due to addition of silica fume and steel fibers to plain cement concrete

Aggregate Type	Mix Type	Time to Cracking of Concrete due to Reinforcement Corrosion (Hours)	% Improvement
Abu-Hadriyah	Plain Cement	1350	—
	Silica Fume Cement	1440	7
	Silica Fume + Steel Fibers	1550	15
Riyadh	Plain	1400	—
	Silica Fume	1500	7
	Silica Fume + Steel Fibers	1600	14
Steel Slag	Plain	1820	—
	Silica Fume	2340	29
	Silica Fume + Steel Fibers	2550	40

The use of steel fibers didn't significantly increase the time to initiation of cracking of concrete due to reinforcement corrosion, but it changed the crack geometry from one large crack to smaller cracks. The use of discrete fibers has distributed the stress evenly throughout the material, instead of the stress building around the biggest flaw and causing a larger crack to open there, the stress build-up around several flaws and causing several smaller microcracks to open.

Figure 4.41 shows the plain cement concrete specimen with only one large, easily visible central crack, while Figure 4.42 shows a steel fiber reinforced specimen exhibiting multiple microcracks. The steel fibers help in stitching the cracks at the ends, perhaps shortening the length of crack and reducing the crack area. The stitching effect of steel fiber reinforced concrete observed in this study is in good agreement with the observation made by Rapoport [66].

Figure 4.43 shows the cross sectional view of a concrete specimen with corroded reinforcement bar when subjected to accelerated corrosion, but the discreet steel fibers were still intact. Figure 4.44 shows the corroded bars extracted from same concrete specimens, which show the extent of damage caused to rebars due to accelerated corrosion. Figure 4.45 shows the close up view of damaged bars showing pitting type of corrosion caused due to chlorides ions.

Figure 4.46 shows the effect of aggregate quality on the time to cracking of concrete due to reinforcement corrosion in plain, silica fume and fiber reinforced concrete specimens. It was noted from the experimental results that, the quality of aggregate had significant effect on the time to cracking of concrete due to

Figure 4.41: Development of single central crack due to reinforcement corrosion in plain cement concrete specimen subjected to impressed anodic potential.

Figure 4.42: Close up view of fiber reinforced concrete specimen when subjected to accelerated corrosion showing multiple microcracks.

Figure 4.43: Cross sectional view of fiber reinforced concrete specimen when subjected to accelerated corrosion.

Figure 4.44: Corroded bars extracted from concrete specimens after accelerated reinforcement corrosion.

Figure 4.45: Close up view of damaged bars showing pitting type of corrosion.

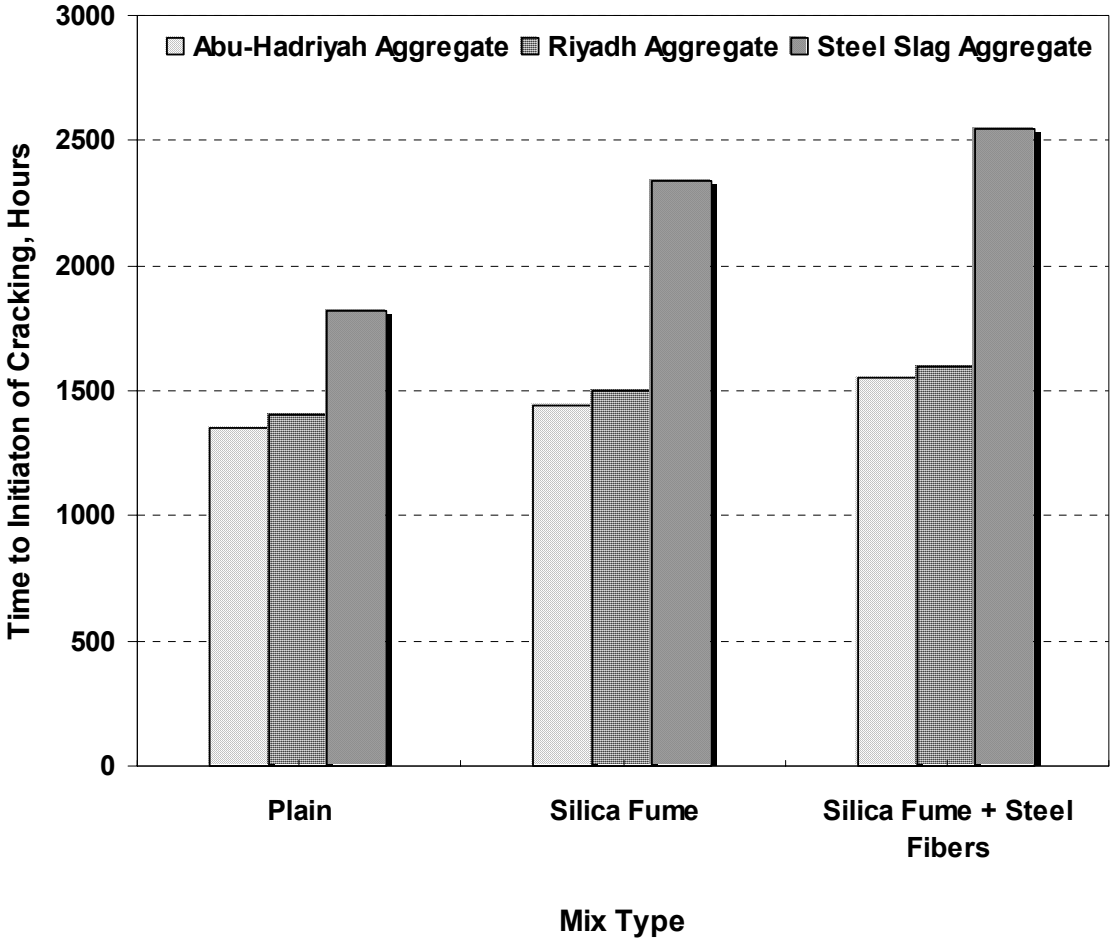

Figure 4.46: Effect of aggregate quality on time to initiation of crack due to reinforcement corrosion when subjected to an impressed anodic potential of 2.5 volts

reinforcement corrosion. The highest time to initiation of cracking was noted in the specimens prepared with steel slag aggregates. In all the three mix designs, the use of steel slag aggregate had considerably delayed the time to initiation of cracking due to reinforcement corrosion. The performance of Riyadh and Abu-Hadriyah aggregates was nearly the same when exposed to accelerated corrosion.

The percentage improvement in the time to cracking in the concrete specimens due to replacement of Abu-Hadriyah aggregate with Riyadh and steel slag aggregate is tabulated in Table 4.9. The percentage improvement in the time to cracking due to reinforcement corrosion, due to the use of steel slag aggregate instead of Abu-Hadriyah aggregate was 35 to 65%, while it was 3 to 4 % when Abu-Hadriyah aggregate was replaced with Riyadh aggregate.

4.5 EFFECT OF AGGREGATE QUALITY ON CHLORIDE DIFFUSSION

The effect of aggregate quality on chloride diffusion was studied in concrete specimens prepared with Abu-Hadriyah, Riyadh and steel slag aggregates. The concrete specimens were immersed in 5% sodium chloride solution for three months with one face exposed to the solution. At the end of the exposure period, the chloride concentration at various depths was determined and the chloride profile was plotted. The chloride profile obtained was utilized to determine the diffusion coefficients by solving Fick's second law of diffusion.

Table 4.10 shows the chloride concentration in the concrete specimens at various depths after the exposure period. The chloride concentration profile for the

Table 4.9: Percentage improvement in time to cracking of concrete due to reinforcement corrosion due to use of Riyadh and steel slag aggregates in place of Abu-Hadriyah aggregate

Mix Type	Aggregate Type	Time to Cracking of Concrete due to Reinforcement Corrosion (Hours)	% Improvement
Plain Cement	Abu-Hadriyah	1350	—
	Riyadh	1400	4
	Steel Slag	1820	35
Silica Fume Cement	Abu-Hadriyah	1440	—
	Riyadh	1500	4
	Steel Slag	2340	63
Silica fume + Steel fibers	Abu-Hadriyah	1550	—
	Riyadh	1600	3
	Steel Slag	2550	65

Table 4.10: Chloride concentration at various depths in concrete specimens

Mix Type	Chloride concentration(% wt. of concrete) at depth of					
	0mm	2.5mm	17.5mm	32.5mm	57.5mm	82.5mm
Abu-Hadriyah *(Plain)*	0.21	0.175	0.05	0.02	0.01	0.01
Abu-Hadriyah *(Silica Fume)*	0.18	0.15	0.015	0.01	0.01	0.005
Abu-Hadriyah *(Silica Fume + Steel Fibers)*	0.155	0.139	0.046	0.023	0.023	0.014
Riyadh *(Plain)*	0.165	0.11	0.025	0.01	0.015	0.01
Riyadh *(Silica Fume)*	0.135	0.165	0.015	0.01	0.01	0.01
Riyadh *(Silica Fume+ Steel Fibers)*	0.12	0.121	0.028	0.01	0.005	0.002
Steel Slag *(Plain)*	0.19	0.2	0.01	0.005	0.005	0.01
Steel Slag *(Silica Fume)*	0.16	0.145	0.025	0.01	0.005	0.01
Steel Slag *(Silica Fume + Steel Fibers)*	0.17	0.125	0.028	0.028	0.005	0.01

concrete specimens prepared with crushed limestone from Abu-Hadriyah is shown in the Figure 4.47. The figure shows the chloride concentration at various depths in plain, silica fume and steel fiber reinforced concrete specimens. As expected, the chloride concentration decreased with depth in all the concrete specimens. The chloride concentration decreased significantly up to a depth of about 30 mm. However, beyond this depth, the change in the chloride concentration was not that significant. The chloride concentration in plain cement concrete was more than that in the silica fume and steel fiber reinforced cement concretes. Figures 4.48 and 4.49 show the chloride concentrations in the concrete specimens prepared with Riyadh and steel slag aggregates, respectively. In these concrete specimens also the chloride concentration decreased with the depth of the specimen.

The chloride concentration in the plain cement concrete prepared with Abu-Hadriyah, Riyadh and steel slag aggregates at the depth of 2.5 mm was 0.175, 0.11 and 0.20% by weight of concrete, respectively while these values at a depth of 32.5 mm were 0.02, 0.01 and 0.01%, by weight of concrete, respectively. The chloride concentration, at other depths, in the plain cement concrete specimens was slightly more than that in the silica fume and fiber reinforced concrete specimens. Further, the chloride concentration in the silica fume cement concrete was more than that in the fiber reinforced cement concretes The lower chloride concentration noted in the silica fume cement concrete, compared to plain cement concrete, may be attributed to the reaction of silica fume with calcium hydroxide to form secondary calcium silicate hydrate, which reduces the pores, leading to a dense structure which decreases the diffusion of chloride ions [67].

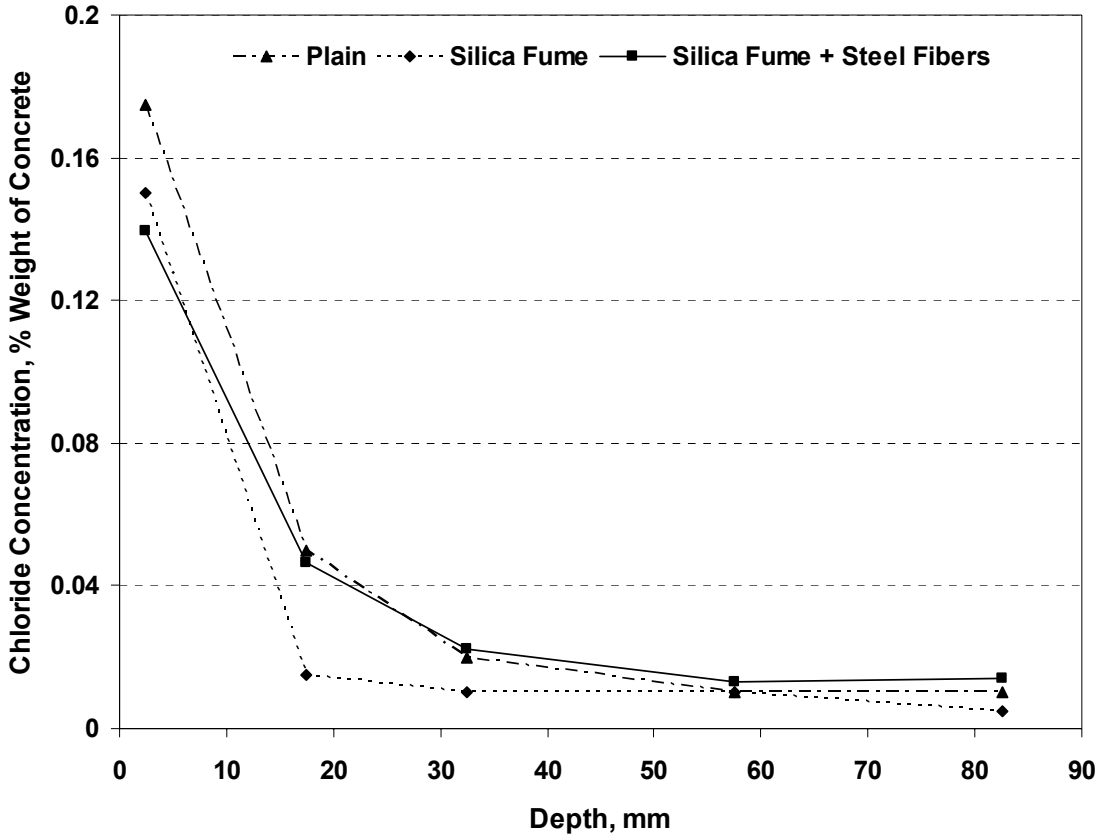

Figure 4.47: Chloride profile for the Abu-Hadriyah aggregate concrete specimens.

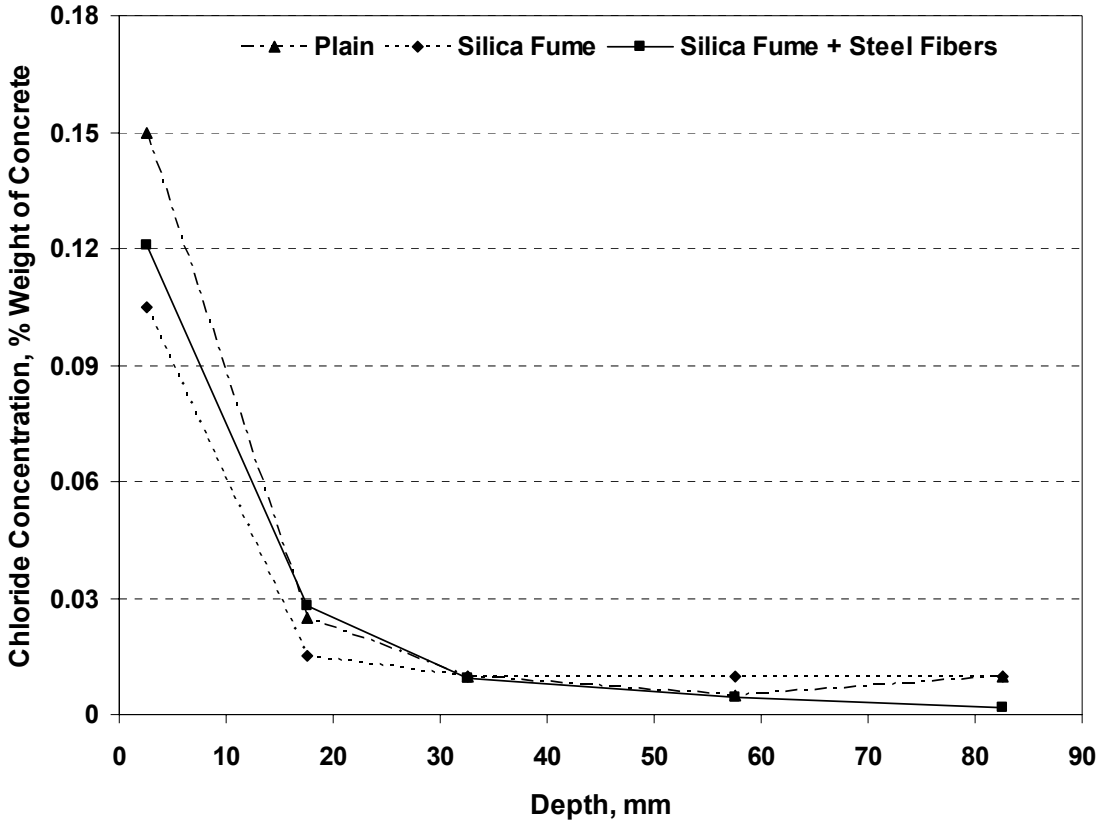

Figure 4.48: Chloride profile for the Riyadh road aggregate concrete specimens.

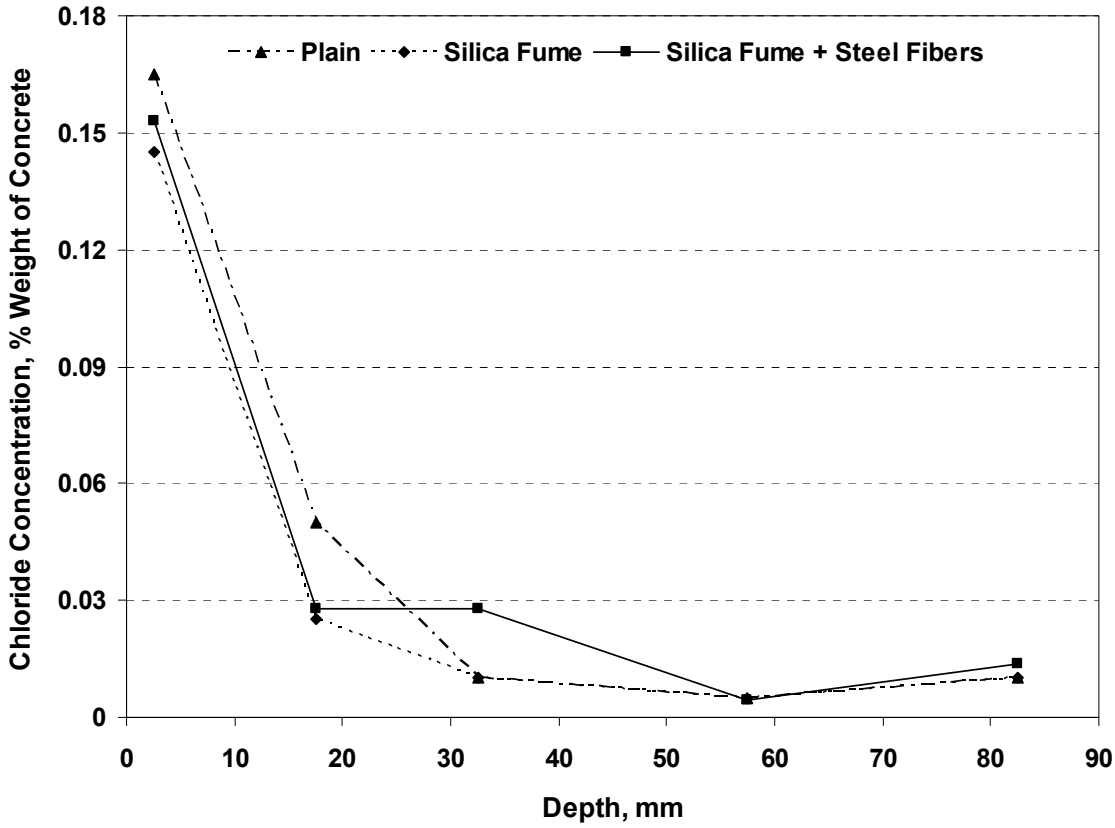

Figure 4.49: Chloride profile for the steel slag aggregate concrete specimens.

Table 4.11 shows the chloride diffusion coefficients in the Abu-Hadriyah, Riyadh and steel slag aggregate cement concrete specimens. The data indicate that the chloride diffusion coefficient for plain cement concrete was more than that of silica fume cement concrete specimens. Figure 4.50 shows the chloride diffusion coefficient for the concrete specimens investigated in this study. The data indicate that the chloride diffusion coefficients did not significantly vary with the type of aggregates. However, the mix design has a significant effect. The chloride diffusion coefficient for Abu-Hadriyah aggregates was higher than that for the other two aggregate types. The values of chloride diffusion coefficient for the Abu-Hadriyah aggregate concrete were in the range of 3.4 to 7.3 x 10^{-8} cm^2/s; in the Riyadh aggregate concrete specimens it was in the range of 3.2 to 6.2 x 10^{-8} cm^2/s, while it was in the range of 3.2 to 6.5 x 10^{-8} cm^2/s for the steel slag aggregate concrete specimens.

4.6 EFFECT OF THERMAL VARIATIONS ON CONCRETE PROPERTIES

The effect of thermal variation on reinforcement corrosion and tensile strength was investigated on the concrete specimens prepared with Abu-Hadriyah, Riyadh and steel slag aggregates by exposing them to thermal variations. After 28 days of water curing, the specimens were kept in an oven for exposure to thermal variation. Each thermal cycle consisted of exposing the concrete specimens at 70 °C for 8 hours and at 25 °C for 16 hours.

Table 4.11: Chloride diffusion coefficients in concrete specimens prepared with the selected aggregates.

Aggregate/Concrete	Coefficient of chloride diffusion, 10^{-8} cm^2/s
Abu-Hadriyah (*Plain*)	7.3
Abu-Hadriyah *(Silica Fume)*	3.8
Abu-Hadriyah *(Silica Fume + Steel Fibers)*	3.4
Riyadh *(Plain)*	6.2
Riyadh *(Silica Fume)*	3.1
Riyadh *(Silica Fume+ Steel Fibers)*	3.2
Steel Slag *(Plain)*	6.5
Steel Slag *(Silica Fume)*	3.4
Steel Slag *(Silica Fume + Steel Fibers)*	3.1

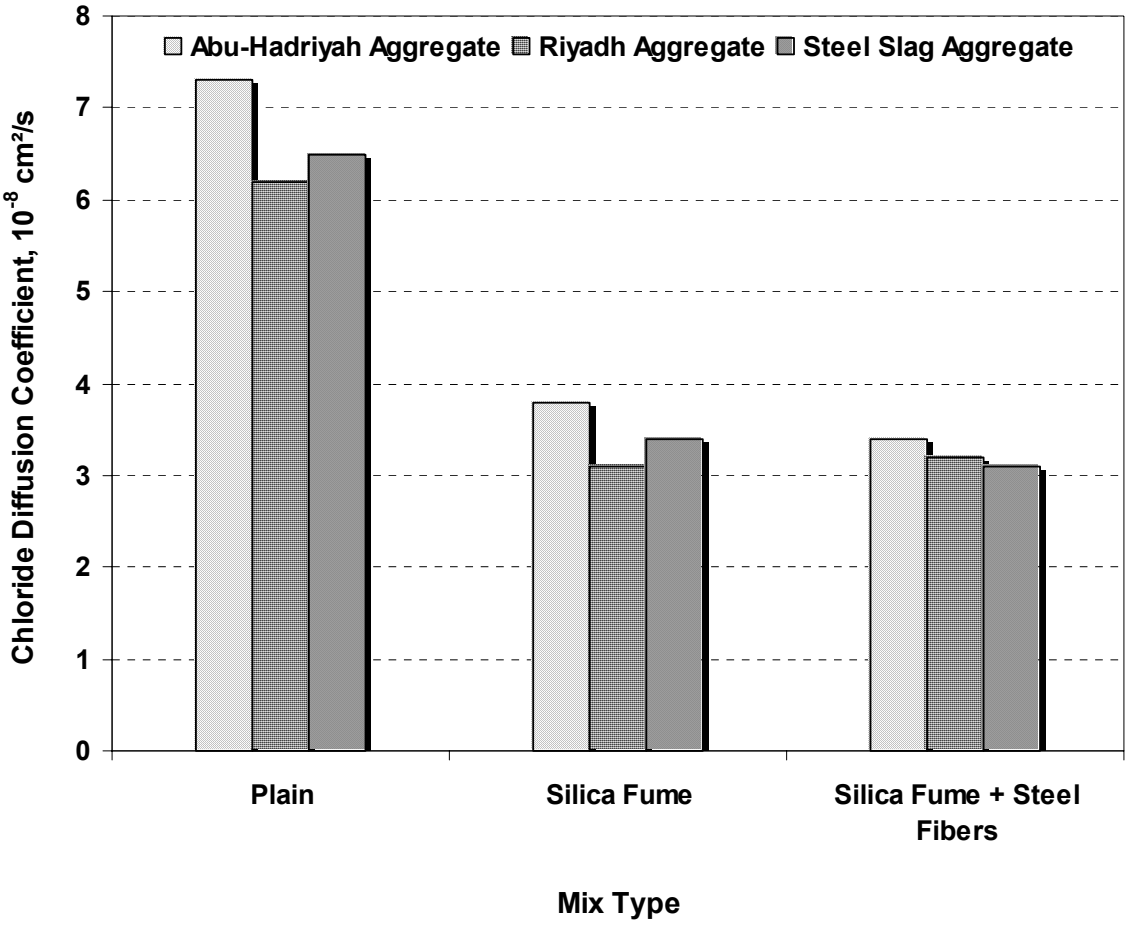

Figure 4.50: Chloride diffusion coefficient for the concrete specimens prepared with selected aggregates.

4.6.1 Effect of Thermal Variation on Tensile Strength

The effect of thermal variation on the split tensile strength of concrete prepared with the selected aggregates was evaluated over a period of 6 months. The concrete specimens were tested after 30, 60, 90 and 180 thermal cycles. The split tensile strength of plain cement concrete specimens increased up to 90 thermal cycles, then a decrease in the strength was noted. A similar trend was noted in the concrete specimens prepared with 1% steel fibers and silica fume cement concrete. However, the split tensile strength of 1% steel fiber concrete specimens was more than that of plain and silica fume cement concrete specimens. After 90 heat-cool cycles, the highest tensile strength of 5.78 MPa was recorded in the fiber reinforced concrete specimens, followed by those prepared with silica fume and plain cement concretes.

Figure 4.51 shows the split tensile strength of the concrete specimens prepared with crushed limestone from Abu-Hadriyah. The split tensile strength values after 90 heat-cool cycles in steel fiber, silica fume and plain cement concrete specimens were 4.07, 4.01 and 3.91 MPa, respectively. A gradual decrease in the split tensile strength, due to exposure to thermal variations, was noted in all the specimens. The split tensile strength values noted after 180 thermal cycles in the fiber reinforced, silica fume and plain cement concrete specimens prepared with Abu-Hadriyah aggregates was 4.01, 3.61 and 3.45 MPa, respectively. The reduction in the split tensile strength, due to thermal exposure, in fiber reinforced, silica fume and plain cement concrete being 1.5, 10, and 12 %, respectively.

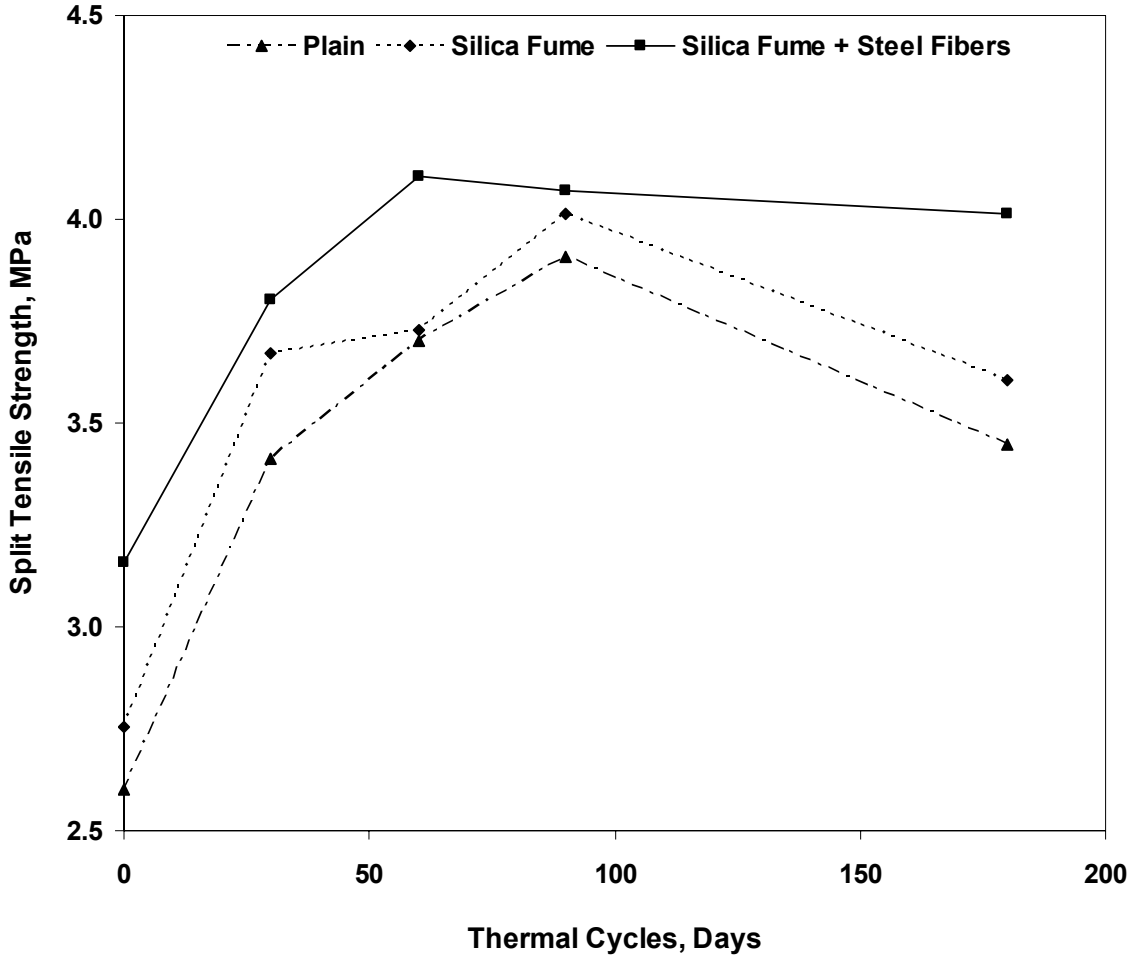

Figure 4.51: Effect of thermal cycling on the split tensile strength of concrete specimens prepared with Abu-Hadriyah aggregates.

Figure 4.52 depicts the effect of thermal variations on the split tensile strength of concrete specimens prepared with Riyadh aggregates. Thermal variation had negligible effect on the split tensile strength of steel fiber reinforced concrete within the time range of this investigation. The split tensile strength of the silica fume cement concrete increased up to 60 thermal cycles, thereafter a decrease was noted. In the plain cement concrete, the decrease in the split tensile strength was noted after 90 thermal cycles. The split tensile strength after 60 thermal cycles in plain, silica fume and steel fiber reinforced cement concretes was 4.06, 4.06 and 4.66 MPa, respectively. The strength after 180 thermal cycles in plain, silica fume and fiber reinforced cement concretes, was 3.55, 3.56 and 4.66 MPa, respectively. The reduction in the split tensile strength due to thermal variation in fiber reinforced, silica fume and plain concrete being, 3, 12, and 16 %, respectively.

The effect of thermal variations on the split tensile strength of concrete specimens prepared with steel slag aggregates is shown in Figure 4.53. In this group of specimens, the split tensile strength of steel fiber reinforced concrete increased with increasing the thermal variations. The split tensile strength of all the concrete specimens increased up to 90 thermal cycles, after which a small reduction in the split tensile strength was noted. After 90 thermal cycles the highest split tensile strength was noted in the fiber reinforced cement concrete, followed by silica fume and plain cement concrete. The split tensile strength in these specimens was 5.11, 5.03 and 4.68 MPa, respectively. The reduction in the split tensile strength due to thermal variation in fiber reinforced, silica fume and plain cement concrete being, 3, 3, and 2 %, respectively.

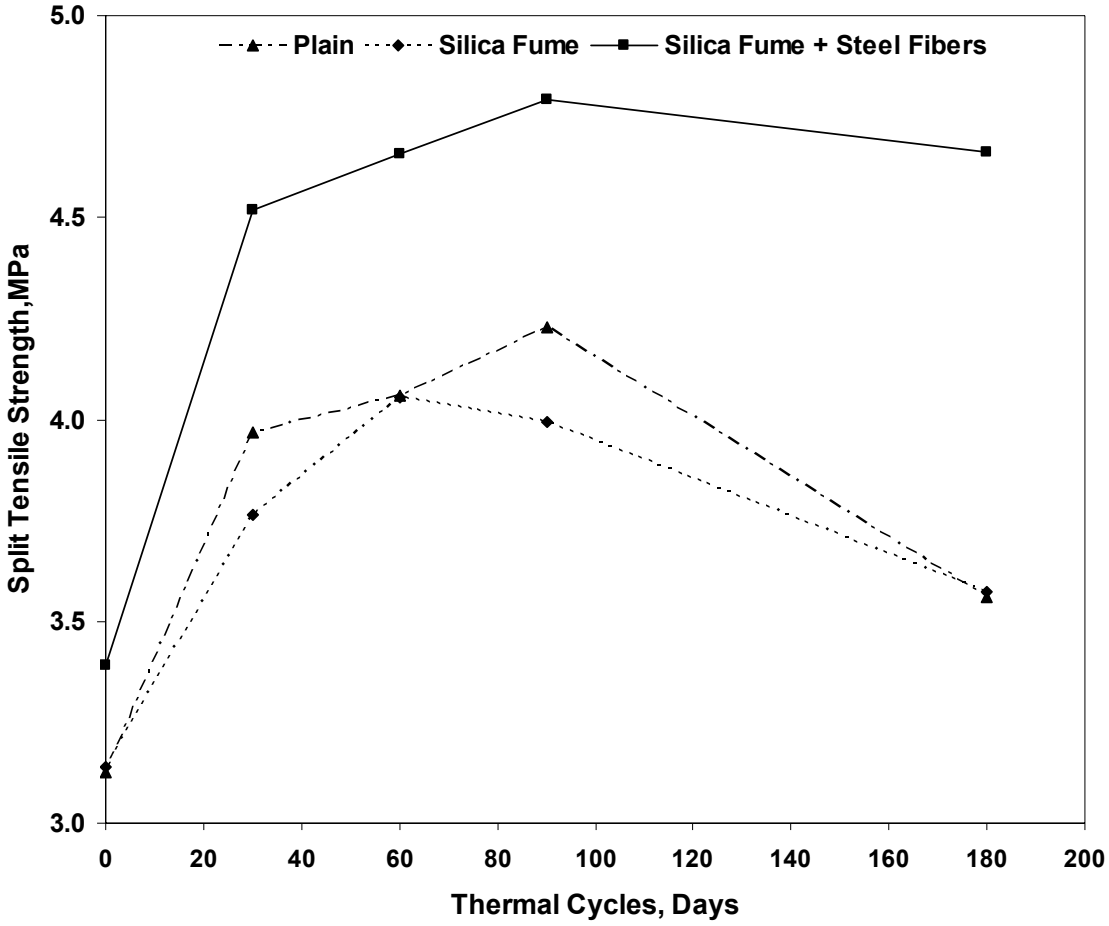

Figure 4.52: Effect of thermal cycling on split tensile strength of concrete specimens prepared with Riyadh aggregate.

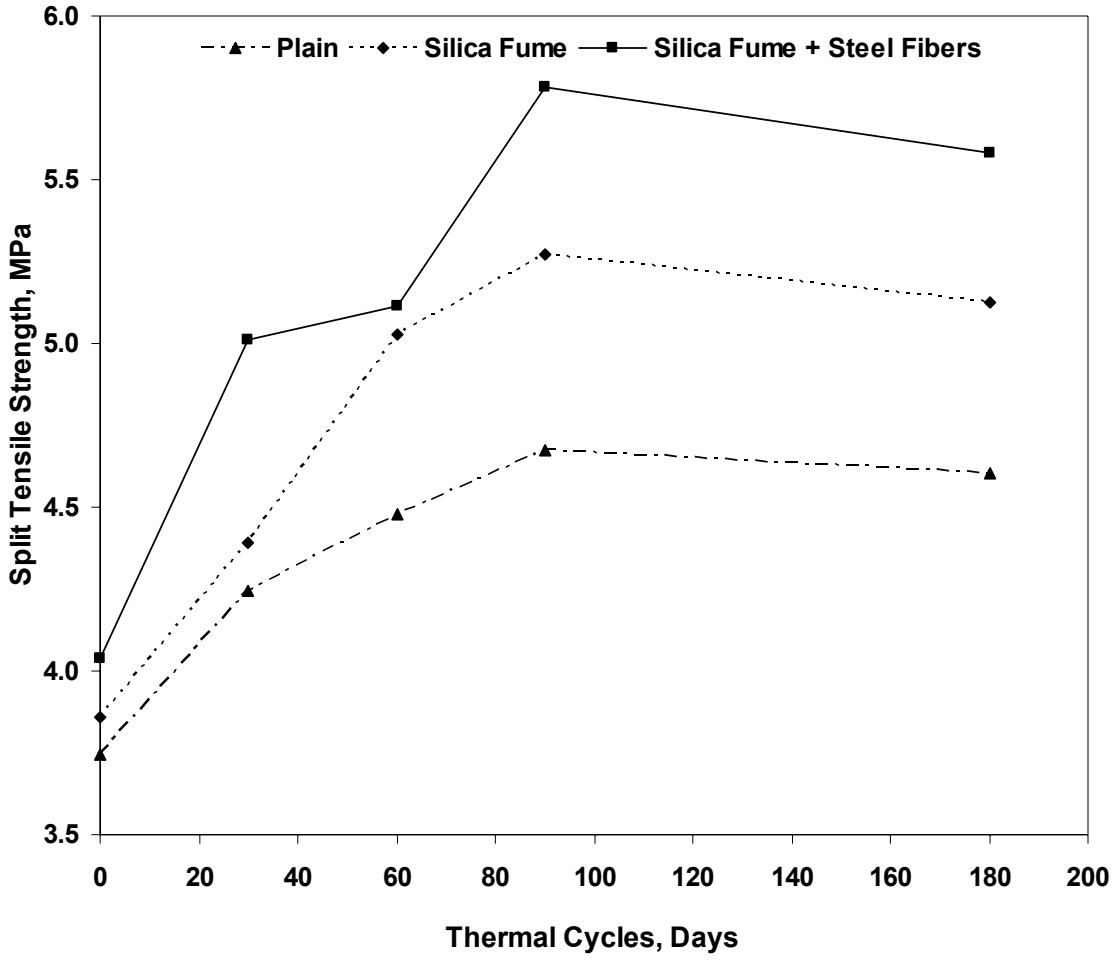

Figure 4.53: Effect of thermal cycling on split tensile strength of concrete specimens prepared with steel slag aggregate

Table 4.12 shows the effect of thermal variation on the percentage improvement in split tensile strength of concrete specimens prepared with the selected aggregates due to addition of silica fume and silica fume plus fibers. The effect of addition of silica fume alone was not significant in some mixes; decrease in the split tensile strength was noted due to addition of silica fume when exposed to thermal cycles. The addition of silica fume plus fibers improved the split tensile in all the concrete specimens prepared with the selected aggregates, even after exposure to 180 thermal cycles.

The superior performance of steel fiber concrete specimens may be due to the random distribution of steel fibers in all the directions of the concrete specimens. The addition of steel fibers had helped in the transferring stresses developed due to thermal variation evenly throughout the concrete matrix, which resulted in more resistant to cracking. The resistance of concrete to elevated temperature depends on several other factors also. According to Khayat and Aiticin [68], factors such as the moisture content of concrete, level and duration of temperature exposure, the size and distribution of pores in the cement paste, and the size of concrete member affect the resistance of concrete to elevated thermal variations.

Depending on the rate and level of temperature exposure, some of the water in concrete can evaporate quickly, leading to shrinkage and cracking of concrete. Painter [69] monitored the relative change in weight and pulse velocity of concrete prisms exposed for 60 days to temperatures of 75, 150 and 300 °C. The concrete specimens were prepared with W/(C+SF) ratios of 0.40 and 0.60 and silica fume

Table 4.12: Percentage improvement in the split tensile strength of concrete specimens after thermal cycles due to addition of silica fume and silica fume plus steel fibers to plain cement concrete

Aggregate Type	Mix Type / Days	Split Tensile Strength, Mpa				% Improvement			
		30	**60**	**90**	**180**	**30**	**60**	**90**	**180**
Abu-Hadriyah	Plain Cement	3.41	3.70	3.91	3.45	—	—	—	—
	Silica Fume	3.67	3.73	4.01	3.61	8	1	3	5
	Silica Fume +Steel Fibers	3.80	4.11	4.07	4.01	4	10	1	11
Riyadh	Plain Cement	3.97	4.06	4.23	3.56	—	—	—	—
	Silica Fume	3.76	4.06	3.99	3.57	-5	0	-6	0
	Silica Fume +Steel Fibers	4.52	4.66	4.79	4.66	20	15	20	31
Steel Slag	Plain Cement	4.24	4.48	4.68	4.60	—	—	—	—
	Silica Fume	4.39	5.03	5.27	5.13	4	12	13	12
	Silica Fume +Steel Fibers	5.01	5.11	5.78	5.58	14	2	10	9

replacement of 0 and 15%, by weight of cement. His results show that both air-entrained and non-air-entrained concrete containing silica fume had greater weight loss and larger reduction in pulse velocity than plain cement concrete.

Reis [70] reported that the inclusion of steel fibers in the concrete resulted in a ductile behavior of the concrete, both at high temperature and at room temperature. He concluded that the properties of high-strength steel fiber reinforced concrete were more affected by high temperature than normal-strength concrete without fibers during the heating phase. It is more difficult for moisture to escape from high-strength concrete elements in a high temperature situation because of the low porosity of this type of concrete. Explosive spalling is therefore a critical problem in the behavior of high-strength concrete during high temperature exposures. The inclusion of steel fibers in the Portland cement concrete has been recognized as a means of improving its resistance to cracking.

Figures 4.54 through 4.56 show the effect of thermal variation on the split tensile strength of plain, silica fume and steel fiber cement concrete specimens prepared with Abu-Hadriyah, Riyadh and steel slag aggregates. The split tensile strength of all the concrete specimens increased upto 90 cycles, then there was a reduction in the split tensile strength. The highest reduction in the strength was noted in the silica fume concrete specimens prepared with Riyadh aggregate. The reduction in the split tensile strength of plain, silica fume, and steel fiber cement concrete specimens prepared with steel slag aggregate was very negligible.

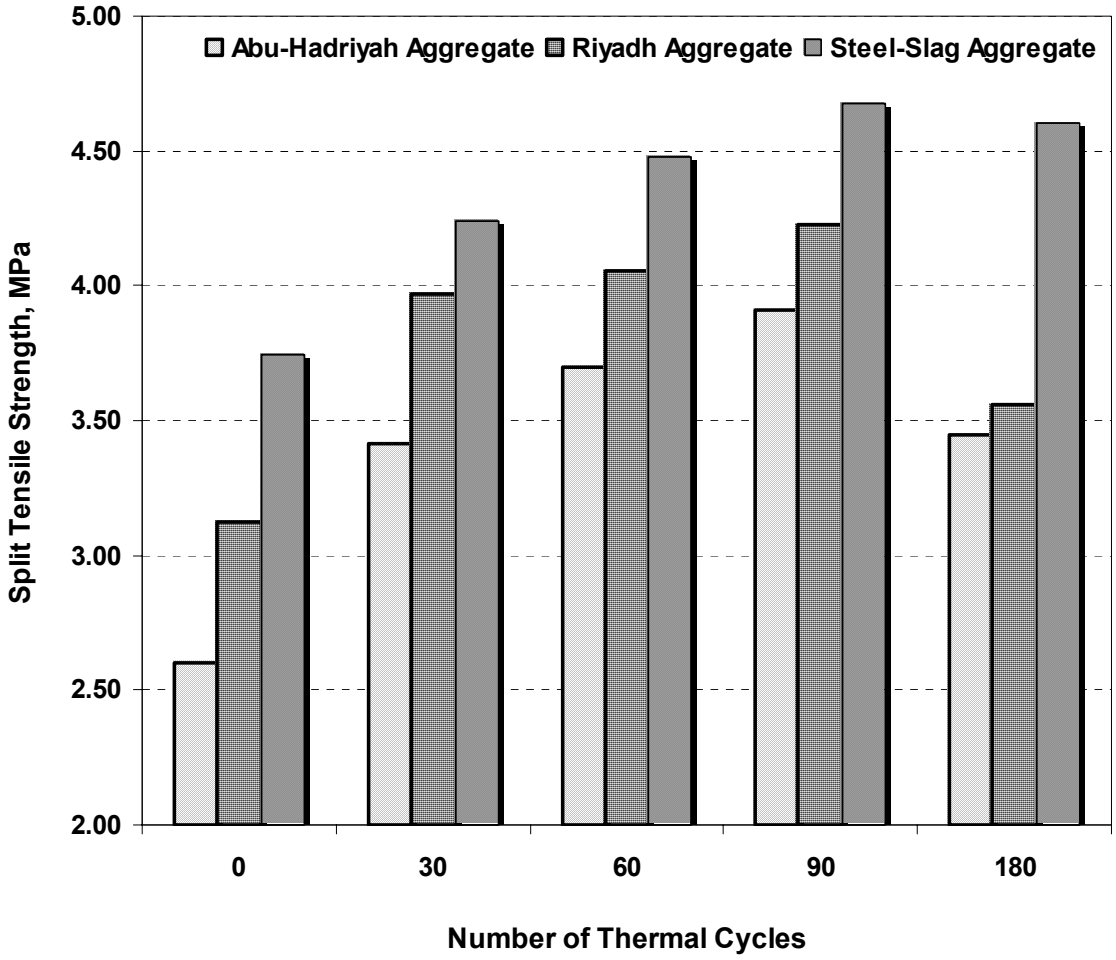

Figure 4.54: Effect of thermal variations on split tensile strength of plain cement concrete specimens.

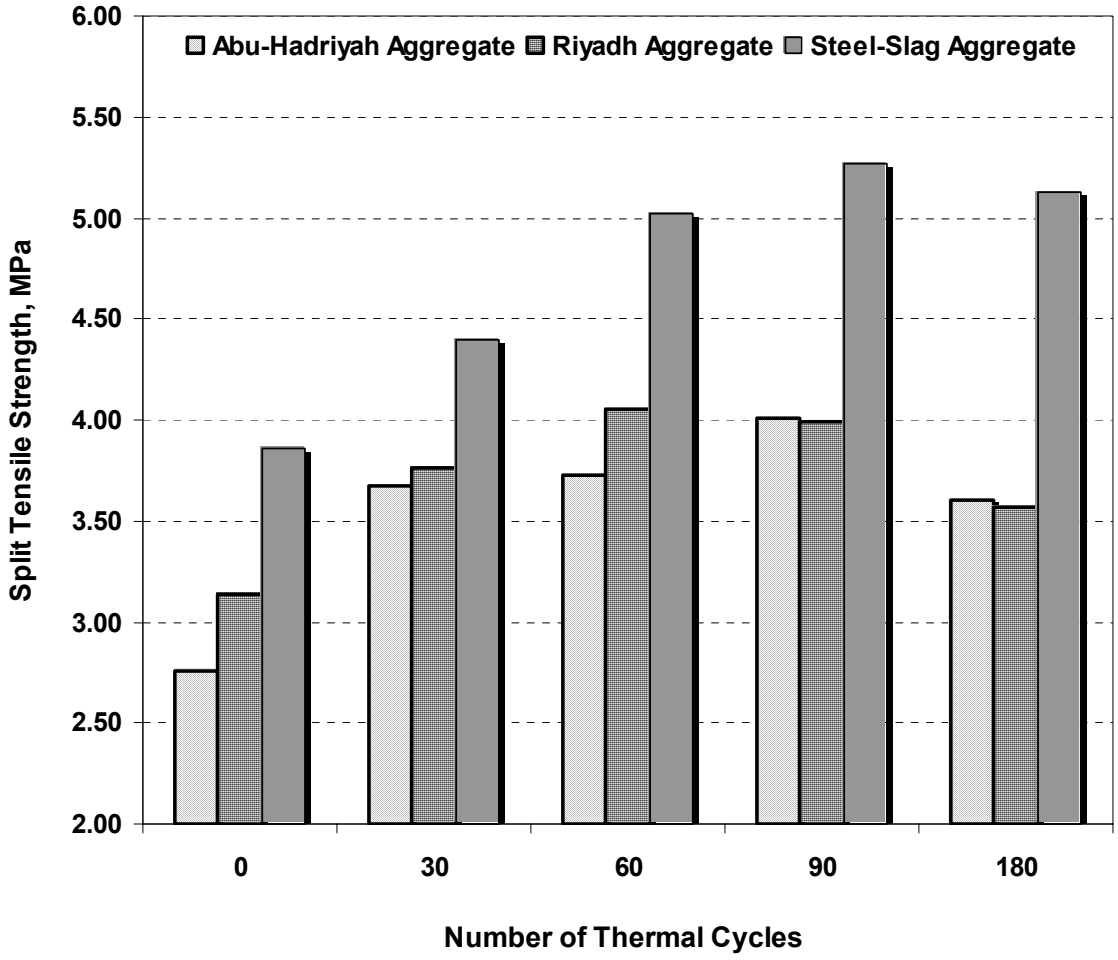

Figure 4.55: Effect of thermal variation on split tensile strength of silica fume cement concrete specimens.

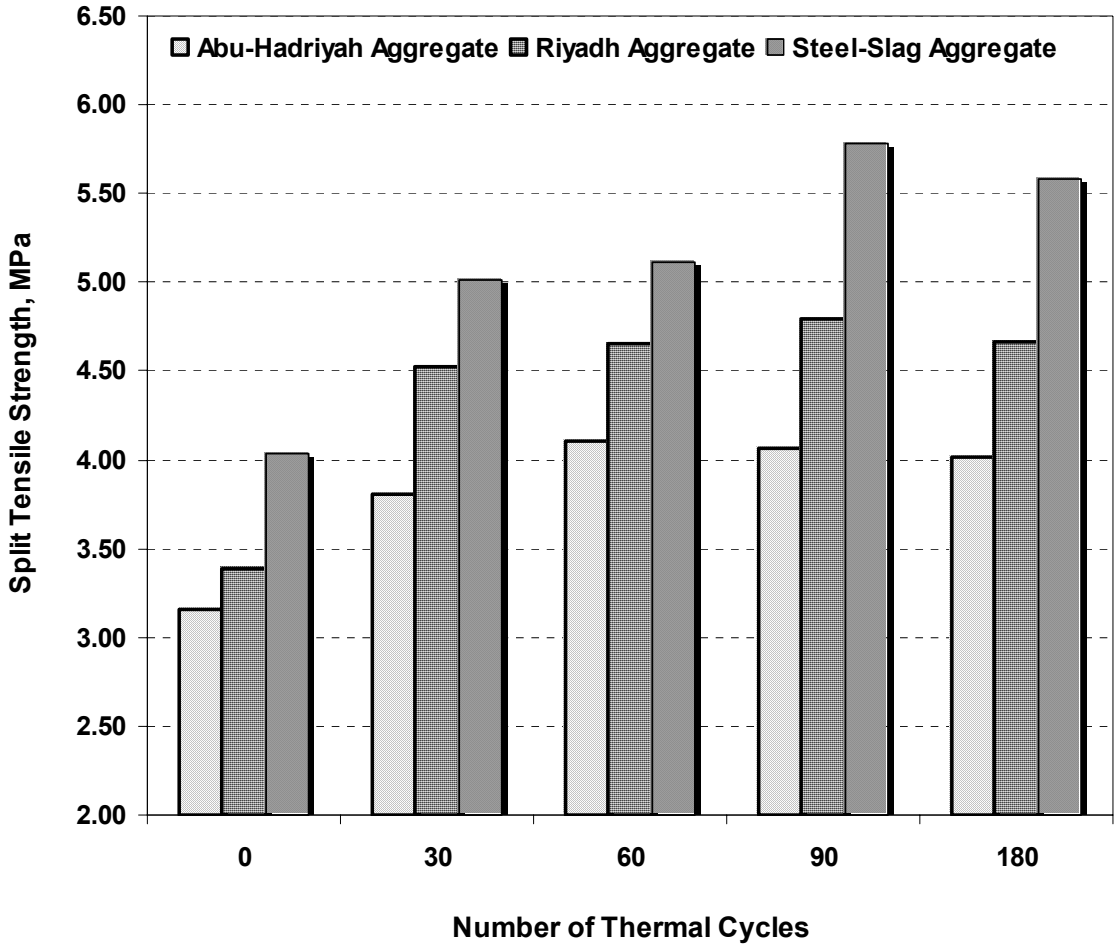

Figure 4.56: Effect of thermal variation on split tensile strength of steel fiber cement concrete specimens.

The data in Figures 4.54 through 4.56 indicate that the thermal performance of concrete is strongly influenced by the thermal properties of the aggregate from which it was prepared. This is because the aggregate constitutes 70 to 80 percent of the total solid volume of the concrete. The character and quality of the bond between aggregate and cement matrix (interfacial zone) also significantly affect the concrete behavior under thermal exposure. Significant amount of internal stresses may develop due to differences in the thermal coefficients of cement paste and aggregate, which results in thermal incompatibility and cracking.

The data in Table 4.13 shows the percentage improvement in split tensile strength of the concrete specimens after exposure to thermal cycles when Abu-Hadriyah aggregate was replaced by Riyadh and steel slag aggregates. The average improvement in the split tensile strength of the concrete specimens due to replacement of Abu-Hadriyah aggregate with Riyadh aggregate was in the range of 0 to 19%, while it was in the range of 7 to 44% when steel slag aggregate was used in place of Abu-Hadriyah aggregate.

4.6.2 Effect of Thermal Variations on Corrosion Resistance

The effect of thermal variation on the corrosion-resistance of concrete specimens prepared using the selected aggregates was also evaluated. The centrally reinforced concrete specimens prepared using the selected aggregates were exposed to 120 heat-cool cycles. After the completion of heat-cool exposure, the specimens were removed from the oven and divided into two batches. The first batch was exposed to 5% sodium chloride solution under normal conditions, then corrosion

Table 4.13: Percentage improvement in the split tensile strength of concrete specimens after thermal cycles when Riyadh and steel slag aggregates were used in place of Abu-Hadriyah aggregate

Mix Type	Aggregate Type / Days	Split Tensile Strength (MPa)				% Improvement			
		30	**60**	**90**	**180**	**30**	**60**	**90**	**180**
Plain Cement	Abu-Hadriyah	3.41	3.70	3.91	3.45	—	—	—	—
	Riyadh	3.97	4.06	4.23	3.56	16	10	8	3
	Steel Slag	4.24	4.48	4.68	4.60	7	10	11	29
Silica Fume Cement	Abu-Hadriyah	3.67	3.73	4.01	3.61	—	—	—	—
	Riyadh	3.76	4.06	3.99	3.57	2	9	0	0
	Steel Slag	4.39	5.03	5.27	5.13	17	24	32	44
Silica Fume +.Steel Fibers	Abu-Hadriyah	3.80	4.11	4.07	4.01	—	—	—	—
	Riyadh	4.52	4.66	4.79	4.66	19	13	18	16
	Steel Slag	5.01	5.11	5.78	5.58	11	10	21	20

potentials and corrosion current density were monitored. The second batch of concrete specimens was then subjected to accelerated corrosion.

Figures 4.57 through 4.59 show the corrosion potentials on steel in the concrete specimens prepared with the selected aggregates and exposed to thermal variations. In all the specimens, the corrosion potentials recorded in the first week were less than -270 mV SCE, the threshold limit specified by ASTM C 876. A comparison of data in Figures 4.8 through 4.15 with those in Figures 4.57 through 4.59 indicates that the corrosion potentials were significantly affected by thermal variations.

Figures 4.60 through 4.62 show the variation in the corrosion current density with time. The corrosion current density in the initial stages of exposure period in all the concrete specimens was more than 0.3 $\mu A/cm^2$, which is evident of the fact that there was active corrosion in all the specimens after thermal exposure. This indicates that the exposure of concrete specimens to thermal variations increases the chance of reinforcement corrosion mainly due to the formation of microcracks.

The I_{corr} on steel bars embedded in the concrete specimens prepared with steel slag aggregates was relatively less than that in the specimens prepared with the other two aggregate types. The I_{corr} on steel in the steel slag aggregate concrete was in the range of 0.3 to 0.68 $\mu A/cm^2$, while in Riyadh aggregate concrete it was in the range of 0.32 to 1.72 $\mu A/cm^2$. In the concrete specimens prepared with Abu-Hadriyah aggregate, it was in the range of 0.61 to 1.74 $\mu A/cm^2$. Further,

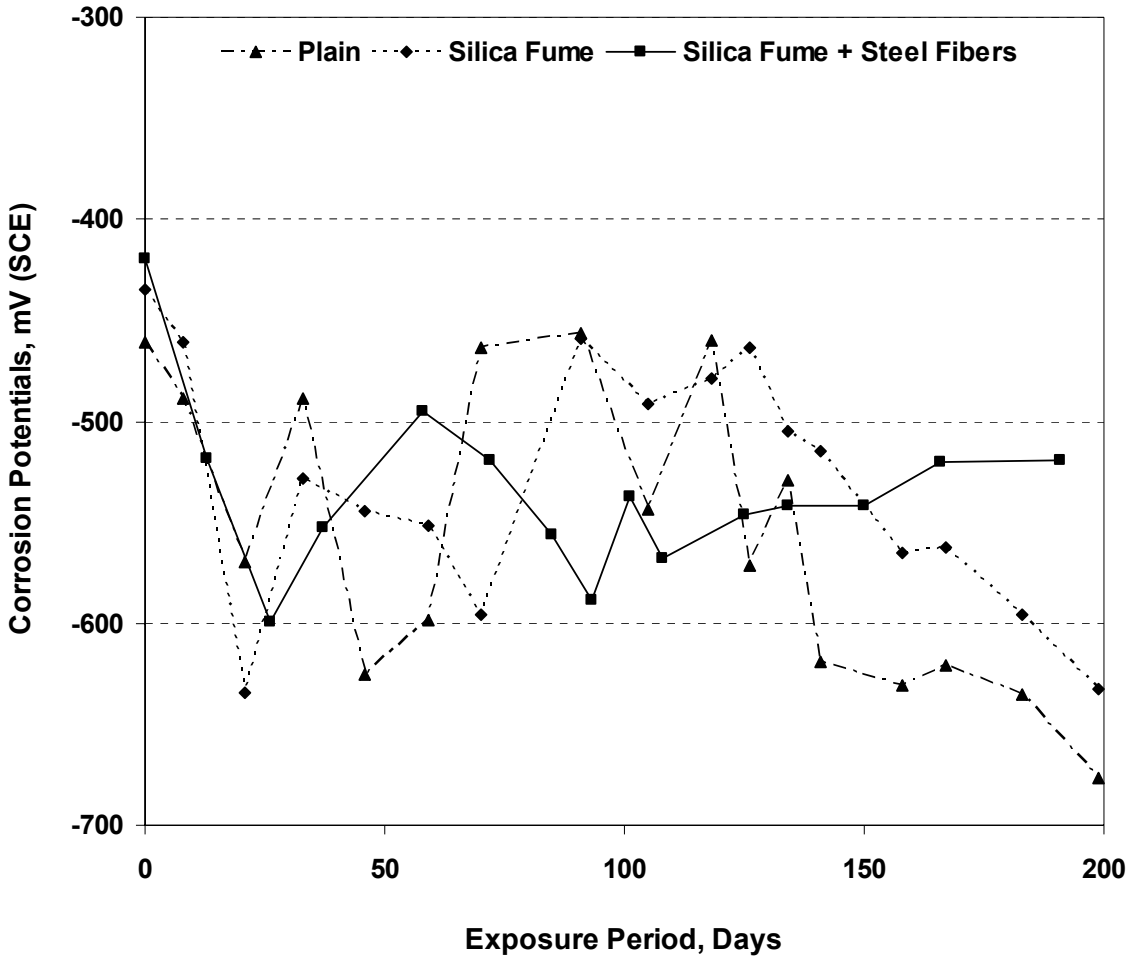

Figure 4.57: Variation of corrosion potentials on the steel in the Abu-Hadriyah aggregate concrete specimens exposed to thermal variations.

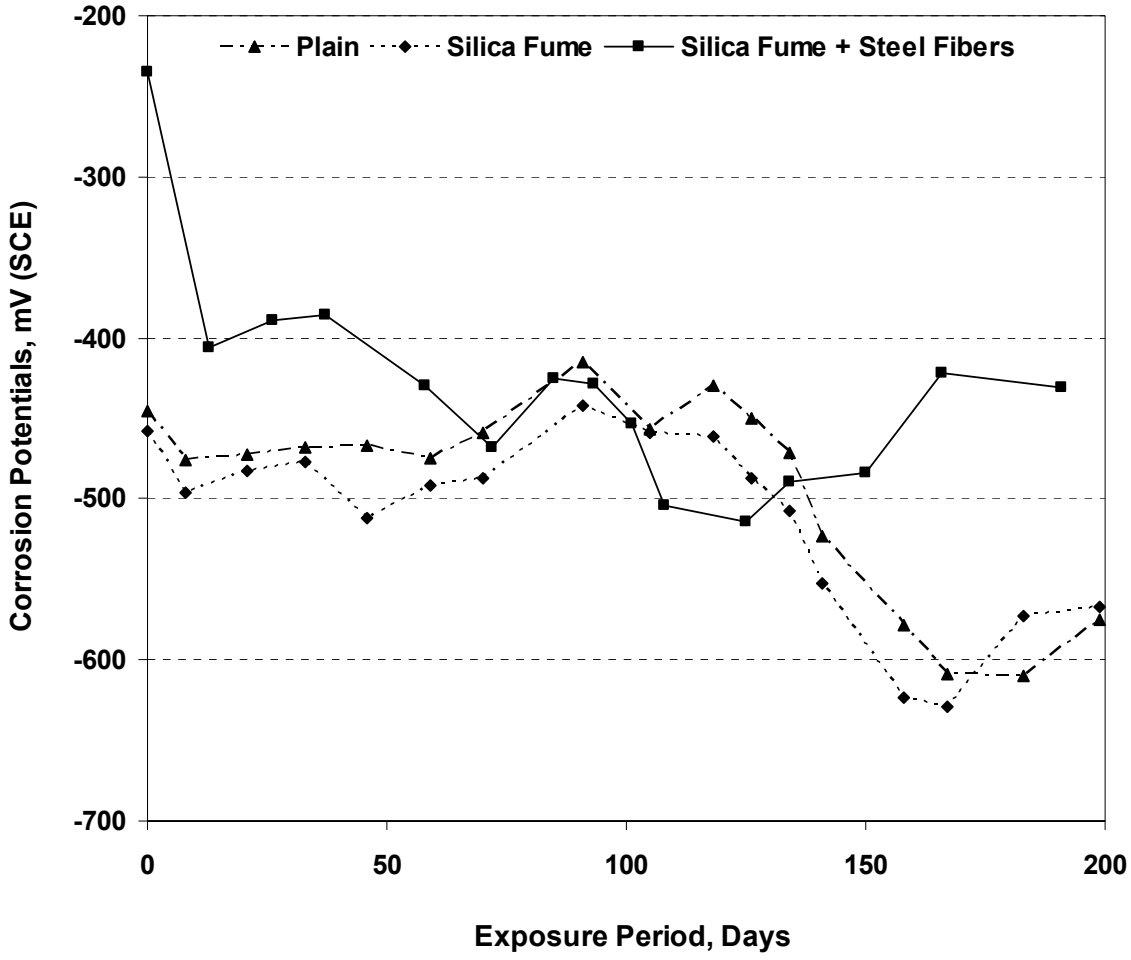

Figure 4.58: Variation of corrosion potentials on the steel in the Riyadh aggregate concrete specimens exposed to thermal variations.

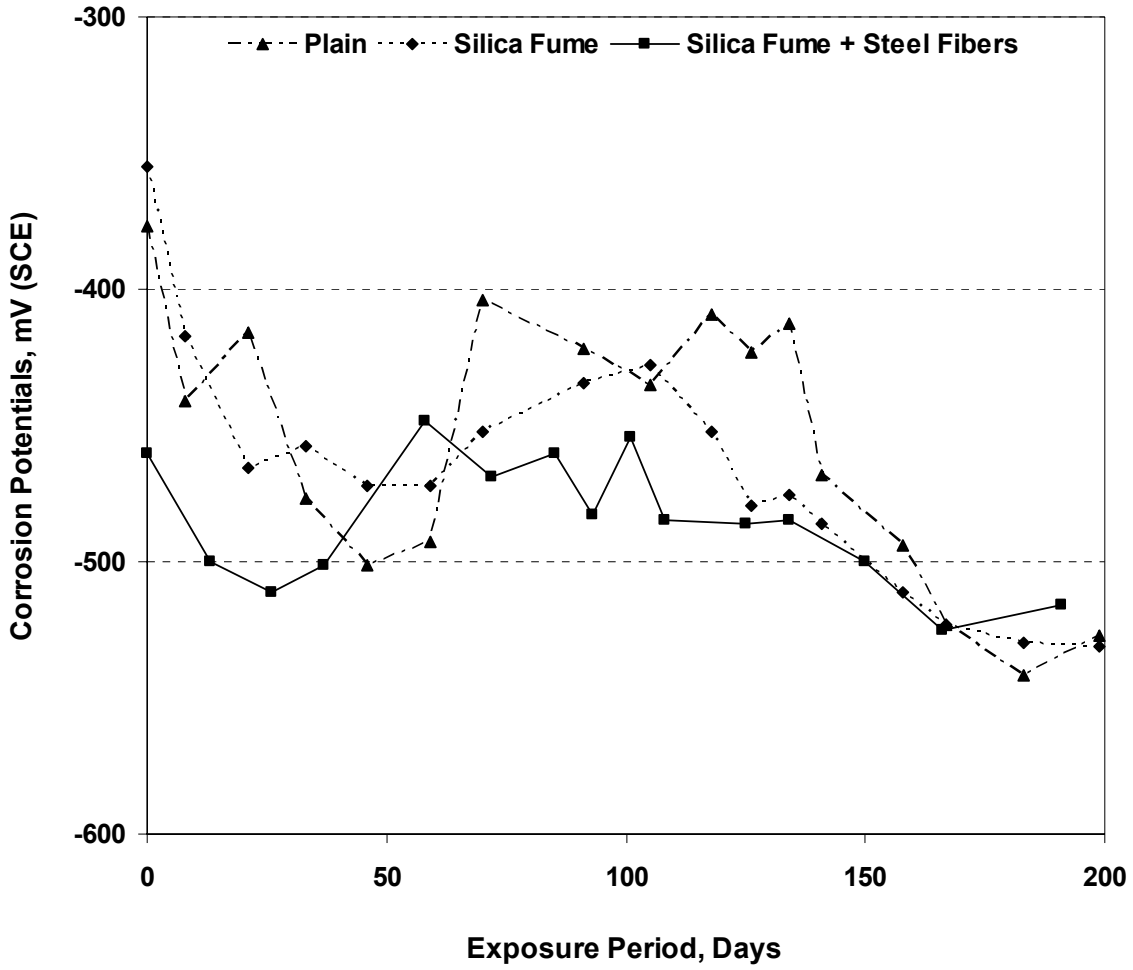

Figure 4.59: Variation of corrosion potentials on the steel in the steel slag aggregate concrete specimens exposed to thermal variations.

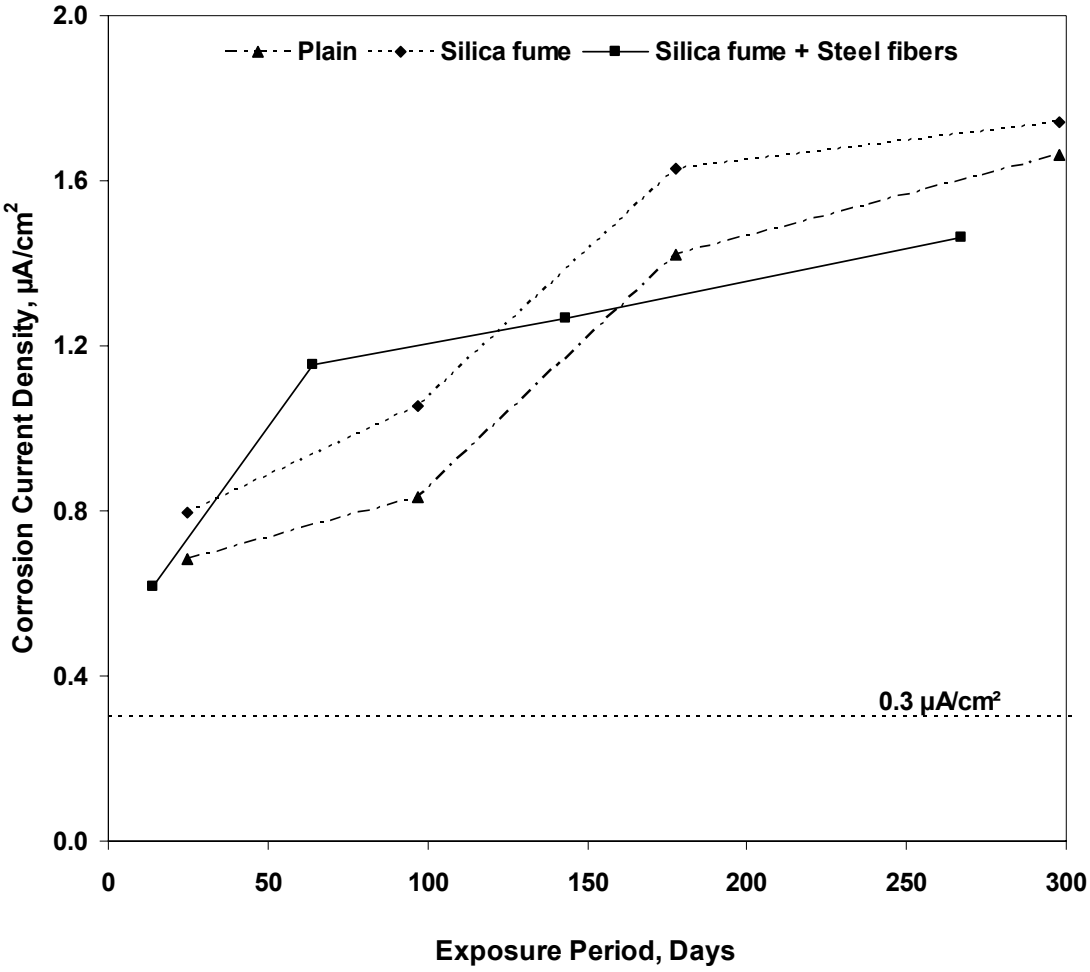

Figure 4.60: Variation of corrosion current density on steel in the Abu-Hadriyah aggregate concrete specimens after thermal exposure.

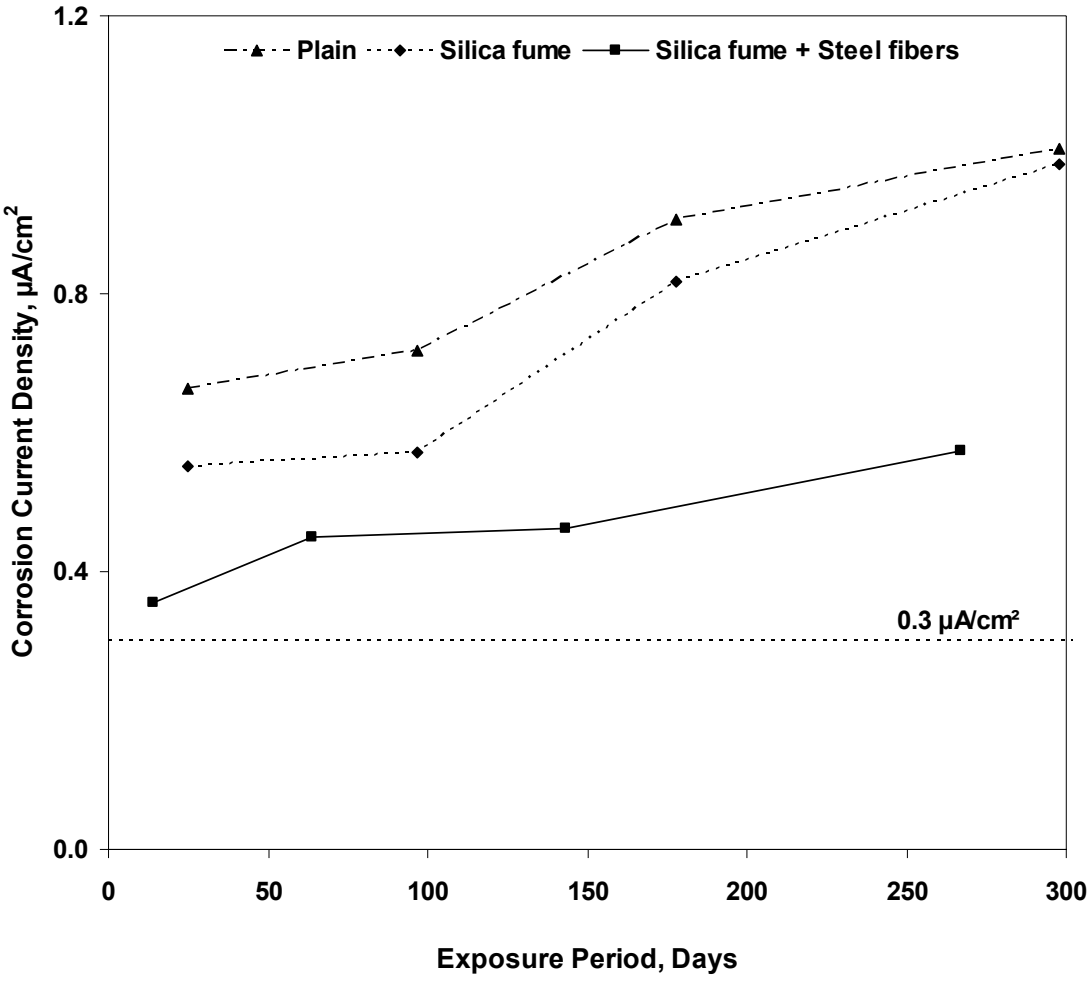

Figure 4.61: Variation of corrosion current density on steel in the Riyadh aggregate concrete specimens after thermal exposure.

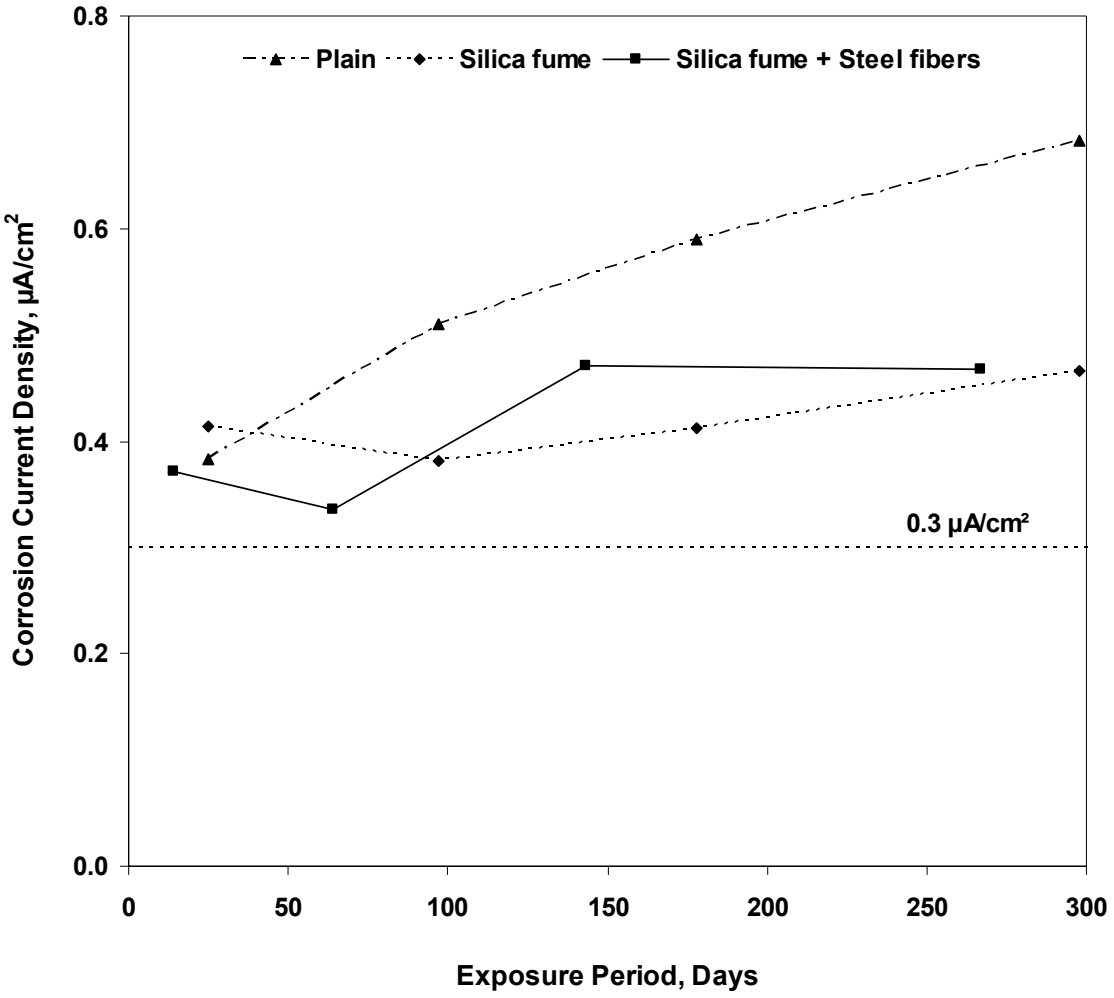

Figure 4.62: Variation of corrosion current density on steel in the steel slag aggregate concrete after thermal exposure.

I_{corr} in the fiber reinforced concrete specimens was less than that in the plain and silica fume cement concrete specimens.

The corrosion in the second batch of concrete specimens exposed to thermal variations was evaluated by impressing an anodic current of +2.5 volts on the steel bars and measuring the current required to maintain that potential. The current flowing through each specimen was plotted against time as shown in Figure 4.63 through 4.68. The time–current curves were utilized to evaluate the time to cracking of concrete due to accelerated reinforcement corrosion.

Figures 4.63 and 4.64 show the time current curves of the concrete specimens prepared with Abu-Hadriyah aggregate. The time–current curves for the Riyadh aggregate concrete specimens are shown in Figure 4.65 and 4.66. The time–current curves of the steel slag aggregate concrete specimens are shown in the Figure 4.67 and 4.68. A comparison of above discussed time–current curves with those for concrete specimens shown in Figure 4.31 through 4.39 shows an increase in initial current required for maintaining an anodic potential of +2.5 volts on the steel bar. The initial current required in all the concrete specimens not exposed to thermal variations was below 2 mA whereas in the concrete specimens subjected to accelerated corrosion after thermal exposure was above 4 mA. This may be due to the formation of microcracks in the concrete due to temperature fluctuations.

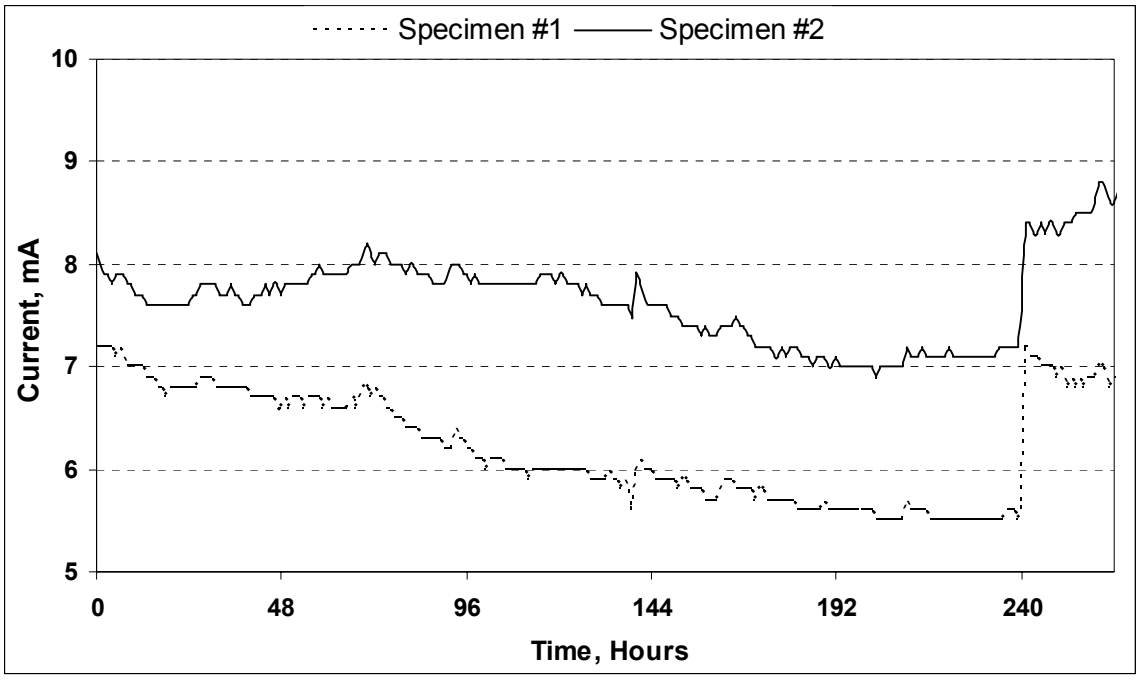

Figure 4.63: Variation of current with time in the plain cement concrete specimens prepared with Abu-Hadriyah aggregate.

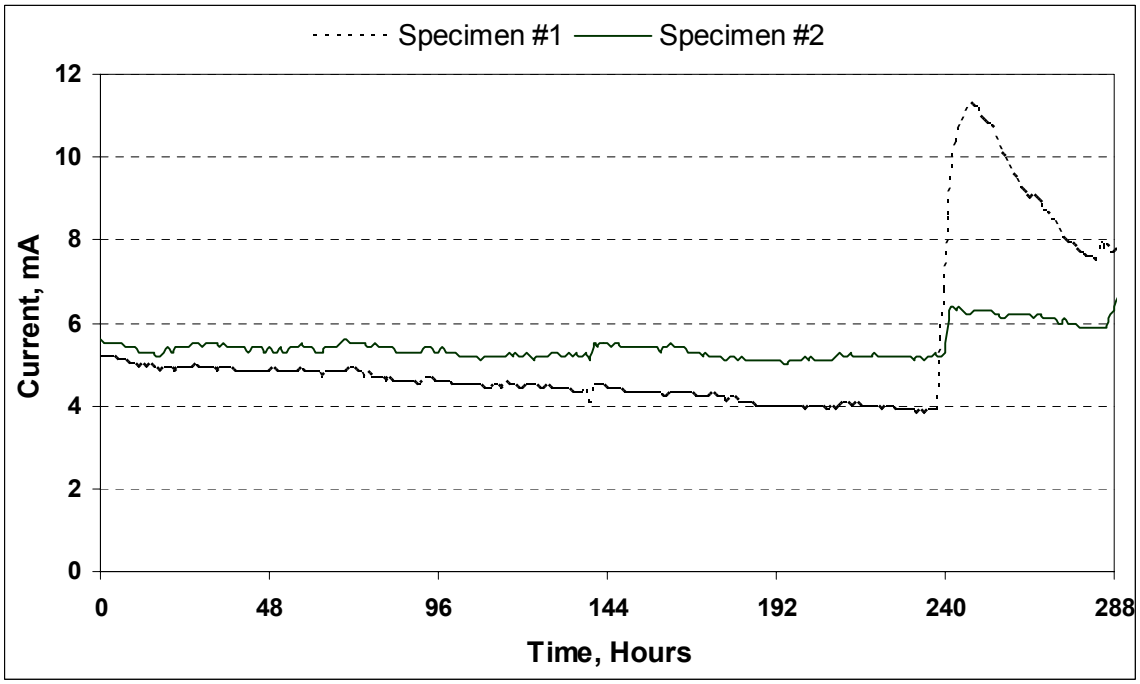

Figure 4.64: Variation of current with time in the silica fume cement concrete specimens prepared with Abu-Hadriyah aggregate.

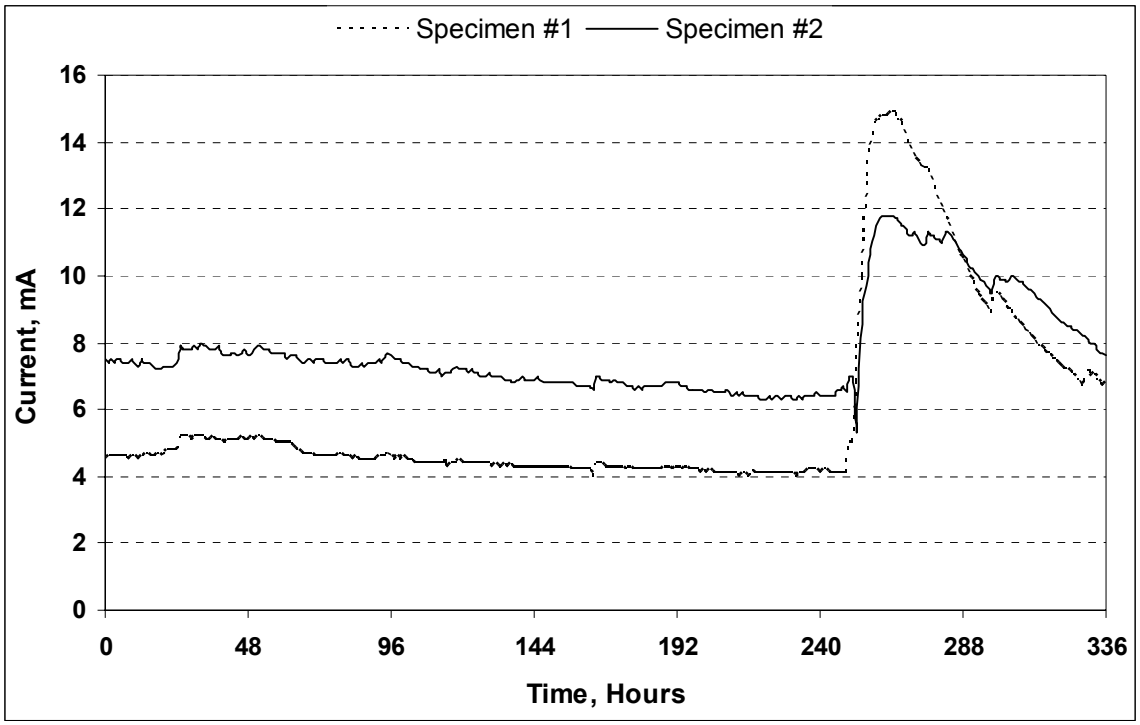

Figure 4.65: Variation of current with time in the plain cement concrete specimens prepared with Riyadh aggregate.

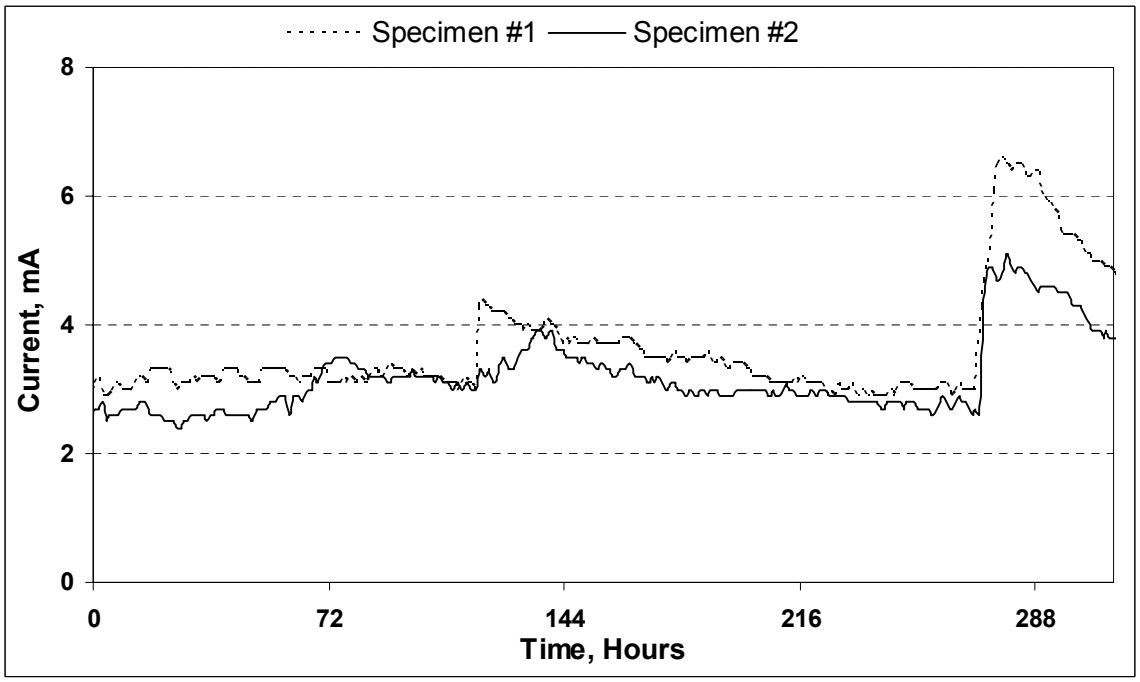

Figure 4.66: Variation of current with time in the silica fume cement concrete specimens prepared with Riyadh aggregate.

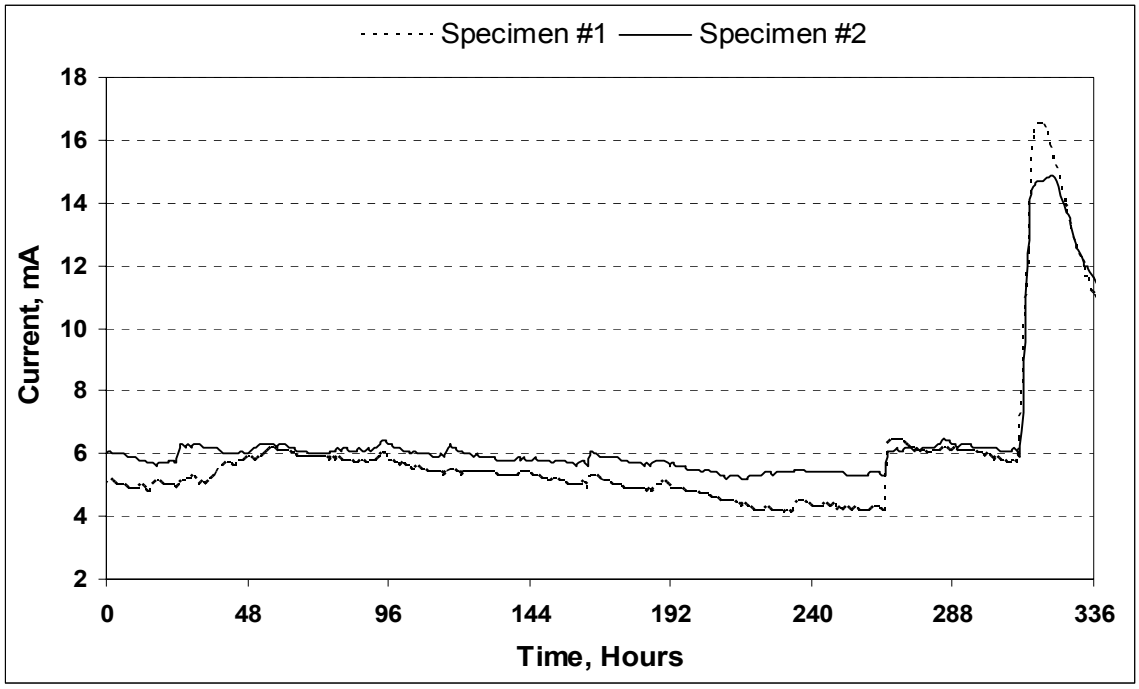

Figure 4.67: Variation of current with time in the plain cement concrete specimens prepared with steel slag aggregate.

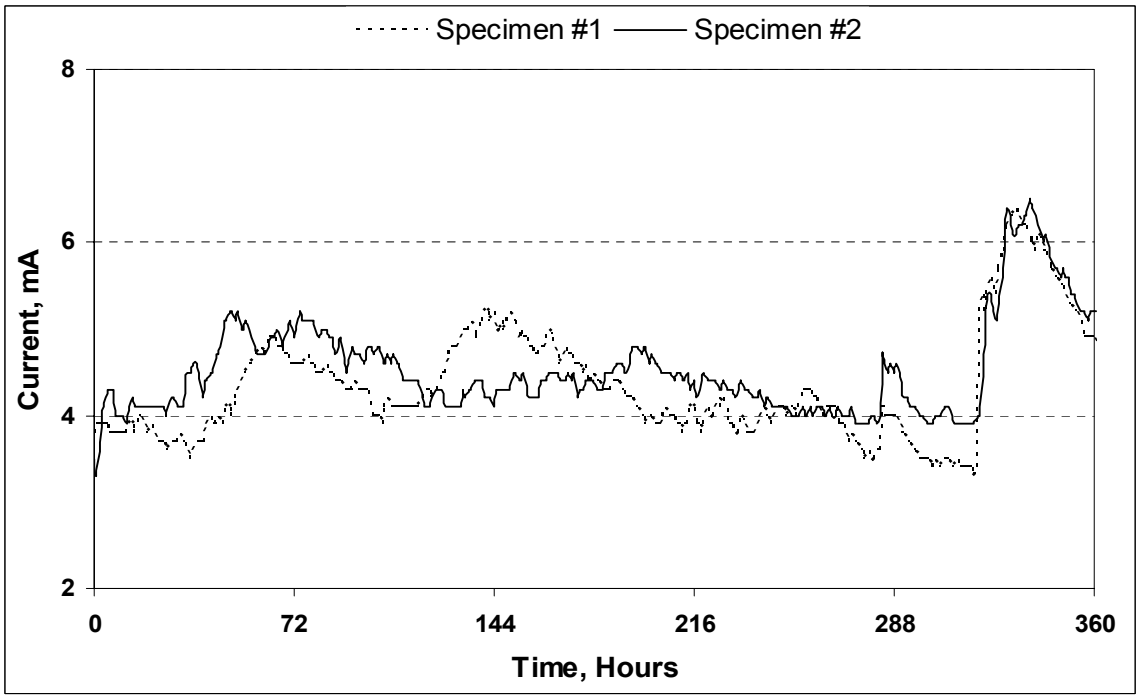

Figure 4.68: Variation of current with time in the silica fume cement concrete specimens prepared with steel slag aggregate.

Figure 4.69 shows the time to initiation of crack due to reinforcement corrosion in the concrete specimens exposed to thermal variations. The comparison of test results of the accelerated reinforcement corrosion obtained before and after thermal exposure along with percentage reduction in the time to cracking of the concrete specimens due to thermal exposure is tabulated in Table 4.14. The result indicates the significant effect of thermal variations on reinforcement corrosion.

The time to cracking due to the accelerated reinforcement corrosion in the concrete specimens exposed to thermal cycles was reduced by 83% when compared to the concrete specimens tested without thermal exposure. The concrete specimens prepared with Abu-Hadriyah aggregates were the first to crack within 235 to 295 hours. The concrete specimens prepared with Riyadh aggregate cracked next with the cracking time in the range of 250 to 300 hours. The highest time to initiation of cracking was recorded in the concrete specimens prepared with the steel slag aggregates. In this set of specimens, the time to initiation of crack due to accelerated reinforcement corrosion was in the range of 310 to 370 hours. The highest percentage of reduction in time to cracking after thermal exposure was recorded in the concrete specimens prepared with the steel slag aggregates.

4.7 SERVICE LIFE PREDICTION

The service life of reinforced concrete is predicted using two models, as discussed in Chapter 2, the physical model derived by Bazant [46] and the empirical model based on the experimental data developed by Morinaga [47]. In

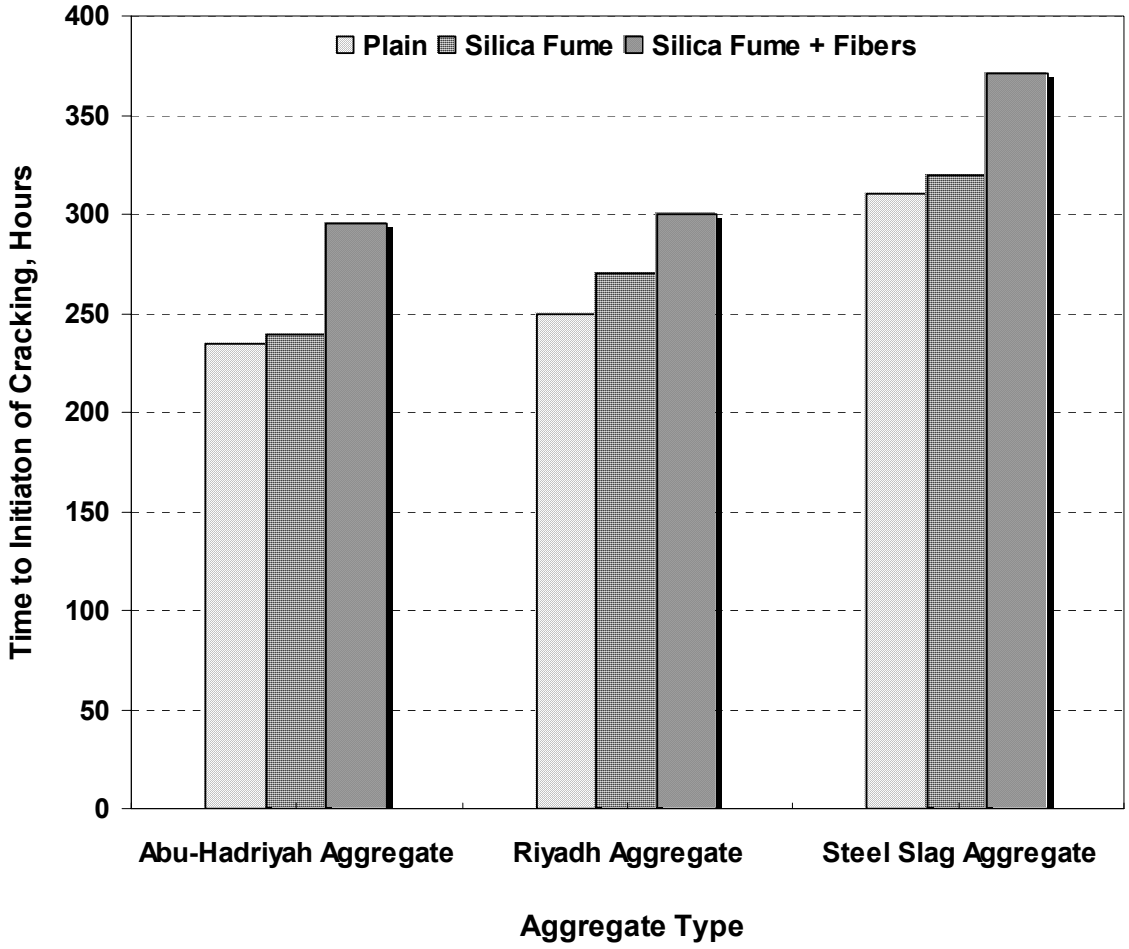

Figure 4.69: Variation of current with time in the silica fume cement concrete specimens prepared with steel slag aggregate.

Table 4.14: Comparison of time to cracking of the concrete specimens due to the accelerated reinforcement corrosion before and after thermal cycles

Mix Type	Aggregate Type	Time to Cracking of Concrete Due to Accelerated Reinforcement Corrosion (Hours)		% Reduction in Time to Cracking
		Normal Exposure	Thermal Exposure	
Plain Cement	Abu-Hadriyah	1350	235	81
	Riyadh	1400	250	82
	Steel Slag	1820	310	83
Silica Fume Cement	Abu-Hadriyah	1440	239	83
	Riyadh	1500	270	82
	Steel Slag	2340	320	86
Silica Fume + Steel Fibers	Abu-Hadriyah	1550	295	80
	Riyadh	1600	300	81
	Steel Slag	2550	370	86

Bazant's model, the known values of corrosion current density of rebar, thickness of the concrete cover over rebar, diameter of the rebar, tensile strength and modulus of elasticity of concrete in contact with the rebar is used to predict the service life. Whereas in the Morinaga's model [47], the corrosion current density I_{corr}, diameter of rebar and cover over rebar are the only factors needed to predict the service life; it does not use any data related to the properties of concrete. To get better picture of the service life of concrete prepared with the selected aggregates, the average of the two models was taken as the service life of the concrete.

The service life predicted using Bazant [46] and Morinaga [47] models for the concrete specimens prepared with the selected aggregates is tabulated in Table 4.15. The average service life of concrete specimens obtained using the two models is plotted in Figure 4.70. The highest service life of 83 years was recorded in the fiber reinforced concrete specimens prepared with steel slag aggregate, whereas the lowest service life of 25 years was obtained in the plain cement concrete specimens prepared with Abu-Hadriyah aggregate. The service life of the concrete specimens prepared with the steel slag aggregates was 1.7 to 2.3 times more than that prepared with the other two aggregate types. The effect of silica fume alone was insignificant in improving service life of concrete, but the addition of 1% fibers along with silica fume to the concrete increased the service life by 1.5 to 2 times. The addition of 1% steel fibers along with silica fume to concrete prepared with low quality aggregate from Abu-Hadriyah improved its service life by 200%.

Table 4.15: Service life prediction of the concrete specimens prepared with selected aggregates.

Mix Type	Aggregate Type	Service Life Years		Average Service Life (Year)
		Bazant's Model [46]	Morinaga's Model [47]	
Plain Cement	Abu-Hadriyah	22.42	27.84	25
	Riyadh	24.56	29.83	27
	Steel Slag	57.19	59.67	58
Silica Fume Cement	Abu-Hadriyah	28.09	34.80	31
	Riyadh	24.98	37.96	31
	Steel Slag	61.59	69.79	66
Silica Fume +Steel Fibers	Abu-Hadriyah	49.09	50.78	50
	Riyadh	47.75	46.40	47
	Steel Slag	83.09	83.51	83

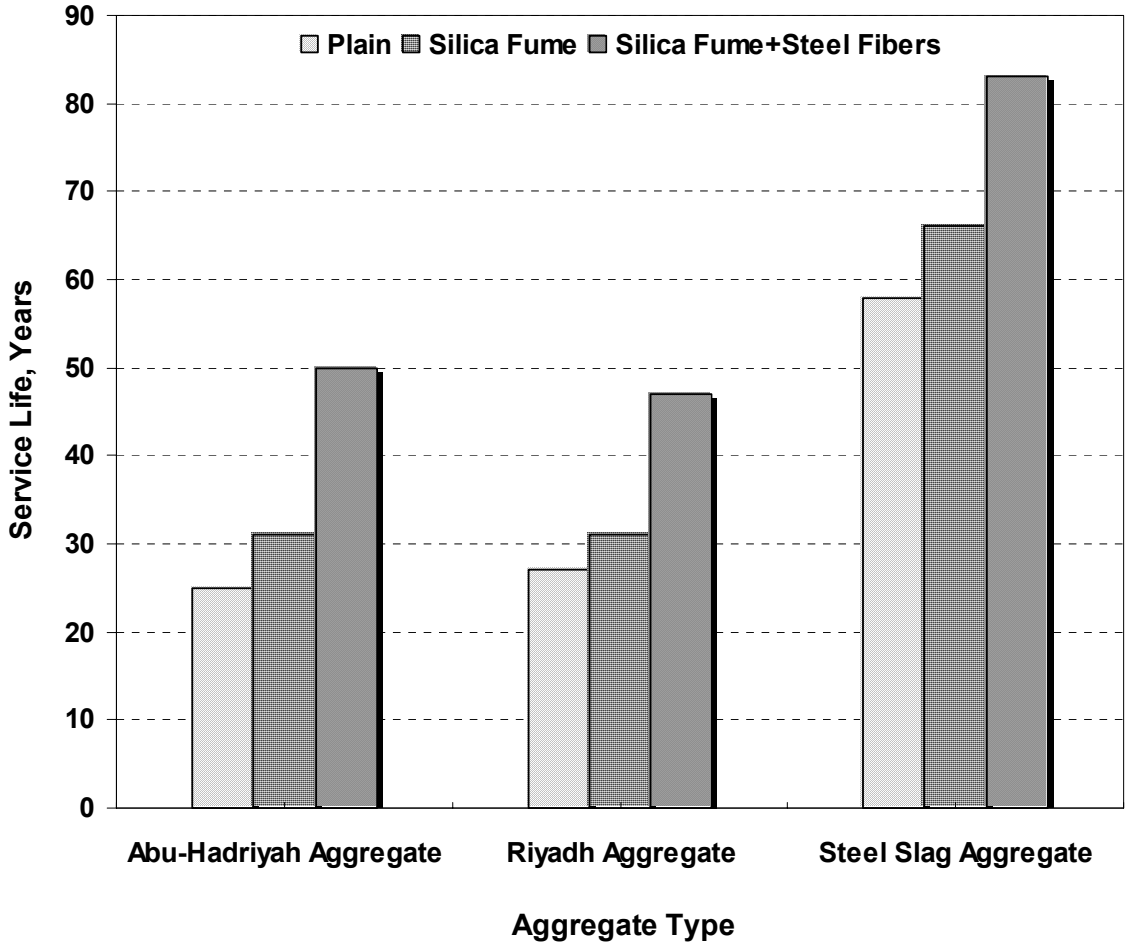

Figure 4.70: Service life of the concrete specimens prepared using selected aggregate.

4.8 COST ANALYSIS OF THE SELECTED AGGREGATES AND MIX DESIGN

When considering durability-enhancing materials, such as silica fume, steel fiber or better quality of aggregates, it is more appropriate to consider the cost per year of service life than the initial capital cost per mixture. Table 4.16 gives the materials cost of the selected concrete mixes. The rates were ascertained by a survey of the ready mix concrete market in the Eastern Province of Saudi Arabia. The steel slag concrete cost 230 to 350 SR/m^3, whereas the cost of the Abu-Hadriyah and Riyadh aggregate concrete lies in the range of 200 to 310 SR/m^3. The high cost of the steel slag aggregate concrete could be attributed to high price of steel slag aggregate.

Figure 4.71 shows the cost per year for the concrete prepared with the selected aggregates. The high cost per year was noted in the silica fume cement concrete prepared with Abu-Hadriyah and Riyadh aggregates. The cost per year of plain cement concrete prepared with steel slag aggregate was the lowest. Table 4.17 summarizes the materials cost per mix and the performance rating of the selected mixes. The performance ratings were assigned after evaluating their performance under the conditions investigated in this study. This information provides a relationship between the cost and the performance of concrete mixes.

Table 4.16: Mix and Cost/year of the selected concrete mixes

Mix Type	Aggregate type	Mix Cost (SR/m^3)	Service Life (Years)	Cost/Year of Service Life (SR/Year)
Plain Cement	Abu-Hadriyah	200	25	8.00
	Riyadh	200	27	7.40
	Steel Slag	230	58	4.00
Silica Fume Cement	Abu-Hadriyah	250	31	8.06
	Riyadh	250	31	8.06
	Steel Slag	280	66	4.24
Silica Fume +Steel Fibers	Abu-Hadriyah	310	50	6.25
	Riyadh	310	47	6.60
	Steel Slag	350	83	4.22

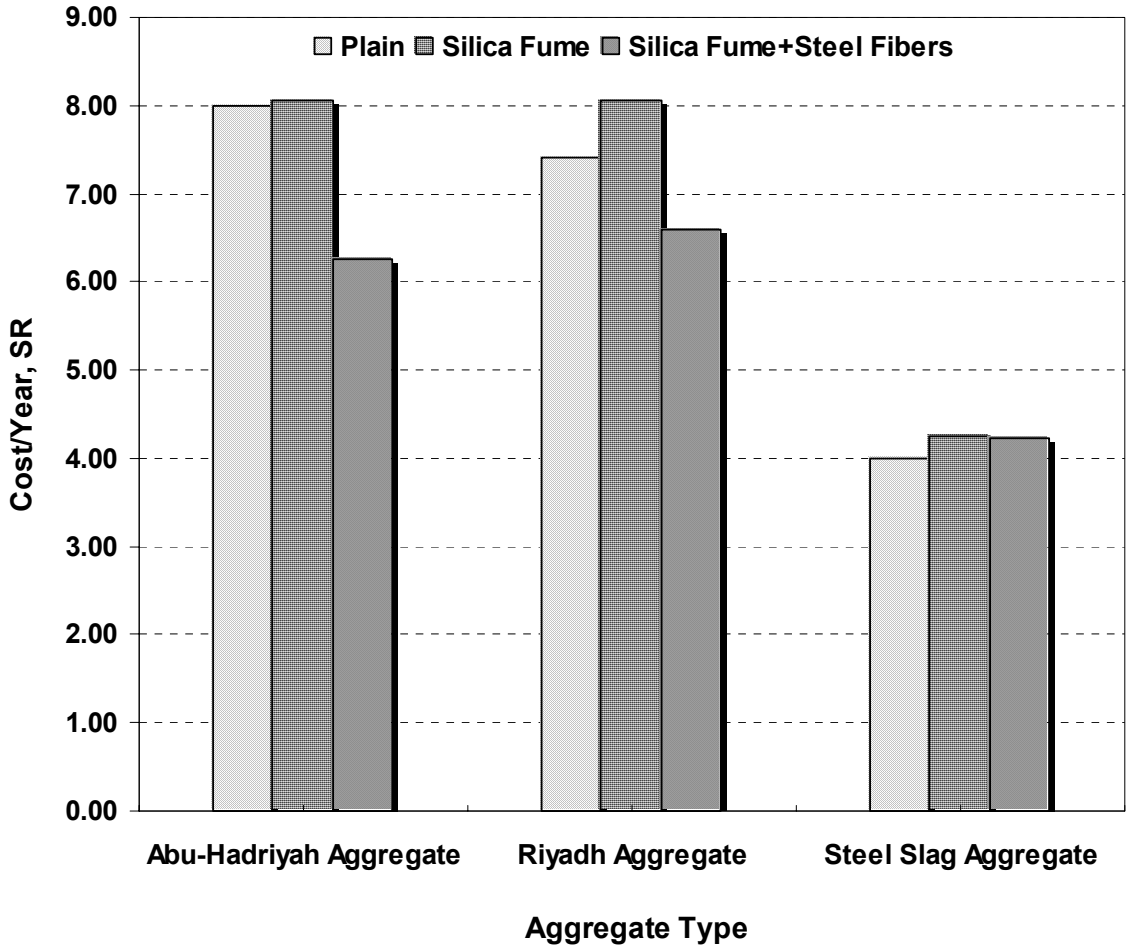

Figure 4.71: Cost/year of the concrete specimens prepared with selected aggregates.

Table 4.17: Performance rating of the selected concrete mixes

Mix Type	Aggregate type	Cost/year of service life (SR/year)	Performance rating
Plain Cement	Abu-Hadriyah	8.00	7
	Riyadh	7.40	6
	Steel Slag	4.00	1
Silica Fume Cement	Abu-Hadriyah	8.06	8
	Riyadh	8.06	8
	Steel Slag	4.24	3
Silica Fume +Steel Fibers	Abu-Hadriyah	6.25	4
	Riyadh	6.60	5
	Steel Slag	4.22	2

CHAPTER 5

CONCLUSIONS AND RECOMMENDATIONS

This study was conducted to assess the effect of aggregate quality and admixtures such as silica fume and steel fibers on the reinforcement corrosion in the concrete specimens exposed to normal and hot-weather conditions. In addition, data on tensile strength and chloride diffusion were developed. The conclusions reached from this study are discussed in the following paragraphs.

5.1 CONCLUSIONS

The following important conclusions can be drawn from the experimental data developed in this investigation:

1. The quality of aggregate has a significant effect on the split tensile strength and corrosion-resistance properties of concrete.

2. Steel slag aggregate is more suitable for preparing high performance concrete.

3. Addition of silica fume plus fibers can improve the properties of concrete prepared with marginal aggregates, such as limestone from Abu-Hadriyah.

4. Thermal variation has a significant effect on the split tensile strength and reinforcement corrosion of high performance concrete.

The other conclusions of this study are presented in the following sections.

5.1.1 Effect of Aggregate Quality on Split Tensile Strength

The quality of aggregate has a significant effect on the split tensile strength of concrete. The split tensile strength of concrete specimens prepared with steel slag aggregates was more than that of concrete specimens prepared with Riyadh and Abu-Hadriyah aggregates. The split tensile strength of concrete specimens prepared with crushed limestone from Abu-Hadriyah was the least. After 28 days of curing, the split tensile strength of plain cement concrete specimens prepared with steel slag, Riyadh and Abu-Hadriyah aggregates was 3.75, 3.12 and 2.60 MPa, respectively.

The split tensile strength of concrete specimens prepared with Riyadh aggregates was 7 to 20% more than that of Abu-Hadriyah aggregate concrete. The split tensile strength of steel slag concrete specimens was 28 to 44% more than that

of the Abu-Hadriyah aggregate concrete. This indicates that steel slag aggregate is more suitable for producing high performance concrete.

The highest split tensile strength was noted in the concrete specimens prepared with steel fiber cement concrete followed by those prepared with silica fume cement concrete. The percentage improvement in the split tensile strength of concrete due to the addition of silica fume and steel fiber was significant in the specimens prepared with the marginal aggregates from Abu-Hadriyah. The average improvement in these specimens was 6% due to the addition of silica fume, while it was 22% due to the addition of silica fume plus steel fibers. The improvement in the split tensile strength of the concrete specimens prepared with Riyadh aggregates was 1% and 9% due to the use of silica fume and steel fiber, respectively, while it was 3 to 8% in the concrete specimens prepared with steel slag aggregates. The data indicate that the split tensile strength due to the addition of silica fume plus fiber to the concrete specimens prepared with marginal aggregate from Abu-Hadriyah increased its split tensile strength to more than that of the Riyadh aggregate.

5.1.2 Effect of Aggregate Quality on the Time to Initiation of Reinforcement Corrosion

The time to initiation of reinforcement corrosion in the concrete specimens prepared with the selected aggregates varied from 72 to 180 days. The longest time to initiation of corrosion was noted in the steel slag aggregate concrete followed by Riyadh and Abu-Hadriyah aggregate concrete. The improvement in the time to initiation of reinforcement corrosion in the concrete specimens due to use of steel

slag aggregates instead of Abu-Hadriyah aggregates was in the range of 81 to 118%, while it was in the range of 2 to 11% due to the replacement of Abu-Hadriyah aggregates with the Riyadh aggregates.

The improvement in the time to initiation of reinforcement corrosion due to the addition of silica fume plus fibers was more than that due to the addition of silica fume alone. The improvement in the time to initiation of reinforcement corrosion due to addition of silica fume was in the range of 11 to 34% while it was in the range of 45 to 75% due to addition of silica fume plus steel fiber.

5.1.3 Effect of Aggregate Quality on Corrosion Current Density

The type of aggregate has a significant effect on the corrosion current density particularly in the later stages of exposure to the NaCl environment. The corrosion current density in the early period of exposure was almost similar in all the concrete specimens prepared with the selected aggregates, but in the later period of exposure, the lowest I_{corr} was recorded in the concrete specimens prepared with the steel slag aggregates. The I_{corr} in the concrete specimens prepared with Abu-Hadriyah aggregates was 1.6 to 2.3 times more than that in the concrete specimens prepared with the steel slag aggregate.

The I_{corr} in the plain cement concrete specimens was more than that in the silica fume and silica fume plus fibers. The lowest I_{corr} was recorded in the concrete specimens prepared with silica fume plus fibers. After 180 days of exposure, the I_{corr} in the concrete specimens prepared with plain, silica fume and fiber reinforced

cement concrete was 0.639, 0.566 and 0.15 μA/cm^2, in the Abu-Hadriyah aggregate concrete.

5.1.4 Effect of Aggregate Quality on Time to Cracking of Concrete Due to Accelerated Reinforcement Corrosion

The effect of aggregate quality has a significant effect on the time to initiation of concrete cracking due to accelerated reinforcement corrosion. The time to initiation of cracking due to accelerated reinforcement corrosion was in the range of 1350 to 2550 hours in the concrete specimens prepared with the selected aggregates. The lowest time to initiation of cracking due to accelerated reinforcement corrosion was noted in the concrete specimens prepared with Abu-Hadriyah aggregates followed by the concrete specimens prepared with Riyadh aggregates. The highest time to initiation of cracking due to accelerated reinforcement corrosion in the range of 1820 to 2550 hours was noted in the steel slag aggregate concrete.

The reduction in the time to initiation of cracking due to accelerated reinforcement corrosion in the Riyadh aggregate concrete was 3 to 4% compared to the of Abu-Hadriyah aggregate concrete while in the steel slag aggregate concrete it was 35 to 65%.

The time to initiation of cracking due to reinforcement corrosion in the concrete specimens prepared with silica fume plus steel fibers was the highest followed by silica fume and plain cement concrete. The reduction in the time to initiation of cracking due to the addition of silica fume and fibers was in the range

of 14 to 40% while it was in the range of 7 to 29% due to the addition of silica fume alone.

5.1.5 Effect of Aggregate Quality on Chloride Diffusion

The chloride concentration in the plain cement concrete was more than that in the silica fume and silica fume plus steel fiber cement concretes. The lower chloride concentration noted in silica fume cement concrete, compared to plain cement concrete is expected since silica fume reacts with calcium hydroxide resulting in the formation of secondary calcium silicate hydrate that fills up the pores formed as a result of cement hydration. This leads to a dense structure which decreases the diffusion of chloride ions.

The chloride diffusion coefficient for plain cement concrete was more than that for silica fume cement concrete specimens. The diffusion coefficient for plain cement concrete were in the range of 7.3 to 6.5 $*10^{-8}$ cm^2/s, while in the silica fume cement concrete specimens they were in the range of 3.1 to 3.4 $*10^{-8}$ cm^2/s. In the concrete specimens prepared with silica fume plus steel fiber the diffusion coefficient was in the range of 3.1 to 3.4 $*10^{-8}$ cm^2/s. The addition of steel fiber to the concrete did not significantly reduce the chloride diffusion coefficient.

The chloride diffusion coefficients do not vary significantly with the type of aggregates. The chloride diffusion coefficient for plain cement concretes prepared with Abu-Hadriyah, Riyadh and steel slag aggregate was 7.3, 6.2 and 6.5 $*10^{-8}$ cm^2/s, respectively. The chloride diffusion coefficient in the concrete specimens prepared with silica fume cement with Abu-Hadriyah, Riyadh and steel slag

aggregates was 3.8, 3.1 and 3.4 *10^{-8} cm^2/s, respectively, while in the fiber reinforced concrete it was 3.4, 3.2 and 3.1 *10^{-8} cm^2/s, respectively.

5.1.6 Effect of Thermal Variation on Concrete Properties

The split tensile strength of concrete was significantly affected by the thermal variations. The split tensile of almost all the concrete specimens increased up to 90 thermal cycles, then a decrease in the split tensile strength was noted. After 180 thermal cycles the highest split tensile strength was recorded in the concrete specimens prepared with steel slag aggregates. The steel fiber concrete specimens showed better resistance to thermal variations followed by plain and silica fume cement concretes. The silica fume cement concrete specimens were significantly affected by exposure to thermal variation due to its brittleness.

The corrosion resistance of concrete was also significantly affected by the thermal variation. The corrosion potentials on the steel in all the concrete specimens were less than -270 mV SCE in the early period of exposure to NaCl solution.

The I_{corr} was also affected by the thermal cycles. The I_{corr} values in all the concrete specimens were more than 0.3 $\mu A/cm^2$ that indicates active reinforcement corrosion.

The time to cracking, due to accelerated reinforcement corrosion, when tested after exposure to thermal cycles, decreased significantly. It was almost reduced by

83%. The time to cracking after thermal exposure was in the range of 235 to 370 hours.

5.1.7 Service Life of the Concrete

The service life of the concrete prepared with the selected aggregates was in the range of 25 to 83 years. The highest service life was noted in the concrete specimens prepared with steel slag aggregate. The service life of the concrete specimens prepared with Abu-Hadriyah and Riyadh aggregates was almost similar. The highest service life of 83 years was noted in the concrete specimens prepared with steel slag aggregates incorporating silica fume plus steel fibers. The service life of the concrete specimens prepared with steel slag was 1.66 to 2.32 times more than that of Abu-Hadriyah aggregate concrete specimens.

5.2 RECOMMENDATIONS

Based on the results presented in this investigation and their analysis, the recommended type of aggregate mix composition, from the reinforcement corrosion perspective, is listed below:

1. Steel slag aggregate with silica fume plus steel fiber concrete
2. Steel slag aggregate with silica fume cement
3. Steel slag aggregate with plain cement
4. Abu-Hadriyah aggregate with silica fume plus steel fibers

5. Riyadh aggregate with silica fume plus steel fibers
6. Riyadh aggregate with silica fume cement
7. Abu-Hadriyah aggregate with silica fume cement
8. Riyadh aggregate with plain cement
9. Abu-Hadriyah aggregate with plain cement

5.3 RECOMMENDATIONS FOR FURTHER STUDY

i) The performance of the local aggregates along with other admixtures, such as fly ash, granulated blast furnace slag and other pozzolans must also be evaluated to get the best combination to produce HPC with least cost.

ii) Future research should be carried out to examine the effect of different fiber sizes, shapes, and percentages.

REFERENCES

1. MacGregor, J. *Reinforced Concrete Mechanics and Design,* 3rd edition, New Jersey, Prentice Hall, 1997.

2. Saricimen H., "Concrete Durability Problems in the Arabian Gulf Region- A Review", *Proceedings Fourth International Conference Deterioration and Repair of R.C. in the Arabian Gulf*, Bahrain, 1993.

3. Shameem, M., Maslehuddin, M., Saricimen, H., and Al-Mana, A. I., "Extending the Life of Reinforced Concrete Structures in the Arabian Gulf Environment", *Proceedings, Structural Faults and Repairs Conference*, London, July 1995, pp. 115-126.

4. Mehta, P. K., and Monteiro, P. J. M., *Concrete: Structure, Properties and Materials,* 2nd Edition, New Jersey, Prentice Hall, 1993.

5. Fontana, M G. *Corrosion Engineering*, McGraw-Hill Book Company, 1986

6. Jones, Denny A., *Principles and Prevention of Corrosion*, Macmillan Publishing Company, New York, NY, 1992.

7. Hoar, T. P., "The Anodic Behavior of Metal", *Corrosion Science,* 7, 1967, pp. 341-355

8. Chao, C. Y., Lin, L. F. and MacDonald, D. D., "A Point Defect Model for Anodic Passive Films. Part I: Film Growth Kinetics. Part II: Chemical Breakdown and Pit Initiation", *Journal of Electrochemical Society*, 128, 1981, pp.1187-1194.

9. Alvarez, M. G. and Galvele, J. R., "The Mechanics of Pitting of High Purity Iron in NaCl Solution", *Corrosion Science,* 1984, 24, pp.27-48.

10. Leek, D. S., and Poole, A. B., "The Breakdown of the Passive Film on High Yield Mild Steel by Chloride Ions", *Corrosion of Reinforcement in Concrete,* Page, Treadaway and Bamforth, Editors, Elsevier Applied Science, London, 1990, pp. 65-73.

11. Rasheeduzzafar, Hussain, S. E. and Al-Saadoun, S. S., "Effect of Tricalcium Aluminate Content of Cement on Chloride Binding and Corrosion of Reinforcing Steel in Concrete", *ACI Materials Journal*, Jan-Feb 1992, pp. 3-12

12. Page, C. L. and Vennesland, O., "Pore Solution Composition and Chloride Binding Capacity of Silica-Fume Cement Pastes", *Materials and Structures*, Vol. 16, No. 91, 1983, pp. 19-25.

13. Tritthart, J., "Chloride Binding in Cement II: The Influence of the Hydroxide Concentration in the Pore Solution of Hardened Cement Paste on Chloride Binding", *Cement and Concrete Research*, 1989 Vol. 19, No. 5, pp. 683-691.

14. Rasheeduzzafar, Hussain, S. E., and Al-Saadoun, S. S., "Effect of Cement Composition on Chloride Binding and Corrosion of Reinforcing Steel in Concrete", *Cement and Concrete Research*, 1991 Vol. 21, No. 5, pp. 777-794.

15. Mangat, P. S., and Gurusamy, K., "Corrosion Resistance of Steel Fibers in Concrete under Marine Exposure", *Cement and Concrete Research*, January 1989, Vol.18, No.1, pp. 44-54.

16. Hausmann, D. A., "Steel Corrosion in Concrete, How does it Occur", *Materials Protection*, Nov. 1967, Vol. 6, pp. 19-23.

17. Gouda, V. K., "Corrosion and Corrosion Inhibition of Reinforcing Steel Immersed in Alkaline Solution", *British Corrosion Journal*, 1970, Vol. 5, pp. 198-203.

18. Mangat, P. S., and Molloy, B. T., "Influence of PFA, Slag and Micro silica on Chloride Induced Corrosion of Reinforcement in Concrete", *Cement and Concrete Research*, 1991, Vol. 21, No.5, pp. 819-834.

19. Al-Amoudi, O. S. B., Rasheeduzzafar, Abdul Jauwad, S. N., and Maslehuddin, M., "Corrosion of Reinforcing Steel in Sabkha Environment", *King Saud University Journal for Science and Engineering.*

20. Holden W. R., Page C L., and Short N.R., "The Influence of Chloride and Sulfates on Concrete Durability", *Corrosion of Reinforcement in Concrete Construction,* Crane A P., Editor, Society of Chemical Industry, London, 1983, pp. 143-149.

21. Al-Amoudi, O.S.B. and Maslehuddin, M., "The Effect of Chloride and Sulfate Ions on Reinforcement Corrosion", *Cement and Concrete Research,* 1993, Vol. 23, No 1, pp. 139-146.

22. Al-Amoudi, O.S.B., Rasheeduzzafar, Maslehuddin, M. and Abduljauwad S N., "Influence of Sulfate Ions on Chloride on Chloride Induced Reinforcement Corrosion in Portland and Blended Cement Concrete," *Cement and Concrete Research,* 1994, Vol. 16, No 1, pp. 3-11.

23. Dehwah, H. A. F., Austin, S. A. and Maslehuddin M., "Chloride-induced Reinforcement Corrosion in Blended Cement Concretes Exposed to Chloride-Sulphate Environments", *Magazine of Concrete Research,* 2002, Vol. 54, No 5, pp 355-364.

24. Maslehuddin, M., Page C. L. and Rasheeduzafar, "Effect of Temperature and Salt Contamination on Carbonation of Cement", *ASCE Journal of Material in Civil Engineering*, 1996, Vol. 8, No 2, pp. 63-69.

25. Hobbs, D.W., "Carbonation of Concrete Containing PFA", *Magazine of Concrete Research*, 1988, Vol. 40, No 14, pp 68-78.

26. Sabir, B. B., "High-strength Condensed Silica Fume Concrete", *Magazine of Concrete Research,* September 1995, Vol. 47, No. 172, pp.27-38.

27. Aitcin, P.C. and Mehta, P K., "Effect of Coarse Aggregate Characteristics on Mechanical Properties of High Strength Concrete", *ACI Materials Journal*, Mar-Apr., 1990, Vol. 87, No. 2, pp. 490-530

28. Baalbaki, W., Benmokrane, B., Challal, O., and Aitcin, P.C., "Influence of Coarse Aggregate on Elastic Properties of High Performance Concrete", *ACI Materials Journal*, Sept-Oct 1991, pp. 499-503.

29. Giaccio, G., Rocco, C., Violini, D., Zappitelli, J., and Zerbino, R., "HSC Incorporating Different Coarse Aggregate", *ACI Materials Journal*, May-June 1992, pp. 242-246.

30. Zhang, M.H., and Gjorv, O. E., "Mechanical Properties of High-strength Light Weight Concrete", *ACI Materials Journal*, May-June 1991, pp.122-126.

31. Beshr, H. A. M., *Durability of High Performance Concrete,* Ph.D. Dissertation, King Fahd University of Petroleum and Minerals, Dhahran, Saudi Arabia, June 2000, pp. 225-238.

32. Mannmohan, D., and Mehta, P.K., "Influence of Pozzolanic, Slag and Chemical Admixtures on the Pore Distribution and Permeability of Hardened Cement Paste", *Cement, Concrete, and Aggregates,* 1981, Vol. 3, No. 1, pp 63-67.

33. Mehta, P K. and Gjorv, O.E., "Properties of Portland Cement Concrete Containing Fly Ash and Condensed Silica Fume", *Cement and Concrete Research,* 1982, Vol.12 No. 5, pp. 587-595.

34. Hustad, T., and Loland, K. E., "Silica in Concrete-Permeability", *Cement and Concrete Research Inst. at the Norwegian Institute of Technology,* Trondheim, Norway, Report No. STF65A81031, June 1981.

35. Gjorv, O. E., "Durability of Concrete Containing Condensed Silica Fume", *Proceeding 1st International Conference on Fly Ash and Slag, ACI Spec.* SP-79, Montebello, Canada, July 1983, pp. 695-708.

36. Al-Amoudi, O.S.B., Abduljauwad, S.N., Rasheeduzzafar, and Maslehuddin, M., "Effect of Chloride and Sulfate Contamination in Soils on Corrosion of Steel and Concrete", *Transportation Research Record*, No 1345, 1992, pp. 67-73.

37. Byfors, K., "Influence of Silica Fume and Fly Ash on Chloride Diffusion and pH Values in Cement Paste", *Cement and Concrete Research,* Vol. 17, 1987, pp. 115-130.

38. Cook, W.D., Miao, B., Aitcin, P. C., and Mitchell, D., "Thermal Stresses in Large HSC Columns", *ACI Materias Journal*, Jan-Feb. 1992, pp. 18-22.

39. ACI Committee 554, Fiber Reinforced Concrete, May 1997.

40. Cady, P. D., Weyers, R E., "Predicting Service Life of Concrete Bridge Decks Subject to Reinforcement Corrosion", *ASTM Special Technical Publication*, No. 1137, 1992, pp. 328-338.

41. Browne, R. D., "Design Prediction of the Life for Reinforced Concrete in Marine and Other Chloride Environments", *Durability of Building Materials*, Vol. 1, No. 2, July 1982, pp. 113-125.

42. Maruya, T., "Simulation of Chloride Penetration into Hardened Concrete", edited Malhotra, V. M., Durability of Concrete *American Concrete Institute*. Detroit, MI, Vol. SP 145, 1994. pp. 519.

43. Andrade, C., "Calculation of Chloride Diffusion Coefficients in Concrete from Ionic Migration Measurements", *Cement and Concrete Research* 1993.

44. Cady, P. D. and R. E. Weyers, "Deterioration Rates of Concrete Bridge Decks," *Journal of Transportation Engineering,* 1984, Vol. 110, No. 1, pp.34-44.

45. Tuutti, K., "Corrosion of Steel in Concrete", Stockholm, Sweden, *Swedish Cement and Concrete Research Institute,* 1982.

46. Bazant, Z P. "Physical model for steel corrosion in concrete sea structures-application", *ASCE Journal of Structural Division*, Vol. 105, June 1979 pp. 1155-1166.

47. Morinaga, S., "Prediction of service lives of reinforced concrete buildings based on the corrosion rate of reinforcing steel", *Proceedings, Building Materials and Components*, Brighton, UK, 7-9 November 1990, pp. 5-16.

48. Wang, X.M., Zhao H.Y., "The Residual Service Life Prediction of Reinforced Concrete Structures", *Durability Building Materials and Components* Edited by Nagataki, S., et al., E & FN Spon, London, 1993, pp. 1107-1114.

49. Dagher H.J., and Kulendran S., "Finite element model of corrosion damage in concrete structures", *ACI Structural Journal*, Vol. 89, No. 6, Nov-Dec 1992, pp. 699-708.

50. Ahmad S., Bhattacharjee B., Wason R., "Experimental Service Life Prediction of Rebar Corroded Reinforced Concrete Structure," *ACI Materials Journal,* Vol. 94 No. 4, July-August 1997, pp. 311-316.

51. Neville, A. M., *Properties of Concrete*, Pearson Education Limited, England, Text, 1999.

52. Cabrera, J G., and Hassan, K G., "The Effect of Polymeric Surface Treatment Compound on the Water Absorption and Chloride Diffusion of Concrete Exposed to Hot Dry Environment," *Proceedings, Intl. Conference on Protection of Concrete*, Edited by Dhir, R. K., and Green J W., E & FN Spon, London, Vol. 1, 1990, pp. 697-715.

53. ASTM C 876-91, "Standard Test Method for Half Cell Potentials of Reinforcing Steel in Concrete," *Annual Book of ASTM Standards,* Volume 04.02.

54. Escalante, E., Ito, S., and Cohen. M., " Measuring the Rate of Corrosion of Steel in Concrete", *Annual Report NBSIR 80-2012,* National Bureau of Standards, Gaithersburg, Md., March 1980, pp. 1-26

55. Escalante, E., Whitenton, E., and Qui, F., "Measuring the Rate of Corrosion of Reinforcing Steel in Concrete", *Final Report NBSIR 86-3456,* National Bureau of Standards, Gaithersburg, Md., Oct. 1986 pp1-27.

56. Clear, K.C., "Measuring Rate of Corrosion of Steel in Field Concrete Structures", *Transportation Research Record,* 1211, pp.28-36.

57. Stern, M., and Geary, A.L., "A Theoretical Analysis of the Shape of the Polarizing Curves", *Journal of Electrochemical Society,* Vol. 104, 1957, pp. 56-63

58. Mansfield, F., "Polarization Resistance Measurements: Experimental Procedure and Evaluation of Data", *Electrochemical Techniques for Corrosion,* NACE, Houston, 1977, pp. 18-26

59. Gonzalez, A.J., Feliu, S., Andrade, C., and Rodriguez, I., "On-site Detection of Corrosion of Reinforced Concrete Structures", *Materials and Structures,* Vol. 24, 1991, pp. 346-350.

60. Ibrahim, M., *Performance Evaluation of Concrete Surface Treatments in the Arabian Gulf*, M. S. Thesis, King Fahd University of Petroleum and Minerals, Dhahran, Saudi Arabia, June 1996, pp. 149- 154.

61. Aitcin, P. C., Sarkar, S. L., and Yahya, D., "Microstructural Study of Different Types of Very HSC", *Materials Research Society*, Pittsburgh, Vol. 85, 1987, pp. 261-272.

62. Wu K R., Chen B., Yao W., Zhang D., "Effect of Coarse Aggregate Type on Mechanical Properties of High-Performance Concrete", *Cement and Concrete Research,* Vol. 31, 2001 pp. 1421-1425

63. Baalbaki, M., Sarkar, S. L., Aitcin, P. C., and Isabelle, H., "Properties and Microstructures of HPC Containing Silica, Slag, Fly Ash", *ACI SP-132,* Detroit, May 1992, pp. 921-941.

64. Iravani, S., "Mechanical Properties of High-Performance Concrete", *ACI Materials Journal,* Sept-Oct. 1996, pp. 416-426.

65. Carrasquillo, R. L., Nilson, A. H., and Slate, F O., "Microcracking and Engineering Properties of High-Strength Concrete", *Report No. 80-1,* Feb. 1980, Structural Engineering, Cornell University, Ithaca, New York.

66. Rapoport, J., et al, "Permeability of Cracked Steel Fiber-Reinforced Concrete", *ASCE Journal of Materials in Civil Engineering,* Vol. 14, No. 4, July-August 2002. pp. 355-358.

67. Ramezanianpour, A. A., and Malhotra, V. M., "Effect of Curing on the Compressive Strength, Resistance to Chloride-Ion Penetration and Porosity of Concrete Incorporating Slag, Fly Ash or Silica Fume", *Cement and Concrete Composites,* No. 17, 1995, pp. 125-133.

68. Khayat, K. H., and Aiticn, P. C., "Silica Fume in Concrete -An Overview", *ACI SP-132*, Detroit, May 1992, pp. 835-872.

69. Painter, K. E., "A Note on the Pulse Velocity of Silica Fume Concrete Prisms after Exposure to Elevate Temperatures", *CANMET International Report MRP/MSL 86-35*, Energy, Mines and Resources Canada, Ottawa, Feb 1986.

70. Reis, M, L, B, C., Neves, C, I., Tadeu, A, J, B., "High-Temperature Compressive Strength of Steel Fiber High-Strength Concrete", *Journal of Materials in Civil Engineering,* Vol. 13, No. 3, May-June 2001, pp. 230-234.

VITAE

NAME: Syed Imran Ali

PLACE OF BIRTH: Hyderabad, INDIA.

ADDRESS: Flat No. 303, Block "A", Akbar Towers,
New Malakpet
Hyderabad 500024,
INDIA.

E-MAIL: imran699@hotmail.com
imran699@yahoo.com

EDUCATIONAL QUALIFICATIONS:

M.S ***(Civil Engineering-Structures)***
April 2003
King Fahd University of Petroleum and Minerals
Dhahran, Saudi Arabia.

B.E ***(Civil Engineering)***
May 1998
Osmania University
Hyderabad, India.